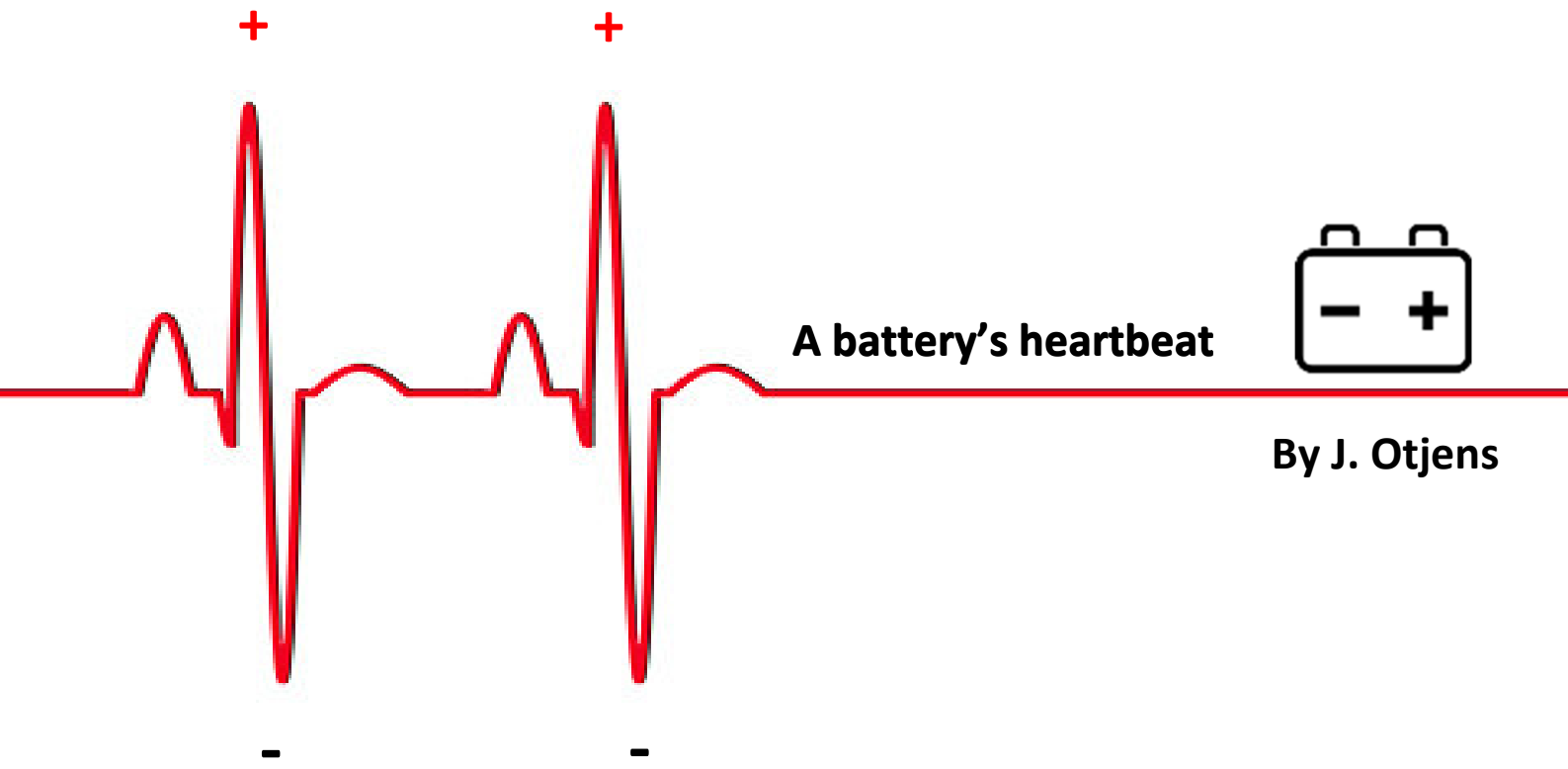

A battery's heartbeat

By J. Otjens

"how to estimate the state of health of an online battery by use of non-invasive measuring methods"

TU Delft Faculty of Mechanical, Maritime and Materials Engineering

A battery's heartbeat

How to estimate the state of health of an online battery by use of non-invasive measuring methods

By

J. Otjens

in partial fulfilment of the requirements for the degree of

Master of Science

In Mechanical Engineering

at the Delft University of Technology,

to be defended publicly on Tuesday January 10, 2017 at 11:30 AM.

Supervisors: Prof.dr.ir. Lodewijks
Dr.ir. Godjevac

Summary

The ANWB, a professional association which enables high level technical assistance on passenger vehicles nationwide, is experiencing an increasing number of battery related failures. Their future goal is to predict an upcoming battery failure and to create the opportunity to respond to the problem in advance. This thesis examines a method capable of determining the battery's state of health and indicating upcoming battery failure. Non-invasive measuring methods are investigated to make the method implementable in practical solutions.

The working principle of batteries applied in the automotive sector will be investigated first to obtain an understanding of the technology which is involved in battery design. Battery technology comprises a combination of chemistry, material, mechanical and electrical science. An aggregation of these technologies yields to a small electrical-energy producing device, referred to as a battery. In the automotive sector lead acid batteries are used in cranking applications

The state of health (SOH) of lead acid batteries is decreasing with age revealing a reduced battery performance. The performance of lead acid batteries is expressed in capacity and peak power delivery. To estimate the battery's SOH the effective performance has to be determined.

The effective performance and therefore the SOH of the battery is gradually decreasing until a cranking failure manifests itself. Batteries can have different failure modes caused by a combination of underlying failure mechanisms. A battery is a closed system and progressing failure mechanisms cannot be observed without the use of invasive methods i.e. to really reveal the battery's SOH the casing has to be opened enabling the internals to be examined which will destroy the battery. Most failures are caused by a combination of different failure mechanisms. Using a non-invasive SOH estimator groups all progressing failure mechanisms together, but enables the SOH to be estimated without destroying the battery. Non-invasive SOH estimators are based on the effective capacity and internal resistance of the battery.

The main task of a battery is to power a cranking system which is cranking a reciprocating combustion engine. The combustion engine produces a variable load on the cranking system which will be observable in the voltage values of the cranking system. Capturing the discharge voltage of the battery while cranking reveals a distinctive shape from which the same kind of general points can be derived. These general points represent features contained by the discharge voltage. In this study the discharge voltage signal is referred to as the "cranking voltage trace" (CVT). The shape of the CVT changes with the battery age and a decreasing SOH. It is expected that features extracted from the CVT change along with the CVT shape. A method is proposed to discover a relation between the change in features and battery SOH.

The proposed SOH monitoring method involves non-invasive measuring of the CVT utilizing a standardized connection implemented in all European vehicles since 2002. To capture the cranking voltage trace measuring equipment is prototyped which is able to sample an analog voltage signal at the required frequency and resolution. A successful prototype proved the feasibility of measuring the CVT with simple hardware as the ANWB is intending.

CVT data of batteries with a decreasing SOH is required to research the existence of a relation between features extracted from the CVT and battery SOH. A test setup has been created to generate CVT data. The test setup is used to produce CVT data by cranking two combustion engines

of different fuel type while capturing the CVT. Five test batteries will be used to crank the engines of the test setup. Three of the five test batteries will be subjected to an accelerated aging process, which ages the batteries in weeks instead of years. For this purpose an accelerated battery aging device was constructed which successfully aged the batteries in a relatively short period. At certain intervals during the aging period the test setup was used to generate CVT data which resulted in approximately 200 CVT's usable for analysis.

Before the CVT data can be analysed it has to be processed first. The data is made identifiable by use of a personal table of labels for each test battery and a CVT identification number. Using these identifiers generated CVT data can be linked to that particular battery and cranking event. A Matlab script imports the CVT data and performs a selection of the peaks and valleys contained by the CVT signal shape. All features of the CVT data are based on these peaks and valleys. After the peak and valley selection has finished the Maltab script will start with the extraction of features. 27 features are extracted from the CVT data and stored in a table of features containing an unique set of features in each row of the table. Once the table of features is filled with features originating from the cranking events executed by the test setup, a data analysis can be performed.

A data analysis is performed to research the existence of a relation between features extracted from the CVT and the battery SOH. The features are classified according to the battery SOH and put through different types of analysis. In the process of analysis, the unusable features are discarded resulting in a select set of features which is most capable of revealing a relation to battery SOH. Two features survived the process of data analysis and are selected to be implemented in the proposed SOH monitoring method. As expected, it is discovered that these features are temperature dependent.

The proposed method SOH monitoring method is a continuous method and therefore needs a reference value to map the change in battery SOH over time. To make the feature values of different battery engine combinations comparable they are normalized by scaling them to a personal baseline. A personal baseline belongs to a particular battery engine combination and uses the feature values captured on first use of the battery. Scaling all succeeding feature values to the baseline values creates normalized values capable of revealing a change relative to the baseline. Since the baseline belongs to new batteries, the change will indicate that batteries are getting older and their SOH is changing. The normalized values are still able to reveal a relation to battery SOH and produce an upcoming failure warning. Three failure warning methods are tested from which two predicted an upcoming failure of one of the test batteries with 100% accuracy.

Table of Contents

Table of Contents. 1

1 INTRODUCTION. 5

1.1 BACKGROUND. 5
1.2 PROBLEM DESCRIPTION. 5
Research question . 5

2 THE AUTOMOTIVE BATTERY . 6

2.1 BASIC STRUCTURE . 6
2.2 A SINGLE CELL . 6
2.2.1 Working principle . 7
2.2.2 Observations in working cells . 9
2.2.2.1 Polarisation effects . 9
Activation polarisation . 9
Concentration polarisation . 9
Ohmic polarisation . 9
2.2.2.2 Electrode surface passivation . 9
2.3 FROM CELLS TO BATTERY . 10
2.4 LEAD ACID BATTERY TYPES . 11
2.4.1 Flooded battery . 11
2.4.2 Valve regulated batteries . 11

3 BATTERY PERFORMANCE . 13

3.1 BATTERY RELATED VARIABLES . 13
3.1.1 Voltage . 13
3.1.2 Current. 13
3.1.3 Temperature. 13
3.1.4 Weight . 13
3.2 RATINGS . 13
3.2.1 Capacity . 14
3.2.2 Cold Cranking Amps . 15
3.3 BATTERY STATES . 15
3.3.1 State of charge . 16
3.3.1.1 Estimating the state of charge . 16
Open circuit voltage measurement. 16
Coulomb counting . 17
Specific gravity . 17
3.3.2 State of health . 18

4 BATTERY FAILURE . 19

4.1 FAILURE MODES . 19
4.1.1 Serviceable . 19
4.1.2 Damaged . 19
4.1.3 Open circuit . 20
4.1.4 Short circuit . 20
4.1.5 Pate/Grid . 20
4.1.6 Worn out/Abused . 20
4.2 FAILURE MECHANISMS . 20
4.2.1 Loss of electrolyte . 21

4.2.2 Electrolyte stratification *21*
4.2.3 Cathode grid corrosion *21*
4.2.4 Positive electrode active material softening and shedding *22*
4.2.5 Electrolyte contamination *22*
4.2.6 Formation of sulphate with crystalline structure *22*
4.2.7 Inter-cell shorting *23*
4.2.8 Inter-cell open circuit *23*
4.3 AGING SERVICE LIFE 23
4.4 SOH ESTIMATORS 24
4.4.1 Estimating SOH considering impedance and resistance *24*
4.4.1.1 Considering increasing internal resistance 25
4.4.1.2 Considering increasing impedance 26
4.4.2 Estimating SOH considering capacity *28*
4.4.2.1 20 hour capacity check C_e 28
4.4.2.2 Reserve capacity check $C_{r,e}$ 29

5 CRANKING SYSTEM AND COMBUSTION ENGINE 30

5.1 COMPONENTS CRANKING SYSTEM 30
5.1.1 Battery *30*
5.1.2 Starter *30*
5.1.3 Ignition switch *30*
5.2 COMBUSTION ENGINE 31
5.3 CRANKING VOLTAGE TRACE 32

6 CRANKING VOLTAGE TRACE BASED SOH MONITORING 33

6.1 PROPOSED SOH MONITORING METHOD 33
6.2 PREVIOUS WORK 34
6.2.1 US patent No: 6472875 ..... *34*
6.2.2 US patent No 2009/0326841 ..... *35*

7 MEASURING THE VOLTAGE CRANKING TRACE 36

7.1 MEASURANDS 36
7.1.1 Sampling the cranking voltage trace *36*
7.1.1.1 Aliasing 36
7.1.1.2 Determination of minimum sample rate 37
7.1.1.3 Limiting data size 38
7.2 CONNECTION IN VEHICLE 38
7.2.1 Future implementation in dongle *39*
7.3 MEASURING EQUIPMENT 40
7.3.1 Prototyped measuring equipment *40*
7.3.1.1 Hardware 41
Controller chip 41
Sampling voltage 41
Temperature 42
Timestamp 43
Data storage 43
Audio-visual comunication 43
7.3.1.2 Software 43
Initialization 43
Looping part 44
7.3.2 Backup measuring equipment *45*

8 DATA GENERATION 47

8.1 TEST SETUP 47
8.2 TESTING PROCEDURE 49
8.2.1 Accelerated aging process. 49
8.2.1.1 Accelerated aging method. 49
8.2.2 Test battery pool 51
8.2.3 Testing preparations 52
8.2.3.1 Temperatures 52
8.2.3.2 State of charge 52

9 CVT DATA PROCESSING 53

9.1 TABLE OF LABELS 53
9.1.1 SOH estimators. 53
9.1.2 Upcoming failure indicator. 54
9.1.3 CVT ID. 54
9.2 CVT DATA STORAGE 54
9.3 PEAK, VALLEY AND CRANK ENDING EXTRACTION 56
9.3.1 Determine preliminary crank ending and catch corrupted data 57
9.3.2 Cleaning data 57
9.3.3 Peak selection. 59
9.3.4 Redefine crank ending. 61
9.3.5 Valley selection. 62
9.3.6 Visual check. 62
9.4 FEATURE EXTRACTION. 62
9.4.1 [redacted] *62*
9.4.2 ..... *63*
9.4.3 ..... *63*
9.4.4 ..... *64*
9.4.5 ..... *65*
9.4.6 ..... *65*
9.4.7 ..... *66*
9.4.8 ..... *67*
9.4.9 ..... *67*
9.4.10 ..... *68*
9.5 TABLE OF FEATURES 69

10 DATA ANALYSIS 71

10.1 CLASSIFYING AND PLOTTING. 71
10.2 FEATURE ANALYSIS FROM A DATA PERSPECTIVE 73
10.2.1 Frequency of occurrence 73
10.2.2 Correlation coefficient between features. 74
10.2.3 Standard deviation. 75
10.3 FEATURE ANALYSIS FROM A RELATION PERSPECTIVE 76
10.3.1 Feature correlation with failure indicators 76
10.3.2 Feature value change over the cycle aging classes. 77
10.3.3 Linear regression solving for aging cycle classes 77
10.3.4 Linear regression solving for 3 classes 78
10.3.5 Linear regression SOH indicators 79
Internal resistance 80

Heavy loading capacity . 82
10.3.6 Selected features. *84*
10.4 RELATION ANALYSIS. 85
10.4.1 3d plots . *85*
10.4.2 Plotting pairs of features . *85*
[redacted] 86
87
87
10.5 CHOSEN PAIR OF FEATURES. 88
10.5.1 Motivation considering polarisation effects . *88*
[redacted] . 88
89
10.5.2 Motivation considering battery SOH indicators. *89*
[redacted] 89
89
10.5.3 Motivation considering the cranking system . *90*
[redacted] 90
90
10.5.4 Temperature dependence . *90*
11 CONTINUES STATE OF HEALTH MONITORING AND FAILURE WARNING . 92
11.1 BASELINE . 92
11.2 NORMALIZED CHANGE . 95
12 CONCLUSION & RECOMMENDATION . 98
12.1 CONCLUSION . 98
12.2 RECOMMENDATION . 99
LIST OF FIGURES 100
LIST OF TABLES 103
REFERENCES . 105

1 Introduction

1.1 Background

The electrical system is a vital part of vehicles used in the automotive sector. The electrical system consists of an energy storage device (battery), an energy producing device (alternator) and consumers (lights, starter motor, ECU, electrical power steering, etc.).

One of the main consumers which the battery has to energize is the electric starter-motor while cranking the combustion engine. At this particular mode of operation a substantial amount of energy has to be supplied by the battery. Once the engine has started the battery will act as an energy buffer which is maintained by the alternator. This buffer is required in case of insufficient energy supply by the alternator or to provide extra capacity for powering large loads (electric power steering) for short amount of times.

A healthy battery is of most importance for a proper engine crank. Unhealthy batteries will cause a complete system failure since they are required to initiate system operation i.e. they have to crank the combustion engine. A battery can be compared to a black box i.e. there is no way of seeing on the outside what happens on the inside, which makes it difficult to reveal an unhealthy battery. On top of this, the service life of a battery is strongly depended on operating conditions. With this in mind one can imagine that a battery forms the system's Achilles heel.

1.2 Problem description

As described in the problem background the ANWB is in search of a battery state of health (SOH) monitoring system. On top of this, the system has to be implementable in a vehicle without any alterations to the electrical system. The vehicles taken into consideration all contain an on-board diagnostics port. This port contains direct connections to the positive terminal of the battery and the negative vehicle ground. Utilizing this connections non-invasive electric measurements can be executed. Methods and possibilities have to be investigated relating this measurements to the battery's cranking performance i.e. it's state of health. If this can be accomplished a continues state of health monitoring system can be constructed enabling an upcoming battery failure prediction. A main research question is formulated as stated in section 0.

Research question

How to estimate the state of health of an online battery by use of non-invasive electric measuring methods?

2 The automotive battery

This chapter will describe the type and working principle of batteries applied in the automotive sector. It is important to obtain an understanding of the technology is involved in battery design since this study researches battery failure. Battery technology involves a combination of chemistry, material, mechanical and electrical science. A aggregation of these technologies yields to a small electrical-energy producing device, referred to as a battery.

2.1 Basic structure

Batteries used in the commercial automotive sector produce a potential of approximately 12 volt originating from six 2 volt cells connected in series. The electromotive force of the battery is produced by electro chemical reactions inside these cells. The cells are encapsulated by a plastic container which incorporates two electrical connections forming the battery terminals. A single cell is the smallest repetitive element inside a battery. Understanding the working principle of a single cell explains working principle for the complete battery.

2.2 A single cell

A cell consists of two electronically conducting electrodes which are in contact with an ionically conducting phase, the electrolyte. Transfer reactions occur on the interaction surface between the electrodes and electrolyte. Electrons are interchanged from the electrodes to the ions in the electrolyte and vice versa, these reactions generate electrical current and define the characteristics of the cell. The upper side of the electrodes is not in contact with the electrolyte and act as cell connections. A distinction can be made between the negative electrode (anode) and the positive electrode (cathode). When an electrical load is connected between the electrodes, an electrical circuit is completed, which enables electrons to flow and power the load.

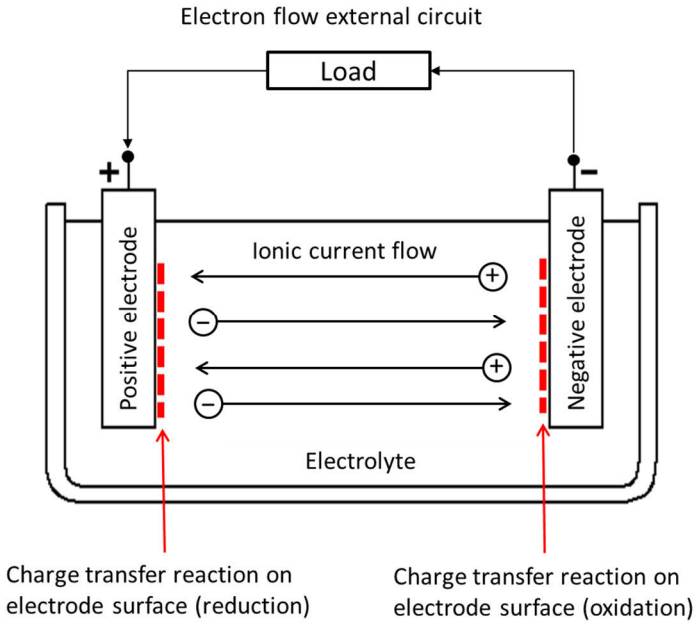

Figure 2-1 : Lead Acid Cell

A distinction can be made between two type of cells, primary and secondary cells. A primary cell can only be discharged once and is not rechargeable. The secondary type is rechargeable. Cells used in automotive batterie are of the secondary type.

2.2.1 Working principle

As described in the previous section a cell contains a fluid electrolyte together with two electrodes. The majority of automotive batteries contain an acidic electrolyte together with lead containing electrodes. For this reason, this type of battery is referred to as the “lead acid” battery. Lead acid batteries are build-up out of lead acid cells. Inside these cells electrochemical reactions take place generating electrical power. Before these reactions can take place, active materials have to be present. The active materials inside a lead acid cell are sulphuric acid (H_2SO_4), lead (Pb) and lead dioxide (PbO_2). Inside a fully charged battery the sulphuric acid is diluted in the electrolyte, the lead is contained by the negative electrode and the lead dioxide is contained by the positive electrode.

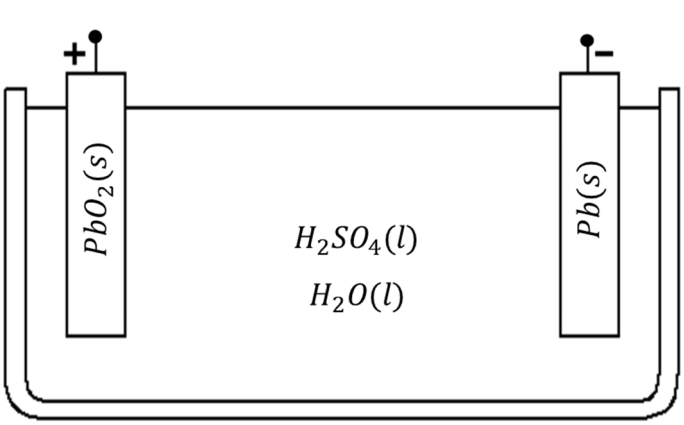

Figure 2-2: Active materials lead in charged lead acid cell

A battery is designed to generate electricity. A lead acid cell generates electricity through a so called double sulphate electro chemical reaction. The active materials on the electrodes react with the sulphuric acid of the electrolyte generating an electrical current. In this process lead sulphate ($PbSO_4$) is produced and deposited on both electrodes. The transfer reactions on discharge are defined by:

Negative electrode reaction:

$$Pb(s) + HSO_4{}^-(aq) \underset{\text{Charge}}{\overset{\text{Discharge}}{\rightleftharpoons}} PbSO_4(s) + H^+(aq) + 2e^-$$

Equation 2-1: Negative electrode reaction

On discharge, lead (Pb) of the negative electrode reacts with hydrogen sulphate ions ($HSO_4{}^-$) of the ionized electrolyte. Reaction products are: lead sulphate ($PbSO_4$) deposited on the negative electrode, hydrogen ions (H^+) left in the electrolyte and electrons (e^-) which are dissipated via the external circuit creating an electrical current. The discharge process of a lead acid cell is depicted in Figure 2-3.

Positive electrode reaction:

$$PbO_2(s) + 3H^+(aq) + HSO_4{}^-(aq) + 2e^- \underset{\text{Charge}}{\overset{\text{Discharge}}{\rightleftharpoons}} PbSO_4(s) + 2H_2O(l)$$

Equation 2-2: Positive electrode reaction

On discharge, lead dioxide (PbO_2) of the positive electrode reacts with hydrogen (H^+) and hydrogen sulphate ions ($HSO_4{}^-$) of the ionized electrolyte. At the same time, electrons (e^-) are delivered by the external circuit. The reaction products are; lead sulphate ($PbSO_4$) deposited on the positive electrode and water (H_2O) left in the electrolyte.

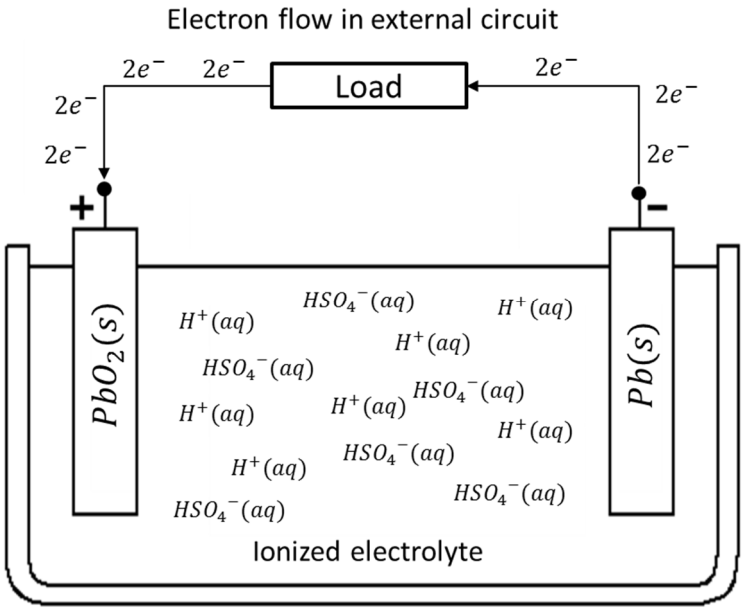

Figure 2-3: Lead acid cell on discharge

Total reaction:

$$PbO_2(s) + Pb(s) + 2H_2SO_4(aq) \underset{\text{Charge}}{\overset{\text{Discharge}}{\rightleftharpoons}} 2PbSO_4(s) + 2H_2O(l)$$

Equation 2-3: Total reaction inside lead acid cell

On discharge reactions on positive and negative electrodes happen simultaneous. Summing those together creates a total reaction in which lead (Pb) and lead dioxide (PbO_2) react with sulfuric acid form the electrolyte. Reaction products are lead sulphate ($PbSO_4$) which is deposited on both electrodes and water (H_2O) left in the electrolyte.

On charge all reactions are reversed. The electron supply from an external power source converts the lead sulphate on both electrodes back to lead (Pb) on the negative electrode and lead dioxide (PbO_2) on the positive electrode while a part of the watery electrolyte is converted back to sulphuric acid (H_2SO_4). As explained in section 2.2, a rechargeable cell is in literature referred to as a cell of the secondary type. A lead acid cell is of the secondary type.

2.2.2 Observations in working cells

A working cell delivers or consumes power i.e. current is flowing through the cell and electro chemical reactions are present. If current flows through a cell a difference in cell potential can be observed. In other words, the voltage of a working cell differs from the open circuit voltage (non-working cell). This is effect is referred to as “polarisation effects”. Polarisation effects have different underlying causes. Another effect in working cells, next to the polarisation effects is electrode surface passivation due to the production of lead sulphate on discharge.

2.2.2.1 Polarisation effects

Three types of polarization effects can be distinguished: activation polarisation, concentration polarisation and resistance polarisation.

Activation polarisation

Theory on reaction kinetics describes an energy barrier which has to be overcome before a reaction starts. Normally thermal energy is used to overcome this barrier, but inside a battery cell the nature of this energy is electrical. Because of this, when starting a reaction, a change in cell potential will be observed. This is referred to as “activation polarisation” .

Concentration polarisation

When current flows through a cell chemical reactions are present. The reactions cause a change in the concentration of reagents (being reduced) and reaction products (being increased). This change in concentration influences the electrode potential. This is referred to as “concentration polarization”

Ohmic polarisation

A cell has a finite electrical resistance. This resistance induces a difference in cell potential when current flows though the cell. This effect is referred to as “ohmic polarisation”.

2.2.2.2 Electrode surface passivation

Another effect in a working cell which is closely related to concentration polarisation is electrode surface passivation. When discharging lead sulphate ($PbSO_4$) is deposited at both electrode surfaces. Lead sulphate is only slightly soluble in the electrolyte and forms a thin layer which obscures both electrodes when discharge progresses. If most of the electrode material is obscured it prevents chemical reactions from taking place. Normally around 50% of the electrodes have to be obscured before a change in voltage is observable. Depending on the amount of current, a certain coverage of the plates will induce a steep voltage drop. This effect can be used to indicate the end of discharge process. As described in section 2.2.1 on charge the lead sulphate is transferred back to lead dioxide on the positive electrode and sulphuric acid dissolved in the electrolyte. In other words, a charging process removes the obscuring layer of lead sulphite.

2.3 From cells to battery

As depicted in Figure 2-4 the electrodes in actual battery design have a metallic supporting gird which holds the active materials place. The grids are made of a lead containing metal alloy fabricated in to a mesh which has the shape of a flat plate. In a complete electrode the active materials are fused together with the supporting grid forming a plate like shape. For this reason, the electrodes inside an actual battery are often referred to as plates. The positive plate is encapsulated by an envelope of separator material. Separator envelops prevent electrical contact between the plates but are porous enough to enable the ion flow through the electrolyte. The grid of the plates acts as a current collector and contains a tab on the upper side to connect plates of the same type together. The plate tabs are welded to a connection bar and are connected in parallel forming a plate set. When positive and negative plates sets are interwoven with each other a plate block or cell is formed. Cells in actual battery design contain more than just the two electrodes (plates). Six cells or plate blocks are connected in series resulting in a total battery potential of approximal 12 volt. At both ends of the series connection pins stick out to realize a connection to the battery terminals. The cells and electrolyte are contained by a propylene container forming the battery casing. The inside of the casing is portioned into six different compartments of equal size containing the cells.

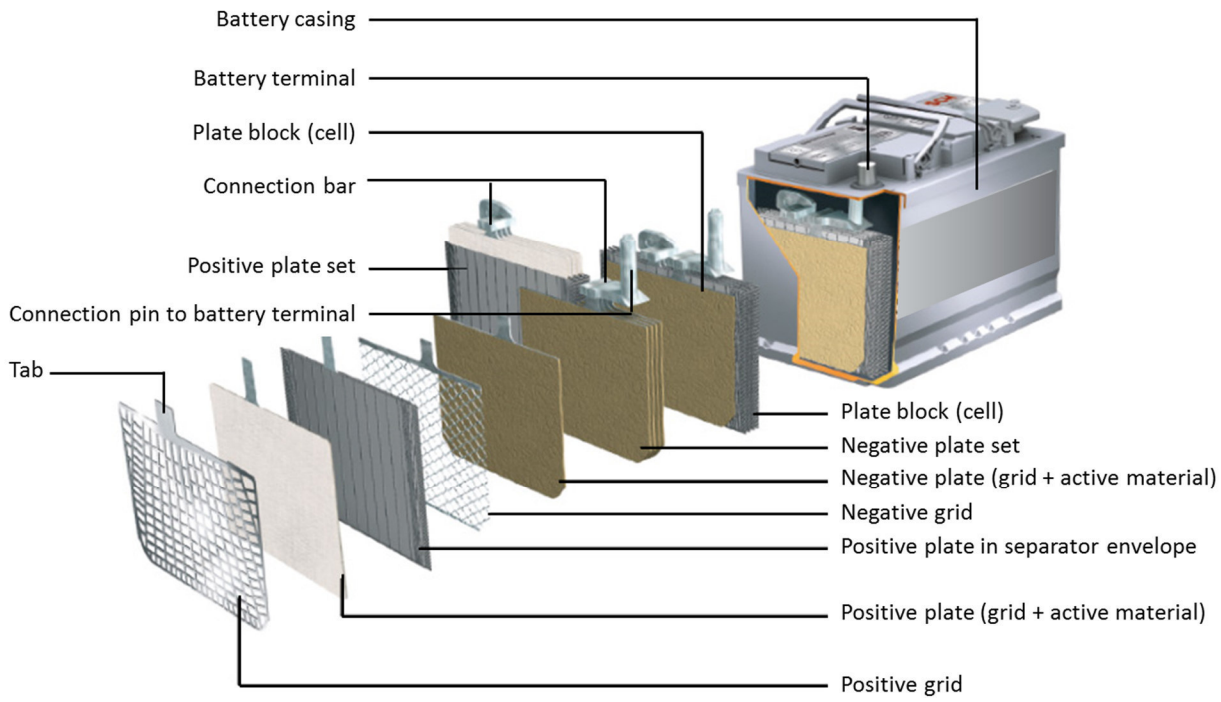

Figure 2-4: Automotive battery design

2.4 Lead acid battery types

Currently two types of lead acid batteries applied are applied for starting application in the commercial automotive sector: the vented wet cell (flooded) and the valve regulated lead acid (VRLA). Both are able to produces a burst of energy for a short periods of time to power heavy loads like a starter-motors. These batteries are referred to as SLI (Staring Lighting Ignition) batteries. There main purpose is powering the starter-motor when cranking the combustion engine. Flooded and VRLA batteries have inferior capabilities in so called “traction applications”. Traction applications require a more gradual energy release over a longer period of time. This study considers SLI batteries only.

2.4.1 Flooded battery

The vented wet cell battery which is also referred to as the flooded battery is the most common used battery type in vehicles without a so called “start-stop system”. A start-stop system stops the combustion engine of the vehicle to prevent fuel consumption when idling at standstill. The engine is restarted quickly when movement of the vehicle is required. Nowadays most vehicles still haven’t got such a system but the marked is shifting towards an increased implementation of this system.

A flooded battery borrows its name from submerged plates/electrodes inside the battery. Ventilation ports and removable caps are mounted on top of the battery casing. The ventilation ports release gasses which emerge from working cells and the caps can be removed to maintain the electrolyte level. This creates an easy maintainable battery, but it has to be placed in a well vented area and can only be placed in the upright position. In comparison to other type of lead acid batteries, flooded batteries have better resistance against high operating temperatures (in excess of 32°C). This creates an advantage when the battery has to be mounted under the bonnet in the vicinity of a warm combustion engine. A disadvantage of the flooded battery design is a higher self-discharge rate in comparison to the VRLA batteries (discussed in the next section). Furthermore, they have a long history of use which shows their robustness and reliability.

2.4.2 Valve regulated batteries

Two types of valve regulated lead acid (VRLA) batteries are applied as SLI battery: the absorbed glass matt (AGM) and the enhanced flooded battery (EFB). Both make use of the same principles. In VRLA batteries the liquid electrolyte is absorbed by a carrier material. Since all fluid electrolyte is absorbed unconventional (not upright) mounting positions are made possible using this battery design. The carrier material in AGM type of batteries consists of fine woven fibre glass matt and in EFB batteries of lose fibres. As described in the previous section, conventional flooded batteries are fitted with a ventilation port to vent produced gasses to the outside world. VRLA batteries work different, they have no ventilation port and are designed to have minimal gas production. In case of gas production, small open connections between the positive and negative plates allow oxygen and hydrogen to recombine. No ventilation to the outside world is needed anymore. In case of excessive gas production, a one-way valve is incorporated into the battery design and acts as a safety valve to release excessive pressure.

VRLA batteries have a lower internal resistance in comparison to flooded batteries, this is an advantage for high power delivery. A disadvantage is the sensitivity to higher operating temperatures. Operating a VRLA battery at under bonnet temperatures will decrease service life significantly in comparison to the flooded battery.

The flooded battery designs is still the most common battery design, therefore this study will focus on flooded battery design only.

3 Battery performance

This study focuses on a method to estimate battery state of health i.e. a decrease in battery performance. The performance of automotive lead acid batteries is expressed in capacity and peak power delivery. New batteries are rated on a specific capacity and peak power delivery. To estimate the effective performance regulations describe different checks on capacity and peak power delivery.

3.1 Battery related variables

To make estimations on capacity and peak power delivery, battery related variables have to be measured. Four important variables are described in this section.

3.1.1 Voltage

The battery voltage is the difference in potential between the two battery terminals. There is a difference between the open circuit voltage (OCV) and the closed circuit voltage (CCV). A typical value of the OCV for an automotive battery is 12,6 Volt. Due to polarization effects the CCV defers from the OCV, as explained in section 2.2.2.1. The SI unit for voltage is Volt [V] and is used in this study to express the voltage.

3.1.2 Current

Current is a flow of electrical charge carriers. In an electrical system these carriers consist of electrons flowing through the electrical circuit. Inside a battery ions flowing in the electrolyte carry and transport the electrons between the battery terminals. The SI unit for electric current is Amperes [A] and is used in this study to express the amperage.

3.1.3 Temperature

Battery temperature is referring to the lumped temperature of the battery. As described in section 4.3 high average operating temperatures have a negative influence on battery service life. On the other hand low battery temperatures have a negative influence on cranking performance. For this reason temperature is an important variable to consider for this study. The SI unit for temperature is Kelvin [K]. In this study the temperatures will be expressed degrees Celsius [°C].

3.1.4 Weight

A battery has a certain weight. Over service life flooded batteries tend to lose some of their electrolyte and therefore show a loss of weight. The SI unit for weight is kilo gram [kg] and will be used in this study to express the weight.

3.2 Ratings

As explained in the introduction of this chapter new batteries are rated on capacity and peak power delivery. Using battery terminology peak power delivery is referred to as cold cranking amps (CCA) since cranking is demanding a peak power delivery of the battery. Capacity and CCA are strongly dependent on rate of discharge and temperature, therefore batteries are rated using a specific regulated process describing temperature and discharge rate. For a better understanding both capacity and CCA are explained in more detail.

3.2.1 Capacity

A battery is able to store a certain amount of electrical energy (charge). The amount of charge a battery is able store is referred to as the capacity of the battery. The capacity of the battery is non-linear and depends on the rate of discharge as depicted in Figure 3-1.

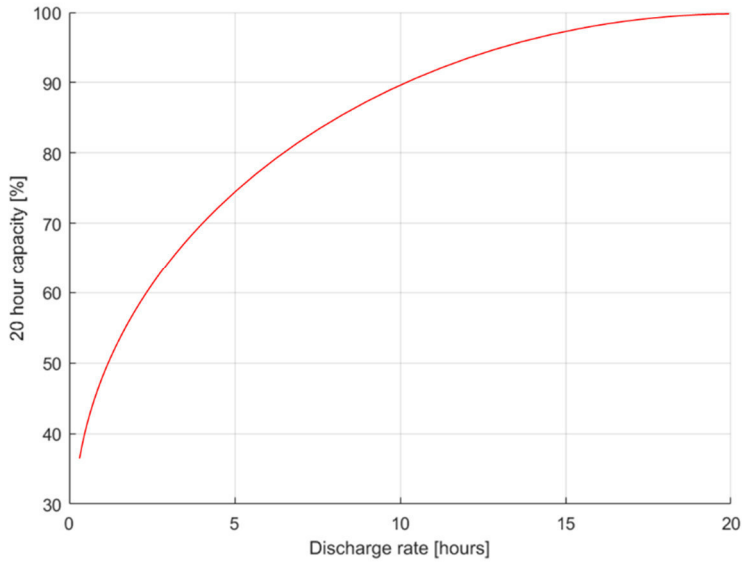

Figure 3-1: 20 hr capacity vs discharge rate at 25°C [1]

The capacity is expressed in Ampere hours. Because of the non-linearity the capacity rating of a battery is related to a discharge rate. The standard capacity rating used for automotive batteries is the 20 hr capacity or in short C_{20}. The C_{20} rating is expressed as the product of the amount of current a battery is able supply for 20 hours at 25 °C multiplied by 20 hours. This means a 50 Ah battery at 25 °C is able to deliver 2.5 A for 20 hours. A battery is rated by the manufacturer when it is new. To check what is left of the rated capacity a C_{20}-check has to be performed which is described in section 4.4.2.1.

A typical C_{20} value for small automotive batteries is 50 Ah. As depicted in Figure 3-1 the C_{20} drops significant if the discharge rate is increased. In high discharge rates the reaction rate of chemical processes becomes a limiting factor resulting in a lower capacity. The higher the discharge rate the lower the capacity. Peukert's law describes the relation between discharge rate and capacity.

$$I^n t = C$$

Equation 3-1: Peukert's law [1]

Where I is the discharge current, t the discharge time and n,C are constants varying with battery model.

n and C can be used to predict the capacity at different discharge rates, which is quite accurate for a large range of discharge rates. However, Peukert becomes inaccurate for high discharge rates. This is related to concentration polarization effects during high rates of discharge.

The capacity is not only depending discharge rate but also on the temperature. Figure 3-2 depicts the dependence of the C_{20} capacity on temperature.

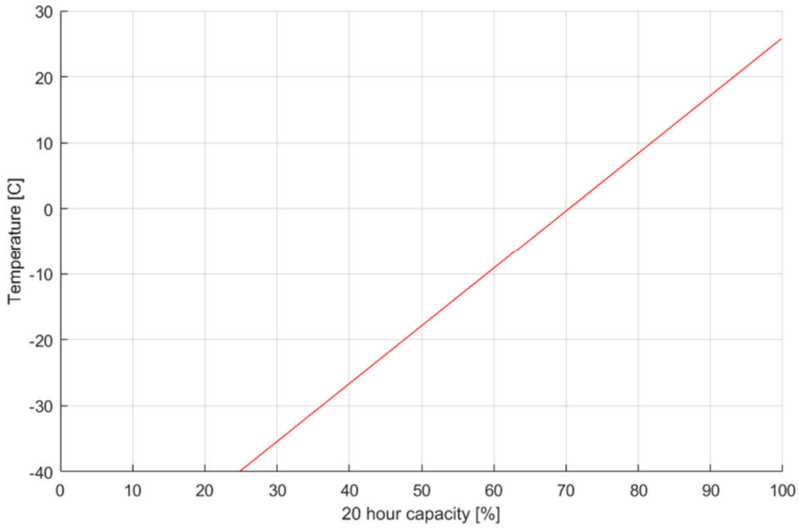

Figure 3-2: Temperature dependence [1]

3.2.2 Cold Cranking Amps

When cranking a combustion engine the battery has to supply currents in excess of 400 A for a short periods of time. This equals high discharge rates in which Peukert's law becomes inaccurate. The C_{20} rating is not suitable for rating this kind of peak performance another type of rating has to be used. This rating is referred to as the cold cranking amps (CCA). Every automotive battery is rated using the C_{20} and CCA ratings.

Globally different standards are used for determining the CCA. Table 3-1 describes four commonly used standards. A typical CCA value for a small automotive battery is around 400 (EN) and for a larger ones 700 (EN). The designation EN is used to indicate which standard is used.

EN CCA Test	SAE CCA Test	IEC CCA Test	DIN CCA Test
Cool down fully charged battery to - 18°C for 24 hours. While at subfreezing temperature, apply a discharge current equal to the specified CCA). To pass the test successfully, the voltage must stay above 7.5 for 10 seconds.	Cool down fully charged battery to - 18°C for 24 hours. While at subfreezing temperature, apply a discharge current equal to the specified CCA). To pass the test successfully, the voltage must stay above 7.2V for 30 seconds.	Cool down fully charged battery to - 18°C for 24 hours. While at subfreezing temperature, apply a discharge current equal to the specified CCA). To pass the test successfully, the voltage must stay above 8.4V for 60 seconds.	Cool down fully charged battery to - 18°C for 24 hours. While at subfreezing temperature, apply a discharge current equal to the specified CCA). To pass the test successfully, the voltage must stay above 9V for 30s and 6V for 150s.

Table 3-1: CCA test standards

3.3 Battery states

In battery analysis two states are very important, the state of charge and the state of health. These two are different from each other but are often misinterpret and misused. This section describes this

states and makes a clear distinction between them. A battery is like a black box, there is no way of knowing what happens on the inside by looking at the outside. Therefore state is estimation based on variables which can be measured on the outside of the battery like voltage and current.

3.3.1 State of charge

The state of charge (SOC) describes the amount of energy left in a battery. The energy level is compared with a reference and expressed in a percentage. Often this reference is the C_{20} as determined by the manufacturer. In some cases the reference for the SOC is the present capacity instead of the rated. This can lead to unreliable estimations because the capacity is gradually decreasing with battery age.

3.3.1.1 Estimating the state of charge

Different methods are used to determine the state of charge of a battery. The most common ones are described. Each of them has its own benefits and drawbacks.

Open circuit voltage measurement

Open circuit voltage measurements can be used for determining the state of charge. Unfortunately electro chemical processes inside the battery have an influence on the OCV and take long time to settle. For accurate SOC estimations using the OVC a 24 hours settling time is required after last battery use.

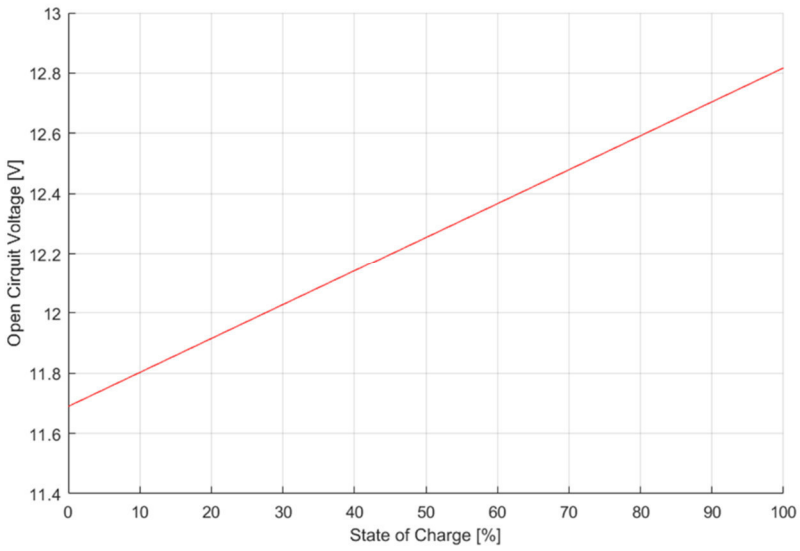

Figure 3-3: State of charge versus OCV [1]

A battery mounted inside a vehicle is always connected to some power consuming systems, even when the ignition is turned off. Real OCV does not exist, but is approximated with ignition off. Some of the electrical systems will continue to consume minimal power which has an advantage on the settling time of the voltage. Tests are showing an average settling time of 30 minutes which is quicker than the 24 hours required in real open circuit voltage applications. This on-board settling voltage (OSV) can be used for an on-board SOC estimation, but has to be corrected for temperature.

Batteries with other chemical compositions, like lithium-ion, often show a relative flat curve with only a steep drop at the end indicating capacity depletion, making an OCV based state of charge estimation difficult.

A difficulty in using the OCV for SOC estimation comes with connecting a measuring device to the battery terminals which creates a closed circuit and annuls the open circuit voltage. Nevertheless the OCV method has proven to be accurate enough for most practical systems provided a suitable settling time is used.

Coulomb counting

This method involves a sensor which measures the positive and negative current flow at one of the battery terminals. The current flow is integrated over time and the net-difference can be used for a SOC indication. A problem with this method is the determination of the starting point of integration i.e. how much charge did the battery contain at beginning of integration?

Another difficulty is the coulombic efficiency of the battery. The coulombic efficiency describes the losses during charge and discharge. For this reason a battery will deliver less charge than was put into it during the charging procces. The coulombic efficiency of the battery depends on battery age, temperature, rate of charge/discharge and SOC which we wanted to determine in the first place. As one can imagine there are accuracy problems using this method and a simple integration has proven to be unreliable. To improve this method a reset of the integration process is needed and the coulombic efficiency has to be taken into account. In some systems the integration process is reset by determining the SOC using the OCV method after a suitable settling time

Specific gravity

Measuring the specific gravity of the electrolyte can be used for reliable SOC estimations. The weight of active chemicals in the electrolyte is changing with the SOC of the battery. During discharge, the electrolyte composition changes. As describes in section 2.2.1 on discharge the sulphuric acid content is reducing leaving a more watery electrolyte with a changed specific gravity. As depicted in Figure 3-4 the specific gravity can be determined by use of a hydrometers which often are scaled directly to the state of charge. In case of a flooded battery design, the electrolyte is extractable via the caps on top of the battery casing. This method does not apply to VRLA type of batteries, since the do not contain a fluid electrolyte.

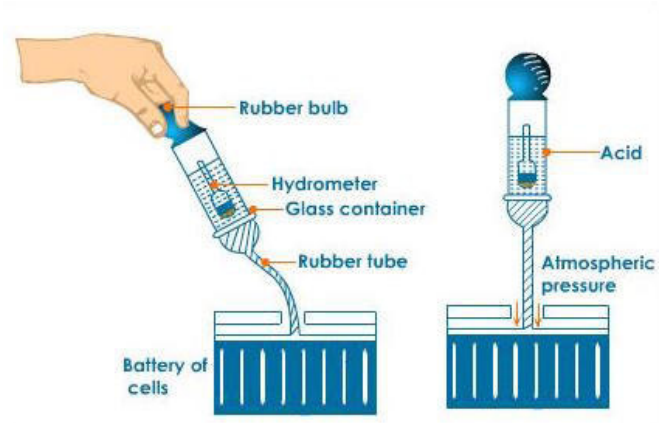

Figure 3-4: Battery hydrometer

Using hydrometers for SOC estimation is slow and can be inconvenient when a battery is placed in a vehicle. To overcome this drawbacks electrical sensors can be placed inside the battery for specific gravity measurements. However in automotive applications this is not a common solution. Sensors are expensive and susceptible to pollution resulting from chemical process. High costs and sensor errors have discouraged a widespread implementation of this method.

3.3.2 State of health

If a battery suffers from a permanent loss in performance it's so called state of health (SOH) has decreased. When discriminating on performance it is very important to have an understanding of the intended battery use. For example when powering a small load the effective C_{20} capacity is a suitable SOH indicator, but for cracking applications the effective CCA is far better one. For this study, the prime task of the battery is to deliver sufficient power for a successful engine crank. This is the reason most of today's automotive battery testing devices correlate SOH of the battery directly to the effective CCA and discard capacity checks. A combination of different failure mechanisms as described in chapter 4 will lead to a gradual decrease in battery state of health. These failure mechanisms all happen inside of the battery and are not observable from the outside. For this reason non-destructive SOH determination can be quite a challenge. For a proper SOH estimation the battery has to be and its internal components have to be examined to determine the progress of the existing failure mechanisms. This is a destructive and invasive method to determine the real SOH of a battery. Non-destructive methods are less accurate and always based estimations coming from common failure indicators measurable on the outside of the battery. Section **Error! Reference source not found.** describes two failure indicators which are usable for SOH estimations.

4 Battery failure

This chapter discusses battery failure. Battery failure manifest itself in different ways referred to as failure modes. Failing components have different underlying failure mechanisms describing the processes responsible for failure. In most cases progressing the failure mechanisms cannot be monitored without tearing the components apart and therefore destroying it. A battery is an example is such a component. For this type of components SOH estimators have to be used. Using SOH estimators the progress of the failure mechanisms can be estimated without destroying the battery. Most failures are caused by a combination of different failure mechanisms .Using a SOH estimator groups all contributing mechanisms together, making a distinction between the responsible failure mechanisms impossible.

4.1 Failure modes

Failure modes describe the manner in which the failure in failing components is represented. Batteries have different failure modes leading to an inability to crank a combustion engine. A Survey conducted on 3000 scrapped passenger vehicle batteries in the USA presented an overview of 6 common failure modes as depicted in Figure 4-1.

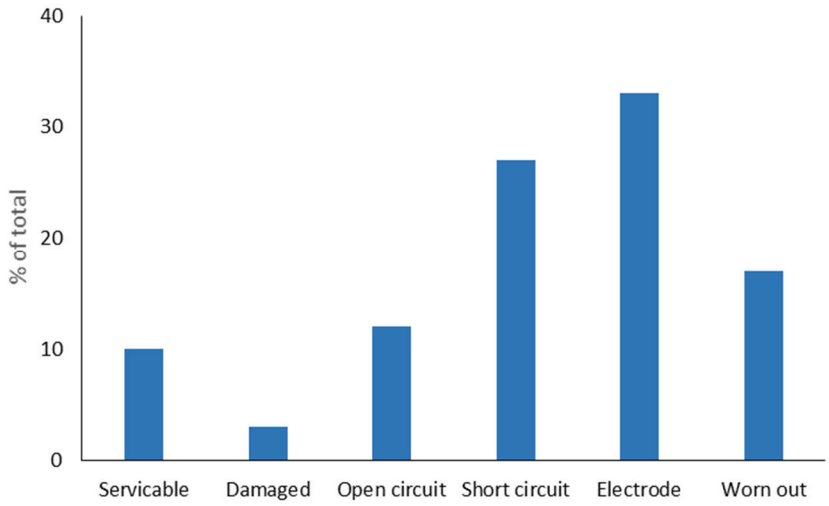

Figure 4-1: Most common failure modes [1]

4.1.1 Serviceable

This is a reversible failure mode. Insufficient SOC is resulting in a depleted battery unable to crank a combustion engine. A simple recharge would be the remedy in this kind of failures. Nevertheless it is one common failure mode, which has to be considered before scrapping a battery. This failure mode is predictable by monitoring the SOC.

4.1.2 Damaged

This is a irreversible failure mode caused by physical means like a car-accidents. It is a very abrupt failure mode evoking instantaneous failure mechanisms like loss of electrolyte due to a broken battery casing. This failure mode is hard to predict, but is in most cases observable on the outside of the battery enabling a conclusion on the leading failure mechanism.

4.1.3 Open circuit

This is an irreversible failure mode is caused by loss of conductivity inside the battery and is hard to predict by used of a failure indicator.

4.1.4 Short circuit

This is an irreversible failure mode is caused by a short circuit between one of the battery's internal components. In most cases the plate pack of a single cell is shorted together. The shorted cell is still conducting but not producing any cell potential. For this reason this failure mode often can be detected by a permeant loss of battery potential equal to the cell potential. This failure mode is hard to predict.

4.1.5 Pate/Grid

This failure mode is caused by deformation of the lead plates/grid. Often this failure mode is triggered by off-design use of battery like extreme temperatures.

4.1.6 Worn out/Abused

Eventually a battery will wear out due to active material being shed from the plates and loss of conduciveness in plate and grid material. This will cause a permanent reduction of capacity and increase in internal resistance.

Failures related to damage, open circuit, short circuit and manufacturing flaws often happen instantaneously and are hard to predict. However, failures which have a serviceable, off-design use and worn out nature can be predicted. The latter failure modes are the most important one for this study.

4.2 Failure mechanisms

When searching the internet on battery failure the term "sulphation" frequently pops up. The term sulphation is adopted by the general public as one common failure cause (mechanism) considering lead acid batteries. However, in specialized textbooks the term "sulphation" is deliberately avoided. In reality sulphation is a natural occurring process inside a lead acid battery and failure is not depending on one failure mechanism alone. Often a combination of different failure mechanisms will cause a battery to fail. Table 4-1 lists the most common failure mechanisms providing an indication of failure mechanisms contributing to battery failure. The failure mechanisms described are applicable to the flooded battery design, failures mechanisms of VRLA type of batteries are outside the scope of this study.

Failure mechanisms
Loss of electrolyte
Electrolyte stratification
Cathode grid corrosion
Positive electrode active material softening and shedding
Electrolyte contamination
Formation of sulphate with crystalline structure
Inter-cell shorting
Inter-cell open circuit

Table 4-1: Failure mechanisms

4.2.1 Loss of electrolyte

When charging a battery gas will be produced resulting from an electrolyze process slowly reducing the amount of electrolyte. This loss reduces the contact area between the electrolyte and the electrode plates. The effective area supporting the electro chemical reactions is reduced leading to a decrease in capacity and peak power delivery. This failure mechanism only exists in flooded batteries since they contain a liquid electrolyte. By adding distilled water this failure mechanism is reversible. Adding water is only possible with flooded battery design. Valve regulated type of batteries do not have the possibility of adding water, but this type of battery has a very low gas production which makes adding water unnecessary. In warmer climates, this failure mode is more relevant since gas production is accelerated by higher temperatures.

4.2.2 Electrolyte stratification

As described in section 2.2.1 during charge one of the reaction products is sulfuric acid (H_2SO_4). Sulfuric acid is contained by the electrolyte, but has a higher specific gravity then water. This causes it to flow down and collect at the bottom of the battery. Therefore, the top of the battery will contain less acid, reducing the active materials in this area. During discharge the sulfuric acid is turned back into water by combining it with lead sulphate ($PbSO_4$). Lead sulphate is a solid material which stick on the electrodes and needs an acidic environment to recombine during charge. When all acidic electrolyte is contained at bottom layers (stratification effect) of the battery the top part of the electrode plates is no longer able to take part of the electro chemical process during discharge. This leads to a loss of capacity which is referred to as electrolyte stratification. Another explanation for the word stratification is layer-shaped, in this case referring to the different layers of acidic material contained by the electrolyte. To counteract the effect of stratification the electrolyte should be mixed. Mixing is accomplished by a gaseous reaction during charge. The generated gas bubbles stir the electrolyte resulting in a better distribution of the sulfuric acid trough the electrolyte. Due to the mixing stratification is a reversible effect, but maintaining a stratified electrolyte for too long will encourage two other failure mechanisms grid corrosion and hard sulphation. As one can imagine stratification is only prominent in flooded battery design. Leaving a discharged flooded battery un attended for too will lead to stratification. In valve regulated battery design stratification effects are minimal since the electrolyte is contained by an absorption material preventing the sulfuric acid from sinking to the bottom

4.2.3 Cathode grid corrosion

The metallic lead of the cathode grid is slowly corroding away. As described in section 2.2.1 the grid holds lead dioxide PbO_2 as active material. When charging a discharged battery lead dioxide is deposited on the metallic lead of the positive grid. In other words, the top layer of the metallic grid is corroded forming the lead dioxide. From this we can conclude that positive grid corrosion is a natural occurring process in every lead acid type of battery. Because of this process the electrical conductivity and mechanical strength of the plates will gradually decline eventually leading to battery failure. This failure mechanism causes the batteries have a finite life, since the grids will disappear by natural corrosion.

It is an irreversible fault and all measures must be taken minimize the rate of corrosion. Batteries failing from this mechanism often have reached their natural and designed service live. If the

electrolyte acidity decreases the battery becomes more susceptible for this failure mechanism. In other words, a battery from which it's charge is maintained regularly has a longer life expectancy.

4.2.4 Positive electrode active material softening and shedding

In theory, the positive plates of a discharged battery contain lead sulphate a active material while the electrolyte contains only water. As described in section xxx during charging this lead sulphate is converted into lead oxide. Lead sulphate has a larger molar volume than lead dioxide meaning with each cycle of the battery the plates will grow on discharge and shrink on charge. Because of this with each cycle the mechanical strength of the active material is weakening and active material is shedded from the plates. Eventually this will lead to a permanent loss of capacity. Positive plates are normally encapsulated by a porous envelope which serves as separator, but also captures this shedded material. Deep discharges will accelerate the process and cause a premature loss of capacity, maintaining the charge of the battery will prevent a premature loss of capacity. This is a irreversible failure mechanism.

4.2.5 Electrolyte contamination

This failure mechanism is user related. As described in section xx flooded batteries are susceptible for electrolyte losses which can be reversed by adding distilled water to top up the electrolyte level. However experience has shown that the water added by the user often is contaminated. The contaminated water still contains minerals which accelerate the self-discharge of the battery. This self-discharge rate can grow to such a level that the battery is unable to accept any charge at all.

4.2.6 Formation of sulphate with crystalline structure

This is one of the most discussed but also misinterpreted failure mechanisms. The general public uses the term sulfation as a common denominator for battery failing including all failure mechanisms. For this failure mechanism the term sulfation could be applicable if we give it the meaning of a sulphate formation procces. As described in section 2.2.1 the formation of sulphate is a naturally occurring procces inside lead acid type batteries. On discharge lead and lead dioxide on the positive electrodes reacts with the sulphuric acid inside the electrolyte. The reaction product is a finely divided form of lead sulphate (…) with an amorous structure. Due to the amorphous structure of the lead sulphate, it is able to converted back to lead, lead dioxide and sulphuric acid on charge. As described this is the natural occurring reaction returning the battery to its former state. But if a battery is discharge deeply and is not recharged soon after, the amorphous structure of the lead sulphate tents to convert to a crystalline structure. In other words when leaving a battery discharged of a longer period of time, lead sulphate will start to form. The difference between an amorphous and crystalline structure are depicted in Figure 4-2.

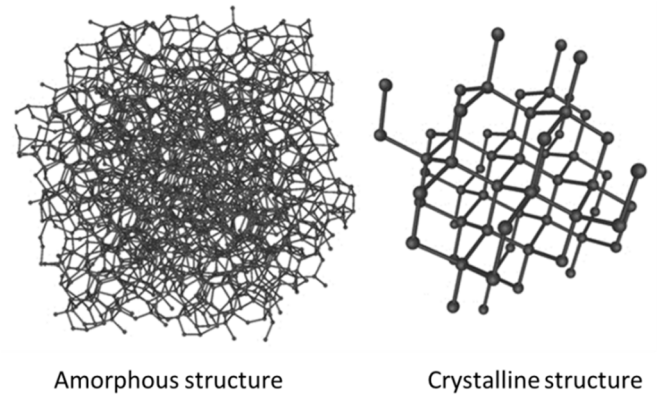

Figure 4-2: Amorphous & crystalline structures

Lead sulphate with a crystalline structure is non-conductive and insoluble. The crystalline mass will become passive and will not take part in further electrochemical activity leading to a loss of capacity. Over time the crystalline lead sulphate tends to form surface layer which coats the plates leading to a significant increase in internal resistance and lower CCA values. This failure mechanism is considered to be irreversible however the effect equalization charging is still debated as a possible solution. Equalization charging means charging at abnormal high voltages. One beliefs charging with this high voltages will convert the crystalline lead sulphate back to sulphuric acid which can be partially thru. Some crystals will be converted back but due to vigorous gassing, which occurs at high charge voltages, the crystalline coating is physically shedded from the plate surface by the gas bubbles. A fresh plate surface is exposed as a result of this leading to better battery performance. Sill active material is lost and the crystalline lead is not converted back but is collected at the bottom of the battery or plate encapsulation.

4.2.7 Inter-cell shorting

A short means a direct electrical connection is established between the positive and negative plates in of a cell. Often this is caused by shedded active material which pushes against plate packaging and separator material evoking an electrical connection. This is an irreversible failure mechanism.

4.2.8 Inter-cell open circuit

Open circuit means the electrical connection is lost. A metallic bars connect the cell plates and cells itself together. The cells are welded to this bar. In some cases this welds will become loose creating an open circuit. This failure mechanism is irreversible, but is not very common.

4.3 Aging service life

A combination of different failure mechanisms as described this chapter will lead to a gradual decrease in battery SOH and cranking performance until end of service life is reached. The average operating temperature has a major influence on battery service life. Increased temperatures will advance most failure mechanisms and lead to premature battery failure. For example batteries in the Netherlands have an service life expectancy of 8 years and in a country with a warmer climate like Australia the life expanse is 5 years. To avoid premature battery failure it is of most importance to operate the battery in its designed temperature range. Figure 4-3 depicts the service life temperature dependence.

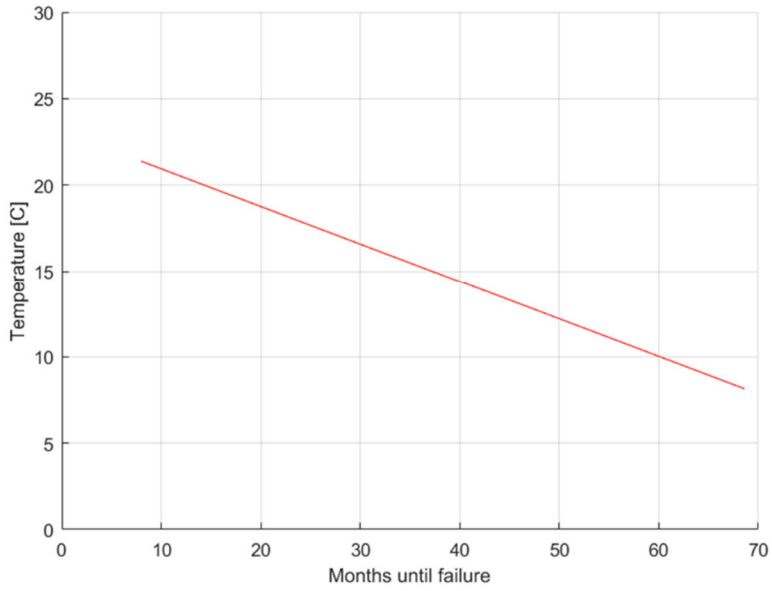

Figure 4-3: Operating temperature vs service life [1]

Next to temperature the operational profile has a major influence on battery service life. Batteries which are charged insufficiently due to short trips are more susceptible to failure mechanisms related to corrosion and stratification. Deep discharge/charge cycles will advance the failure mechanisms related to shedding of active materials.

4.4 SOH estimators

SOH estimators can be used to estimate the battery's SOH and predict upcoming cranking failure. Two non-invasive SOH estimators will be used in this study: the impedance/resistance and effective capacity.

4.4.1 Estimating SOH considering impedance and resistance

Both impedance and resistance can be used as a SOH estimator. In the following two sections this will be discussed, but for a better understanding first a short description is given to clarify the difference between impedance and resistance. A battery is a reactive component, meaning next to the conventional resistance there exists a frequency dependent resistance. This frequency dependent resistance is referred to as the reactance. Impedance a combination of reactance and ohmic resistance. Examples of purely reactive components are a coils and a capacitors. The parallel plates inside a battery show capacitive behaviour therefor a capacitor will be used to explain a reactive component. A resistor is a good example of a purely resistive component. An analogy for the ohmic resistance inside a battery is for example the resistance of the bars connecting the plates as depicted in Figure 2-4.

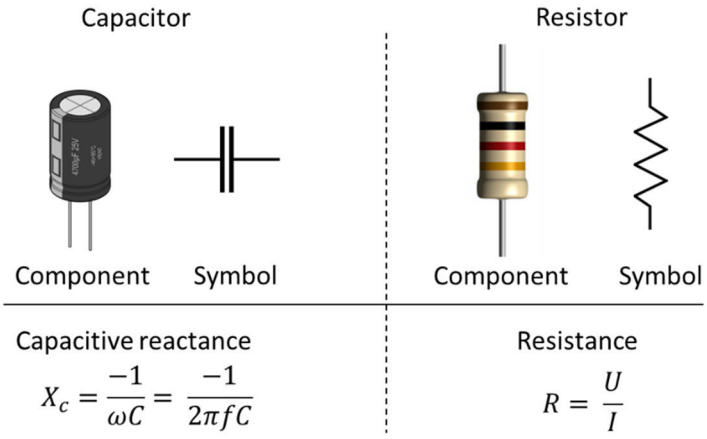

Figure 4-4: Capacitor and Resistor

As can be seen form the equations the capacitive reactance X_c is a frequency dependent component and resistance R is independent of frequency. Both quantities are expressed in ohms indicating a resistance. Impedance can be represented as a complex quantity. Where the real part of the impedance is the resistance R and the imagionary part the reactance X.

$$Z = R + iX$$

Equation 4-1: Impedance (Cartesian form)

4.4.1.1 Considering increasing internal resistance

The internal resistance of the battery can be correlated to the cranking performance. When determining the internal resistance, one should be aware of al resistive components contributing to the total resistance of the battery. However a battery is a reactive component, meaning next to ohmic resistance is carries also reactance. To avoid any confusions between reactance and resistance the resistance will be referred to as ohmic resistance.

One has to keep in mind that when using ohmic resistance for SOH estimation, reactance is neglected which can lead to less accurate SOH inductions. Nevertheless the looking at internal resistance of a battery is the most common method for a SOH estimation and has proven to be reliable enough for automotive applications.

The total internal resistance of a battery can be explained by looking at the equivalent circuit of a single cell as depicted in Figure 4-5.

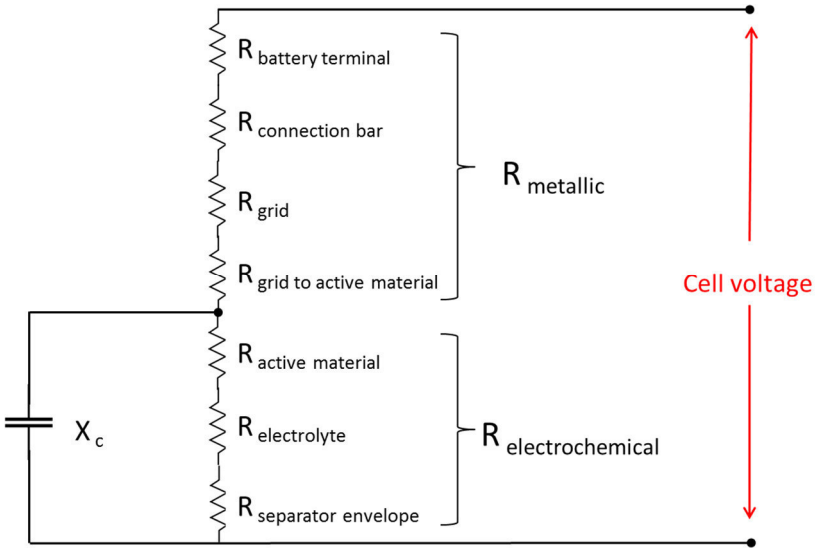

Figure 4-5: Equivalent circuit single cell

As depicted in Figure 4-5, the ohmic resistance can be split into a metallic and an electrochemical path. This ohmic resistance is lives inside the battery therefore also referred to as internal resistance. The capacitor X_c is a reactive component and resembles parallel plates with a dielectric (separator) in between them.

The influence of internal resistance on starting performance is substantial. Due to large currents when starting the internal ohmic resistance will dissipate power and drop the voltage. Electrical power is a function voltage $U$and current I lower voltages of the battery will result in less power deliver to the cranking process.

$$P = U \cdot I$$

Equation 4-2: Electrical power

For this study SOH is related to the cranking performance of the battery. Observing the internal resistance can be a suitable SOH estimator considering cranking performance.

4.4.1.2 Considering increasing impedance

As explained in the previous section a battery is a reactive component which has an impedance. A battery's impedance can be determined by determined by injecting voltage waves into the battery while measure its response, which is a current wave.

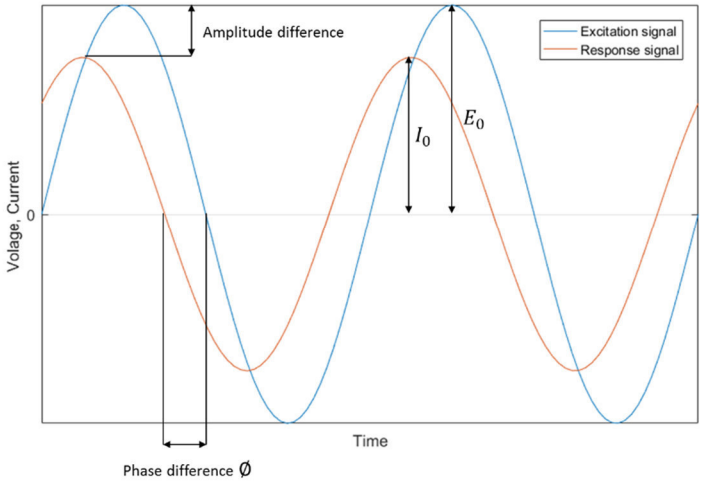

Figure 4-6: Voltage & current waveforms

As depicted the waves reveal a amplitude and phase differences. This can be used to calculate the impedance.

$$\text{Excitation signal: } E(t) = E_0 \sin(\omega t)$$

$$\text{Response signal : } I(t) = I_0 \sin(\omega t + \emptyset)$$

$$\text{Impedance: } Z = \frac{E(t)}{I(t)} = \frac{E_0 \sin(\omega t)}{I_0 \sin(\omega t + \emptyset)} = Z_0 \frac{\sin(\omega t)}{\sin(\omega t + \emptyset)}$$

Equation 4-3: Impedance

Analysing impedance values for a spectrum of frequencies is called “Electro Impedance Spectroscopy” (EIS). Plotting the impedance values of a battery for different excitation frequencies impedance spectrum as depicted in Figure 4-7. Since a battery shows capacitive behaviour, it is common practice to use a negative complex horizontal axis.

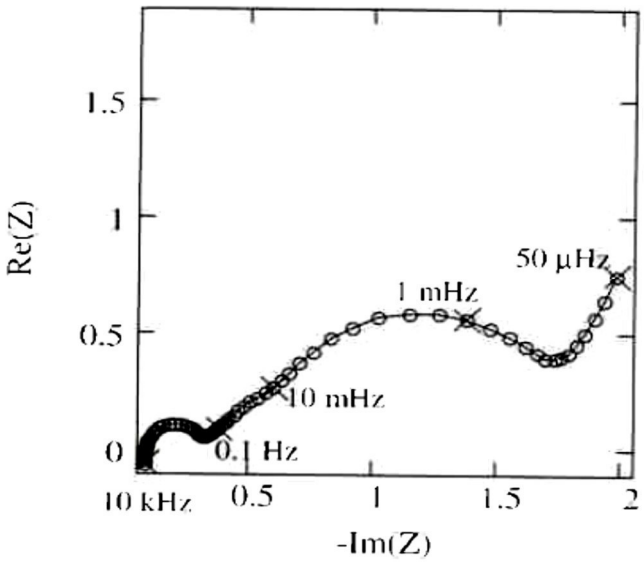

Figure 4-7: Impedance spectrum of a lead acid battery [5]

Analysis of this spectrum can lead to a very accurate SOH estimations. However there are drawbacks to this method. A completed EIS measurement is time consuming and is very sensitive to noise. For a reliable EIS analysis all chemical processes inside the battery have to come to a complete stop which is also time consuming. For reliable measurements the battery has to be completely disconnected from the system, which makes online (in vehicle) testing impossible. The measurement equipment must be in direct connection with the battery terminals otherwise cable length and shape will have an effect on the measured impedance. On top of this the measurement equipment is expansive and bulky.

As one can imagine EIS analysis is not a feasible solution for an non-invasive SOH monitoring method which we are investigating in this study.

4.4.2 Estimating SOH considering capacity

As described in the previous sections an increasing in internal resistance or impedance can be used as a SOH indicator. However measurements based on internal resistance or impedance alone do not reveal the capacity of the battery. A decrease in capacity can be an important SOH estimator which exists next to the resistance and impedance. As described in section 3.2.1a battery is a shows non-linear capacity behaviour which is depended on the discharge rate. As explained a battery is rated on its 20 hour capacity. The effective capacity can be used as a failure indicator. But the 20 hour capacity has not got a strong correlation to the batteries cranking performance due to the non-linearity of the capacity as depicted in Figure 3-1. Regulations also describe reserve capacity check which involves a higher discharge rate compared to the 20 hour capacity check. The reserve capacity test has a stronger correlation to the batteries cracking performance. Next to the capacity checks, regulations also describe a cranking performance test as explained in section 3.2.2. The two capacity checks forming next paragraphs are directly copied in from the regulations with some minor adjustments to make it more readable. The complete regulations can be referenced in appendix xxx.

4.4.2.1 20 hour capacity check C_e

Throughout the duration of the tests, the battery shall be placed in a water bath maintained at a temperature of 25 °C ± 2 °C. The terminal base of the battery shall be at least 15 mm but not more than 25 mm above the level of the water. If several batteries are in the same water bath then the distance between them and also the distance to the walls of the bath shall be at least 25 mm.

The battery shall be discharged with the current I_n kept constant at ± 2 % of the nominal value until the terminal voltage falls to 10,50 V ± 0,05 V.

$$I_n = \frac{C_n}{20}\ [A]$$

Equation 4-4: Nominal discharge current for C_{20} check

Where C_n is the nominal (rated) capacity as defined by the manufacturer. The duration t of this discharge shall be recorded and is expressed in hours. The beginning of the discharge shall take place within a period of 1 to 5 hour from the time of the end of charging.

The effective capacity C_e is defined by:

$$C_e = t \cdot I_n \, [Ah]$$

Equation 4-5: Effective capacity

4.4.2.2 Reserve capacity check $C_{r,e}$

The battery shall be placed in a water bath according to the 20 hour capacity check as described in the section before.

Within a 1 to 5 hour period after the end of charging the battery shall be discharged with a current of 25 A ± 1 % until the terminal voltage falls to 10,50 V ± 0,05 V. The duration t of the discharge shall be recorded and is expressed in minutes.

The reserve capacity $C_{r,e}$ is defined by:

$$C_{r,e} = t \text{ [min]}$$

Equation 4-6: Reserve capacity

5 Cranking system and combustion engine

This chapter describes a combination of the cranking system and combustion engine type used in the majority of automotive vehicles. Since the battery SOH is related to the cranking performance it is important to get a better understanding of the cranking system. The system is cranking a reciprocating combustion engine which produces a varying load on the cranking system while cranking. This will observable in the voltage values of the cranking system.

5.1 Components cranking system

For a successful engine crank several components of the cranking system are working together. The battery is a vital component of the cracking system, but it exist of more parts

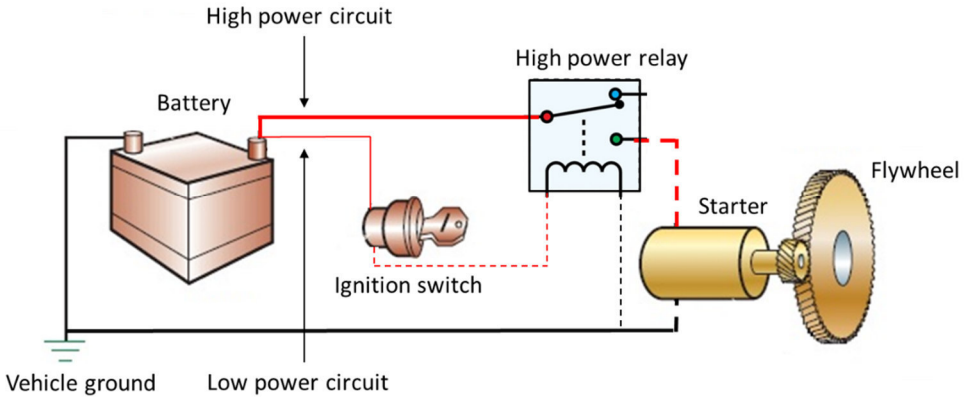

Figure 5-1: Cranking system

Figure 5-1 depicts a simplified cranking system. The battery has to deliver electrical power to turn the starter. The current flow the starter is controlled by a high power relay, which is directly connected to the starter. The relay is of the normally open type and is activated by a low power signal from the switch. Activating the relay closes the high power electrical circuit and powers the starter.

5.1.1 Battery

The cranking process demands high power delivery of the battery for a short amount of time. Currents up to 400 A are no exception. Automotive type of lead acid batteries are especially designed to handle high power delivery for short amounts of time. Most combustion engines are cranked within one second.

5.1.2 Starter

Most starters are permanent magnet electrical machines which operate on direct current. The battery is the power source of the starter.

5.1.3 Ignition switch

As described the ignition switch activates the high power relay on the starter but this is not the only function of the switch. For simplicity the three most important functions related to this study will be explained in Table 5-1.

Ignition off	Ignition on	Cranking
In this switch state, nearly all electric consumers are disconnected from battery.	This switch state connects all electrical components to the battery and keeps them	This switch state activates the starter. As described the starter is directly powered by the

Only really small consumers are still consuming some power like clocks and computer memories. The battery voltage is comparable to the open circuit voltage and can be used for a state of charge estimation as explained in section 3.3.1.1.	powered. Keeping power on this components is needed for successful vehicle operation including running of the combustion engine.	battery via the high power relay. When a successful engine start is noticed by the user the switch is released returned to its former state (ignition on).

Table 5-1: Cranking process

5.2 Combustion engine

As depicted in Figure 5-1 the starter turns a flywheel. This flywheel is directly connected to the crankshaft of the combustion engine. For better understanding of the cranking process the operational principal of an internal combustion engine is described. Figure 5-2 depicts a combustion engine.

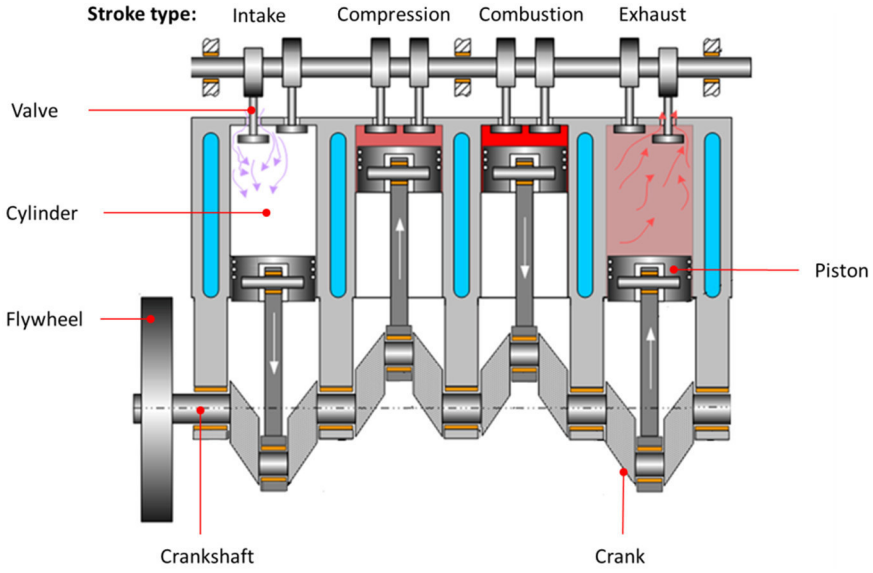

Figure 5-2: Combustion engine

Inside a running engine the crankshaft is turned by the movement of the pistons connected to the cranks of the shaft. The pistons make vertical movements inside the cylinders and are pushed down by expanding gasses resulting from a combustion process. The up movement of the pistons is caused by the inertia of the flywheel which is directly connected to the crankshaft. The up or down movement of a piston is called a stroke. Almost all automotive engines are of the 4 stroke type. In 4 stroke engines each piston encounters 4 types of strokes in a repeating pattern: Intake, compression, combustion and exhaust. On top of the cylinder valves are controlling the type of stroke. The repeating process of piston movement keeps the engine running.

To start up this process the flywheel is turned by the starter. While turning the flywheel some of the pistons will encounter a compression stroke, making it extra hard to turn the crankshaft. In these instances the starter consumes extra electric power resulting in large current flows.

5.3 Cranking voltage trace

Measuring the batteries voltage while cranking and plotting it over time creates a curve as depicted in Figure 2-1. In this study this curve will be referred to as the cranking voltage trace (CVT). In a CVT we can recognize all the parts of the cranking system.

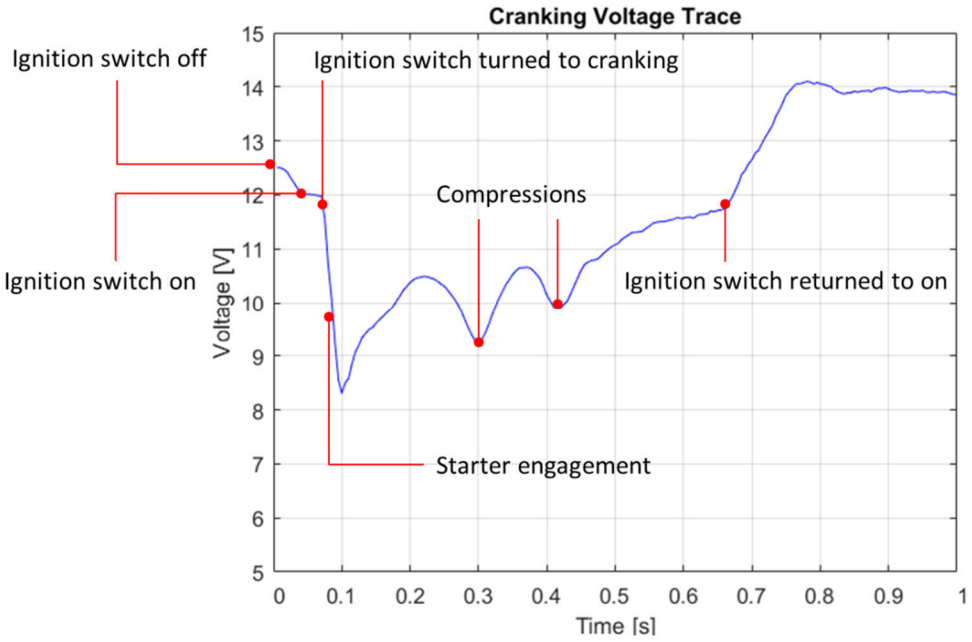

Figure 5-3: Cranking voltage trace

6 Cranking voltage trace based SOH monitoring

This chapter discusses a method to estimate the battery's SOH based on the CVT. A CVT reveals a distinctive shape from which common points occurring in every CVT can be derived. These points represent features of the CVT. As depicted in Figure 6-1, the shape of the CVT changes with battery age and decreasing SOH. It is expected that features extracted from the CVT change along with the CVT shape. A method is proposed to discover a relation between change in features and cranking performance.

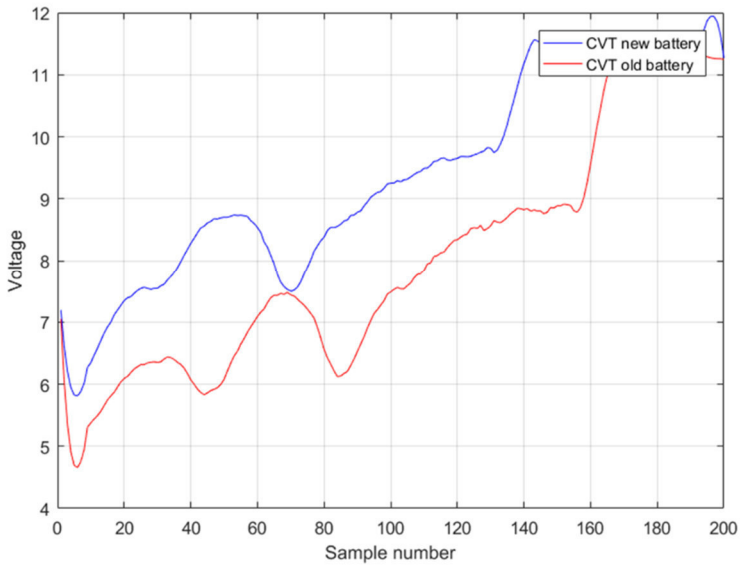

Figure 6-1:Cranking voltage trace of new and old battery

6.1 Proposed SOH monitoring method

A method is proposed which enables non-invasive SOH monitoring and is able of generating an upcoming failure warning. The method is based on the CVT which is captured for every cranking event. The CVT data is procced and features are extracted. The feature values are corrected for temperature and normalized. A particular set of normalized features is related to the SOH. If the SOH is negatively exceeding a predetermined threshold value a failure warning is generated. Figure 6-2 depicts a visual representation of the proposed method.

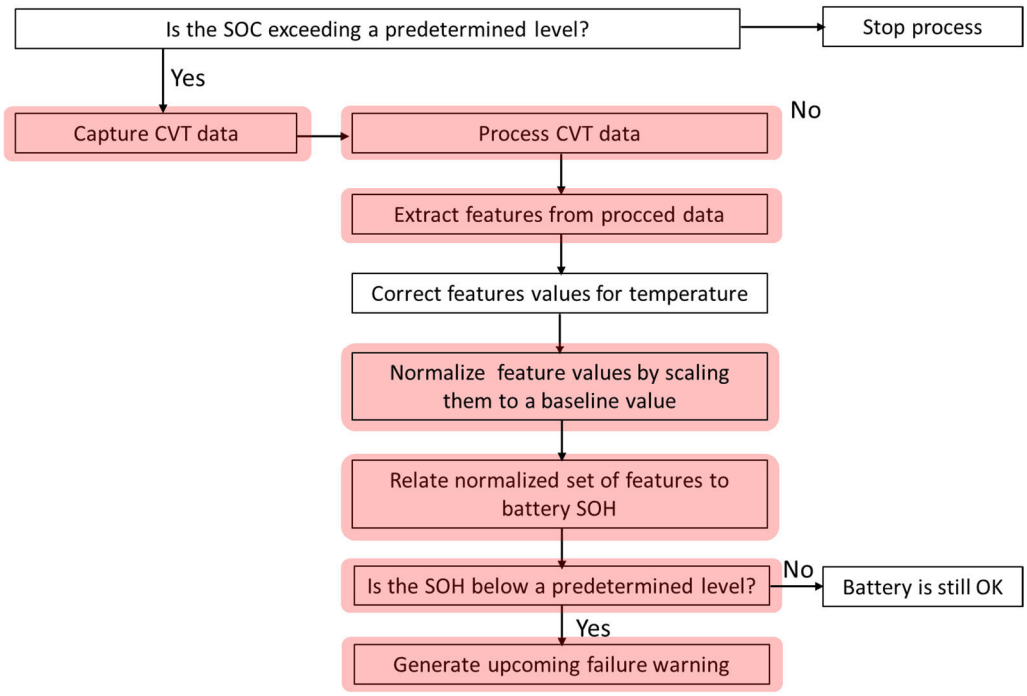

Figure 6-2: proposed SOH monitoring method

This study will focus on the highlighted parts. The state of charge determination and temperature correction are outside the scope of this study. Although the question: if there is a temperature dependence existent will remain within the scope of this study.

6.2 Previous work

The idea of capturing cranking voltage data and try to relate it to battery SOH is not new. Different patents and papers describe this idea. To indicate the differences between this thesis and previous work, a general description will be given of patents and papers showing most resemblance. This is followed by a summation of the differences between the thesis and patents or papers.

6.2.1 US patent No: 6472875

This patent describes a method to determine the SOC of the battery by using the delta of two successive voltage drop values contained by a CVT signal. It is claimed that a state of low charge can be determined by looking at the sign of this delta. If the sign is positive its assumed the battery has a sufficient state of charge, if the sign is negative or equal to zero, it is assumed the battery has a poor state of charge. The battery is declared to be defective if it has a poor state of charge.

As a variant to this method the first derivative of a moving average of the CVT is used. If the first derivative is positive it is assumed the battery has a sufficient state of charge, zero or negative values would indicate a poor state of charge. The battery is declared to be defective if it has a poor state of charge.

The patent briefly touches on the subject of determining the SOH of the battery. According to this patent a battery is declared to be old if a defective SOC is detected (as described in the above aliens) together with an average CVT voltage value below a predefined threshold.

In addition the patent quotes: "*the battery voltage before ignition makes it possible to determine a battery is flat or old*" Right after this quote the patent states if this pre-ignition battery voltage is

below a predetermined threshold the battery has a poor SOC. On the other hand the patent states, that if the voltage value is above the threshold is does not automatically mean the battery is in good condition. Further analysis is needed to determine if the negative exceeding of this threshold is SOC or SOH related. This is contradiction what is quoted previously.

The complete patent can be referenced in appendix xxx

6.2.2 US patent No 2009/0326841

This patent describes a method to determine the SOH of a battery using data collected during the cranking phase. The data compromises battery voltage and engine rotation speed. The voltage and rpm data is normalized and processed in a trained classifier. The classifier uses a trained (predefined) decision boundary to separate the classes. Temperature and SOC are directly processed by the classifier without normalisation. The classifiers output is a battery SOH expressed in a percentage.

The complete patent can be referenced in appendix xxx

7 Measuring the voltage cranking trace

This chapter describes the requirements for non-invasive measuring of the CVT. To capture the cranking voltage trace measuring equipment is required which is able to sample an analog voltage signal at high frequency and resolution. As stated in the research question the measurements have to be non-invasive and are electrical of nature. This means measurement have to be carried oud without making adaptations to the vehicles wiring harness to connect measurement equipment. Non-invasive measuring is achieved utilizing a standardized connection inside the vehicle. To prove the practical applicability of simple hardware measuring a CVT via this connection measurement equipment has been prototyped.

7.1 Measurands

Another way phrasing the CVT is: “time dependent cranking discharge voltage signal”. To capture and CVT time and voltage have to be measured. Voltage is an analog quantity which is captured and digitalized by a sampling process using an analog digital converter (ADC). An ADC maps analog voltage values to a range of digital values. The more digital values contained by the range the higher the resolution of the ADC. A higher resolution enables smaller differences in voltage to be measured. An ADC uses a specific sample rate to capture an analog signal. The sample rate can be used to capture the time dependence of the voltage signal.

Next to voltage and time, battery temperature is important variable since it is expected to have an influence on the cranking performance. The battery temperature can be assumed constant over the cranking period and can therefore be captured using a single sample.

7.1.1 Sampling the cranking voltage trace

A suitable sample rate is required to capture the CVT and prevent the effects of aliasing as explained in the upcoming paragraph. Sampling at high frequencies is more accurate but leads to larger data size since more data is collected. A balance has to be found between accuracy and data size. Data size is important for future dongle implementation purposes as described in section 7.2.1. To minimize data size a minimal sample rate has to be identified, which is still able to capture all voltage data without the effects of aliasing.

7.1.1.1 Aliasing

Aliasing occurs when a continues analog signal is sampled using sample rate unable to capture all the changes in the signal. Sampling at to low sample rates will exclude high frequency changes in contained by the analog signal leading to a false representation of the original signal. The term *aliasing* refers to the measured signal taking a different persona or a false representation of the original signal. If the Nyquist sample criteria is met aliasing will be avoided.

$$f_s \geq 2 \cdot f_c$$

Equation 7-1: Nyquist sampling criteria

Where f_s is the sampling frequency and f_c the highest frequency contained by the signal.

In other words: to prevent aliasing the sampling frequency should be equal or larger than twice the highest frequency contained by the original signal.

7.1.1.2 Determination of minimum sample rate

To meet the Nyquist criteria for sampling first the highest frequency contained by the original signal has to be identified. The signal depicted in Figure 7-1 is sampled with a frequency of 10000 Hz by a use of a lab scope.

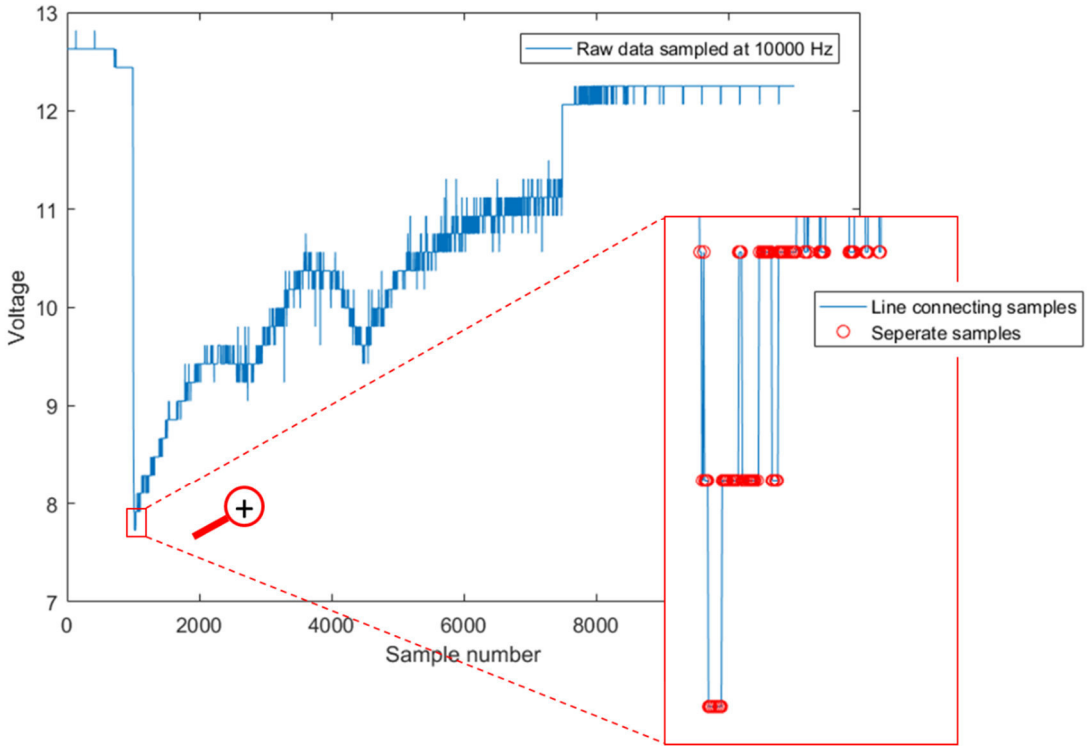

Figure 7-1: CVT sampled at 1000Hz

The highest frequency of the signal is contained by the first voltage drop. Zooming in on this area reveals the number of samples. The zoomed area of Figure 7-1 depicts a small negative spike containing the samples of the absolute minimum voltages. This minimum contains 22 samples. Considering Nyquist criteria and the sample rate used to capture this CVT we are able to calculate a minimal sample rate needed to capture this minimum:

$$\text{number of samples} \;=\; 22\ [samples]$$

$$\text{Time interval between samples} \;=\; \frac{1}{\text{Sample rate}} = \frac{1}{10000}\ \left[\frac{\text{s}}{\text{sample}}\right]$$

$$\text{Time frame minimum} \;=\; \frac{1 \cdot 22}{10000} = \;0.0022\ [\text{s}]$$

$$\text{Higest frequiency contained in signal} \;=\; f_c = \frac{1}{0.0022} = \;454\ [\text{Hz}]$$

$$\text{Minimum sample rate} \;\geq f_s \;\geq 2 \cdot f_c$$

$$\text{Minimum sample rate} \geq 2 \cdot 454 \geq 909 \;\approx 1000\ [\text{Hz}]$$

Calculation 7-1: Minimum sample rate

7.1.1.3 Limiting data size

As explained in the introduction of this chapter, data size has to be kept as small as possible. Zooming in on the minimum reveals noise in the captured signal. This noise can be generated by a variety of electrical components contained by the vehicle and its surroundings. As depicted in fig xx there exits one voltage value which is most prominent. To save data size it is decided capturing this voltage value will be sufficient.

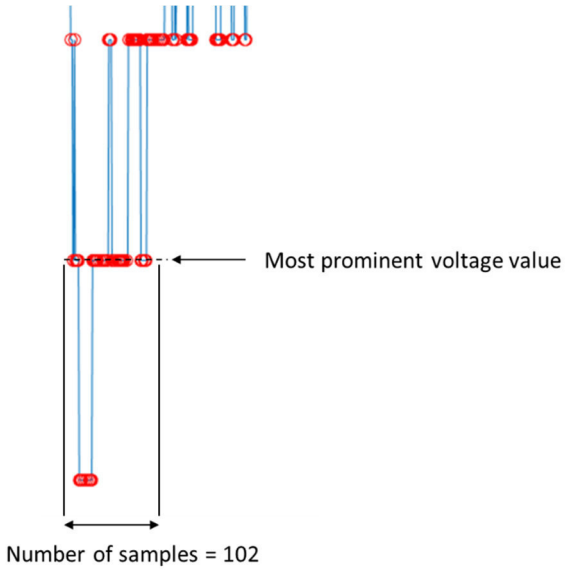

Figure 7-2: Most prominent voltage value in first voltage drop

Using this voltage value for determining the minimum sample rate yields to a sample rate of:

$$\text{number of samples} \;=\; 102\;[samples]$$

$$\text{Time interval between samples} \;=\; \frac{1}{\text{Sample rate}} = \frac{1}{10000}\;\left[\frac{\text{s}}{\text{sample}}\right]$$

$$\text{Time frame minimum} \;=\; \frac{1 \cdot 102}{10000} = \;0.0102\;[\text{s}]$$

$$\text{Higest frequiency contained in signal} \;=\; f_c = \frac{1}{0.0102} = \;102\;[\text{Hz}]$$

$$\text{Minimum sample rate} \;\geq f_s \;\geq 2 \cdot f_c$$

$$\text{Minimum sample rate} \geq 2 \cdot 102 \geq 204 \;\approx 200\;[\text{Hz}]$$

Calculation 7-2: Minimum sample rate based on most prominent voltage value

Using this sample rate to capture the CVT yields to smaller data size and acceptable accuracy.

7.2 Connection in vehicle

All vehicles from the year 2002 and after are equipped with an on-board diagnostics port. The dimensions and pin-out of these ports is standardised. Regulations state the port has to be easy accessible and be placed inside the vehicle's cabin. As depicted in Figure 7-3,the port is often

incorporated in the dashboard and located in the vicinity of steering wheel. Utilizing this port to connect the measurement equipment t enables non-invasive measurements since no alternations to the vehicles wiring harness have to be made. An overview of the available connections on the OBD socked is depicted in Table 7-1

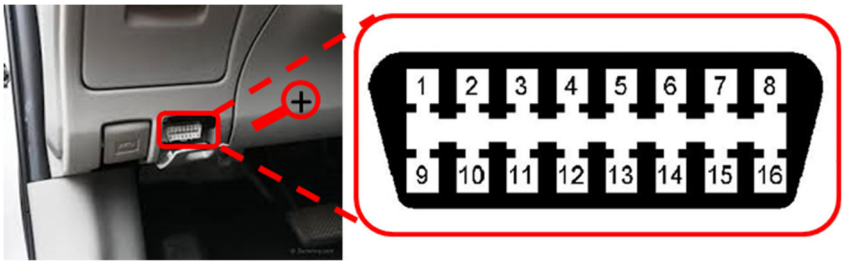

Figure 7-3: On-board diagnostics port

Pin #	Description	Pin #	Description
1	Vendor Option	9	Vendor Option
2	J1850 Bus +	10	J1850 Bus
3	Vendor Option	11	Vendor Option
4	Chassis Ground	12	Vendor Option
5	Signal Ground	13	Vendor Option
6	CAN (J-2234) High	14	CAN (J-2234) Low
7	ISO 9141-2 K- Line	15	ISO 9141-2 Low
8	Vendor Option	16	Battery +

Table 7-1: OBD Socket pinout

Pin 16 connects directly to the battery's positive terminal and pin 4 connects to the battery's negative terminal via the chassis ground of the vehicle. Utilizing this pins enables low power battery voltage measurements required to capture a CVT.

7.2.1 Future implementation in dongle

Ultimately the measurement equipment has to be incorporated inside a dongle. A dongle is a device which can be plugged into the on-board diagnostics port as depicted in Figure 7-4.

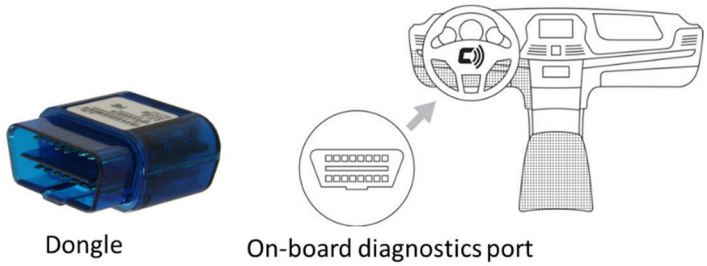

Figure 7-4: Dongle

A dongle is equipped with a wireless data connection to transfer vehicle related data like diagnostic information, vehicle position, acceleration, etc. The data generated by the dongle can be analysed to accommodate fleet management programs. For this reason dongles are currently used by transport companies to make their vehicle fleet connected.

This study focuses on monitoring battery SOH utilizing features coming from the CVT. If a device like a dongle is used to capture the CVT constrains emerging from this type of simple hardware have to be considered.

7.3 Measuring equipment

For testing purposes and prove the applicability of a dongle-like device, a testing device is required with an adjustable sampling rate in a range of 100 till 1000 Hz. These kind of ranges are relative low and uncommon in sampling devices.

The device has to capture a complete CVT, therefore it has to be able to recognize a cranking event. To save data size it important sampling starts just before a cranking event and is automatically stopped right after a successful engine crank. This can be achieved using voltage based triggers in combination timed interrupts of the sampling process. Both have to be highly configurable.

As one can imagine such a device is not buyable form the shelf and the question rises if it is even possible to capture a CVT using simple devices like dongles. To answer this question a device is prototyped using very basic hardware and self-programmed software. The prototype will be used for data collection to prove if dongle-like devices can be used. To have a backup if the prototype fails or if it turns out that data collected by the prototype is not usable, a lab scope is used in parallel with the prototype.

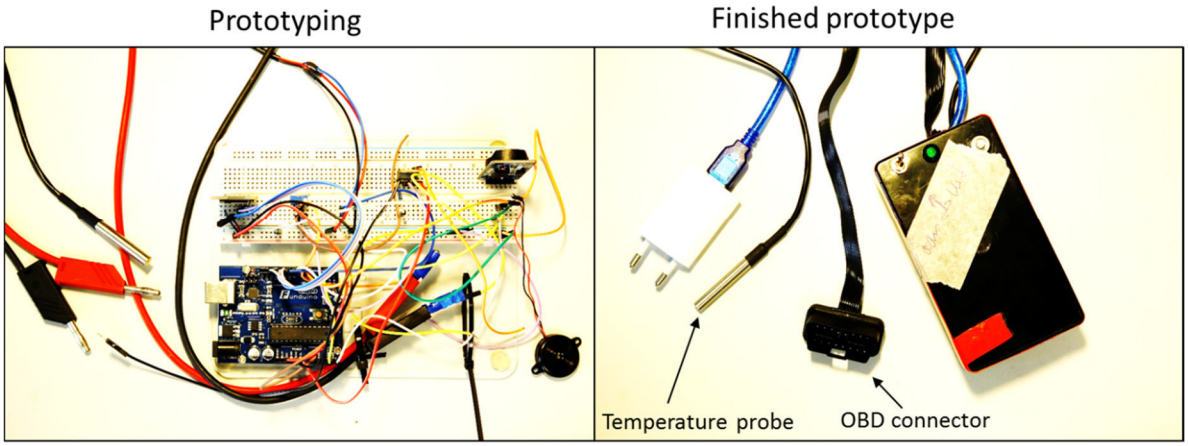

Figure 7-5: Prototyping measuring equipment

7.3.1 Prototyped measuring equipment

Prototyping is time consuming, but has its benefits. In general a prototyped devices are self-build yielding to total control of measurements and data storage. Being in total control of: measurements, data storage, sample rate, resolution, voltage trigger points, timed interrupts etc. leads to better insight in what is possible with this simple hardware. Prototyping will also lead to electronic better feedback for a future dongle manufacturer.

7.3.1.1 Hardware

The prototype is composed of prefabricated hardware components with at its hard a micro controller chip. The controller chip is programable and drives all connected hardware.

Controller chip

An existing micro controller chip is used which is programmable using a C++ like language. The chip is loaded with the Arduino bootloader which makes it easily programmable via free software disturbed by the Arduino community. As depicted in Figure 7-6 the controller chip is the ATMEGA 328p. The most important specifications are provided in the figure. A complete overview of the specifications can be referenced in appendix xxx

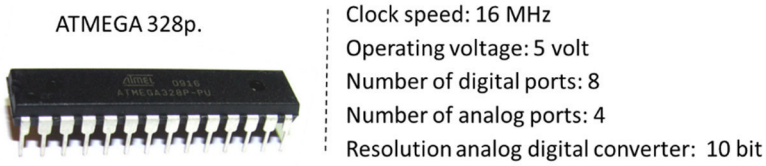

Figure 7-6: Controller chip

Sampling voltage

The digital and analog ports of the controller chip can be configured to input or output's using software programming. The CVT is measured by one of the analog ports which is configured as input. Analog ports can handle signals of 0 to 5 volts. This is problematic since the measured signal can contain voltages up 16 V depending on the alternator operation. To safely measure a CVT a voltage divider is applied as depicted in Figure 7-7.

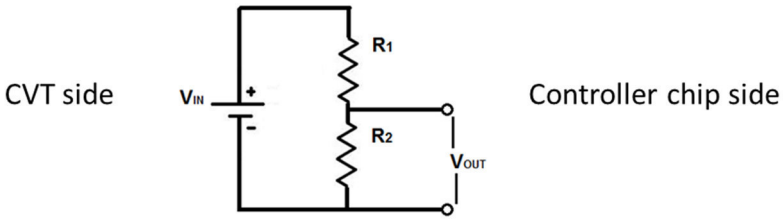

Figure 7-7: Voltage divider

Resistors $\mathbf{R}_1$ and $\mathbf{R}_2$ used in the voltage divider of the prototype have values of: $\mathbf{R}_1$ = 1000 kΩ and $\mathbf{R}_2$ = 100 kΩ. The maximum measurable signal voltage can now be calculated using Ohm's law.

$$U = I \cdot R$$

Equation 7-2: Ohm's law

Where U represents the voltage, I the current and R the resistance.

Appling this to the voltage divider resistor values:

$$U_{in} = I \cdot (R_1 + R_2)$$

Equation 7-3

$$U_{out} = I \cdot R_2$$

Equation 7-4

Rewrite Equation 7-4

$$I = \frac{U_{in}}{(R_1 + R_2)}$$

Equation 7-5

Since the current flows through each of the resistors is equal Equation 7-5 in can substituted in Equation 7-4:

$$U_{out} = \frac{U_{in} \cdot R_2}{(R_1 + R_2)}$$

Equation 7-6

To calculate the maximum signal voltage the maximum allowed voltage for the analog port is used as a constrained, which is 5 volt.

$$U_{in} = \frac{U_{out} \cdot (R_1 + R_2)}{R_2} = \frac{5 \cdot (1000 + 100)}{100} = 55\ [V]$$

Equation 7-7

Using the resistor values as described by Figure 7-7 a maximum of 55 volts can be safely measured without destroying the controller chip. This is well within the ranges of the intended use. The analog port uses an analog digital converter (ADC) with a maximum reading rate of 0.0001 seconds with is equal to a sample rate of 10000 Hz, this is also well within the range of the desired sample rates.

The ADC uses a bit-space of 10 bits to map the voltage values and receives voltage values ranging from 0 to 5 volt. A voltage divider transforms a range of 0 to 55 volt to the 0 to 5 used by the ADC. Mapping 0 to 55 voltage to the possible values inside the bit-space yields to the minimum change in voltage which can be observed by the ADC i.e. the resolution.

$$\text{Number of possible values inside bit space} = 2^{number\ of\ bits}$$

Equation 7-8

Fore a bit space of 10 bits Equation 7-8 yields to 1024 possible values. This leads to a resolution of:

$$\frac{55}{1024} = 0.05\ [V]$$

Equation 7-9: resolution

Temperature

A digital temperature probe is connected to one of the digital ports. Using a digital temperature probe instead of an analog has a some benefits. Most analog temperature sensors are in fact resistors with a negative temperature coefficient (NTC). This means with rising temperature the resistance of the NTC will drop. Using this kind of sensors, the controller has to supply a current flow

resulting in a voltage change over the sensor with varying temperature. Some power is dissipated by the NTC resulting in a temperature increase of the resistor leading to inaccurate readings.
A digital sensor works different. It contains a calibrated chip which supplies a temperature reading on request. The chip has its own specific address, once the address is called (by the software) the sensor communicates its temperature reading. Since each sensor has its own specific address it is possible to connect multiple sensors to the same communication wire (bus) and only power the sensor just before it is called.

Timestamp

To generate a timestamp based on real time, a chip containing a real time clock (RTC) is incorporated into the design. Once a RTC chip is set to the right time and date, it continues to preserves time and date by use of to a small battery which is recharged each the chip receives power.

Data storage

A micro sd card is used to store the sampled voltage values. The voltage values are written to the sd card in real time using a predefined sample rate. For this reason writing speed is very important since the controller chip has not enough data buffer to store a complete CVT and write it to the sd card in a complete package. A chip containing a micro sd card slot is connected to the controller chip enabling the CVT storage space..

Audio-visual comunication

A buzzer together with an light emitting diode (LED) is connected to one of the digital ports of the controller chip for communication purposes. Without this there is no way of knowing if the device is ready for a particular event. Three communications protocols a programed into the device:

- 1 buzz & blink: The sd card is successfully initialized and the device is ready to record.
- 2 buzzes & blinks: The sampling process has finished and new CVT data is stored on the sd card.
- A 3 tone buzz & 3 blinks: The device is not ready to record (sd card is missing or error)

7.3.1.2 Software

As described in the previous section, the controller chip can be programmed with a C++ like language. The program contains to distinctive parts: an initialization part that runs once and a looping part which runs over and over again. Since the clock speed of the controller chip is 16 MHz the program will run thought the loop with this speed. For each part a schematic overview describing the working principle is provided followed by a verbal explanation. The complete program code can be referenced in appendix xxx.

Initialization

A schematic overview of the initialization part is provided accompanied by a verbal explanation.

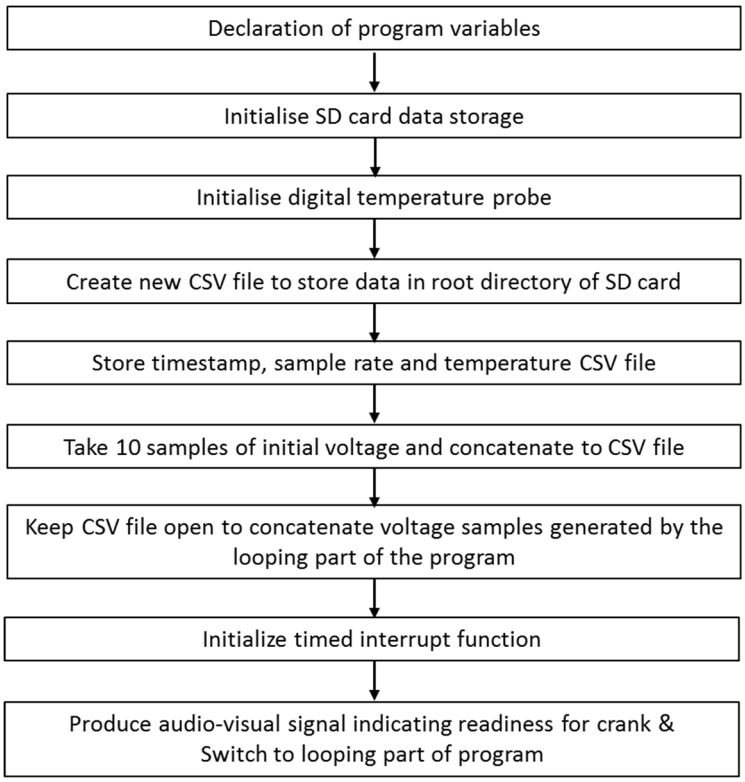

Figure 7-8: Initialization part prototype software

When the controller chip is powered on the initialization part of the program will run once starting with the declaration of program variables. Next the SD card is initialised, if this is successful the temperature proper is initialised and a new comma separated values file (CSV) is added to the SD card. The first values will contain a timestamp, the sample rate, the temperature and 10 samples of the initial voltage. After storing this values the CVT file is kept open, meaning data can be added to the file without opening the file. To prevent corrupted files it is normal practise to open and close files when adding values. Opening and closing is time consuming and because high writing rates have to be achieved the file is kept open for the complete sampling process to be closed at the end.

A timed interrupt function is initialized which is required to achieve an exact sample rate. This function interrupts the program to execute a predefined function. The interrupts are time based and independent of the loop speed. If no timed interrupt function is used the sample rate would be depended on loop speed. The more lines of code contained by the loop, the longer it takes to complete a loop leading to inaccurate sampling rates.

After the timed interrupt function is initialized and set to the required sample rate an audio-visual signal is produced indicating the device is ready for an engine crank. On this instant on the program switches from the initialization to the looping part.

Looping part

A schematic overview of the looping part is provided accompanied by a verbal explanation.

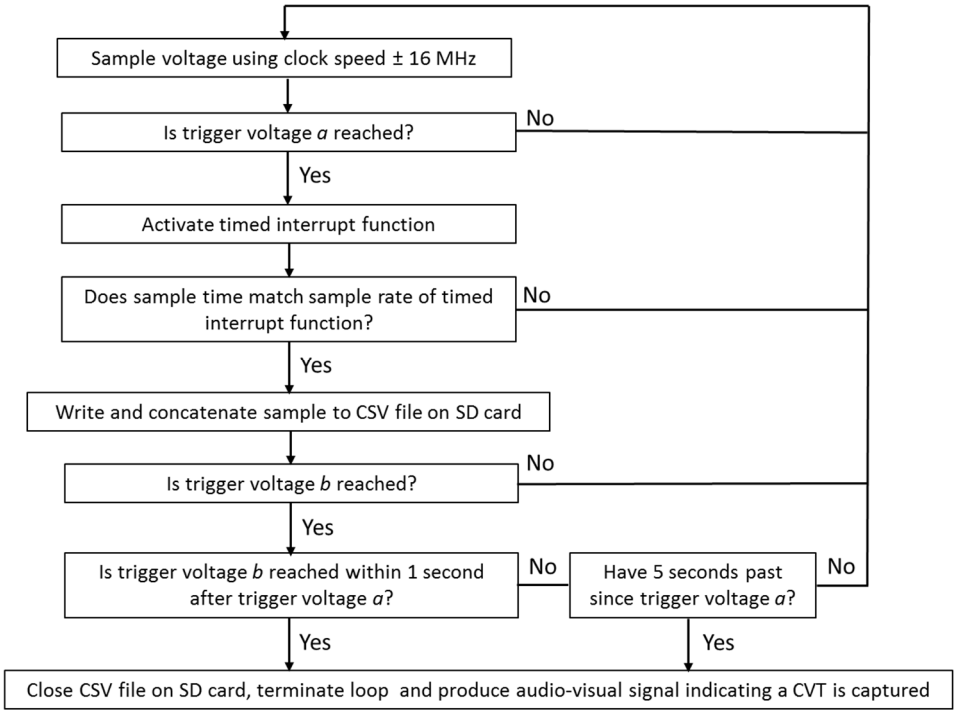

Figure 7-9: Looping part prototype software

Once the program has entered the looping part the voltage is monitored from this loop. The program runs through the loop with a speed of 16 MHz while sampling the voltage. The sampling rate will be a bit less than 16 MHz depending on the code length for the looping part. If a predetermined trigger voltage *a* is reached the timed interrupt function is attached to the program. The timed interrupt function writes the sampled voltage values to the CSV file at intervals matching the sample rate the voltage values are concatenated to the CSV file. If trigger voltage *b* is reached within one second after trigger voltage *a* the concatenation is terminated. If this trigger voltage *b* is not reached concatenation will continue for 5 seconds before termination. When the concatenation process terminated, the program closes the CSV file and produces an audio-visual end signal indicating a CVT is captured and stored on the SD card.

7.3.2 Backup measuring equipment

Next to the prototyped device a oscilloscope is used which is connectable to a personal computer (PC). The signals fed into the oscilloscope can be stored and annualized by the PC. These kind of scopes have high accuracy and are very useful in test setups. The minimum sample rate of these devices still exceeds any practical feasible solution like a dongle. This is one of the reasons a prototyped device is build.

PC connected oscilloscopes are reliable data capturing devices, but are not highly configurable. For example, start and end of data collection have to be controlled manually. As depicted in Figure 7-10 the cranking event is very short in comparison to a complete recording with a scope. This means unnecessary data is generated and useful parts have to be extracted later on.

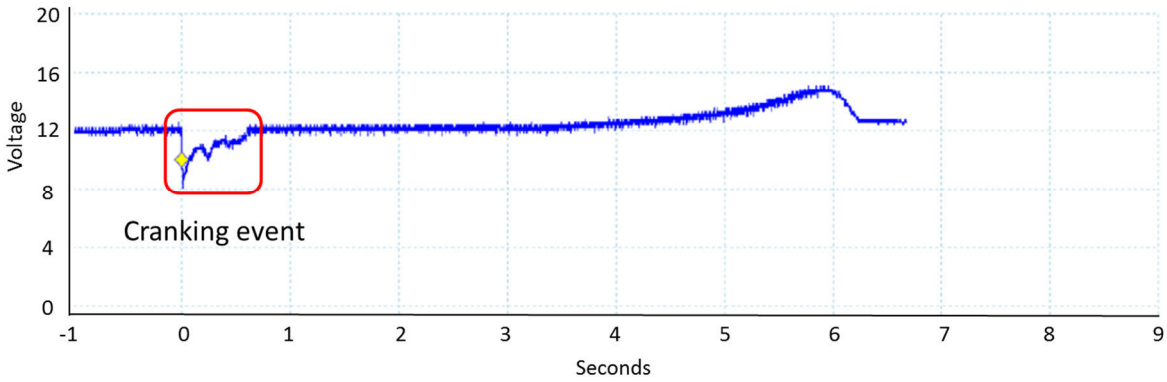

Figure 7-10: cranking voltage captured with an oscilloscope

8 Data generation

As described in section 6.1 a SOH monitoring method is proposed based on CVT data. This data is unavailable and has to be generated in a controlled manner. The generated CVT data has to be labelled and stored to accommodate an analysis process which will be described in the succeeding chapters. A test setup has been created to generate the required CVT data. The test setup is used to produce cranking data of batteries with different and decreasing SOH. To accelerate the decrease of battery SOH an accelerated aging device is constructed which ages the batteries in weeks instead of years.

8.1 Test Setup

This test setup has been created to generate the required CVT data. Batteries with different SOH will be used to crank two internal combustion engines while the CVT is captured. Five test batteries will be used to crank the two engines of the teste setup. The CVT data is captured using the prototyped device in parallel with an PC connectable oscilloscope.



Table 8-1: Test setup

As can be seen the engines are placed on a stand. They are both containing an on-board diagnostics port and have different fuel types (petrol and diesel). Using engines with different fuel types is done to discover differences between the CVT's are appearing. A diesel engine is expected to require cranking more power, due to its higher compression ratio. The expectation is that this will be observable in the CVT's. Another reason using for using two different engines is to discover if a cranking failure is dependent on a certain battery-engine combination or just on the battery itself. If for example one of the battery engine combinations produces a failure but using the same battery in combination with the other engine produces no failure, it can be concluded the failure is dependent on the battery engine combination. The specifications of the two engines used for testing is depicted in Table 8-2.

	1.4 KFV	1.9 TDI PD AXR
Displacement	1360 [cubic centimetres]	1896 [cubic centimetres]
Number of cylinders	4	4

Power	55 Kw	74 kW
Fuel type	Petrol	Diesel
Year of production	2004	2002
Compression ratio	10:1	19:1

Table 8-2: Engine specifications

To be sure that changes in the CVT data are coming from the batteries alone, it is important to keep surrounding variables like engine temperature, ambient temperature, battery temperature, etc. constant. By using engines on stands instead of complete vehicles a higher level of control considering the test environment is achieved .Test setups can be categorized from model to field tests as depicted in Figure 8-1. The test setup used for this study can be categorized as a subsystem test.

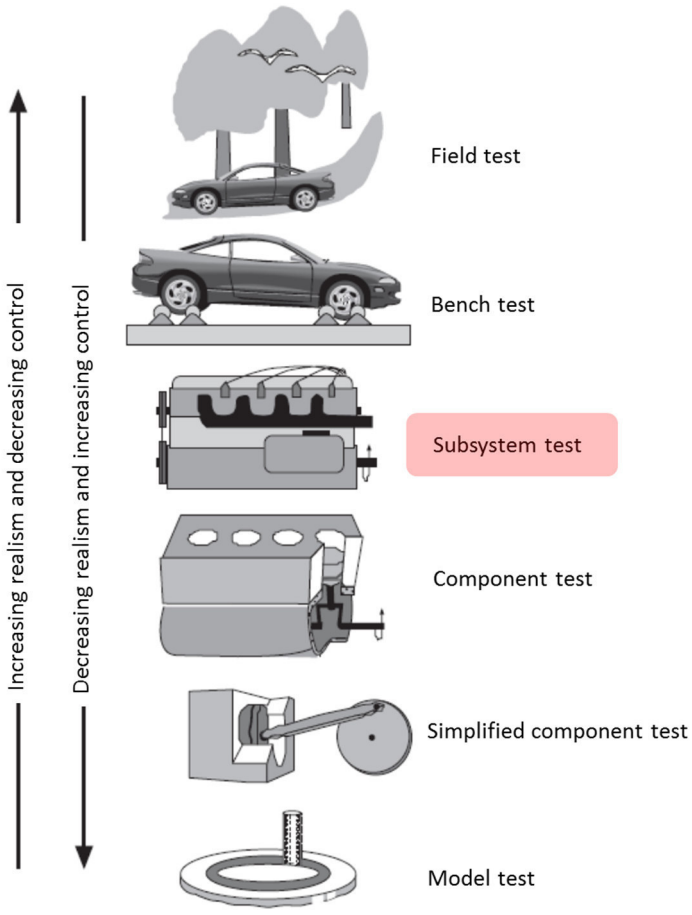

Figure 8-1: Test categories

8.2 Testing procedure

As described five batteries will be used in the test setup to crank both engines while the CVT data is captured and stored for processing and feature extraction . A secmatic representation of the testing procedure is depicted by Figure 8-2.

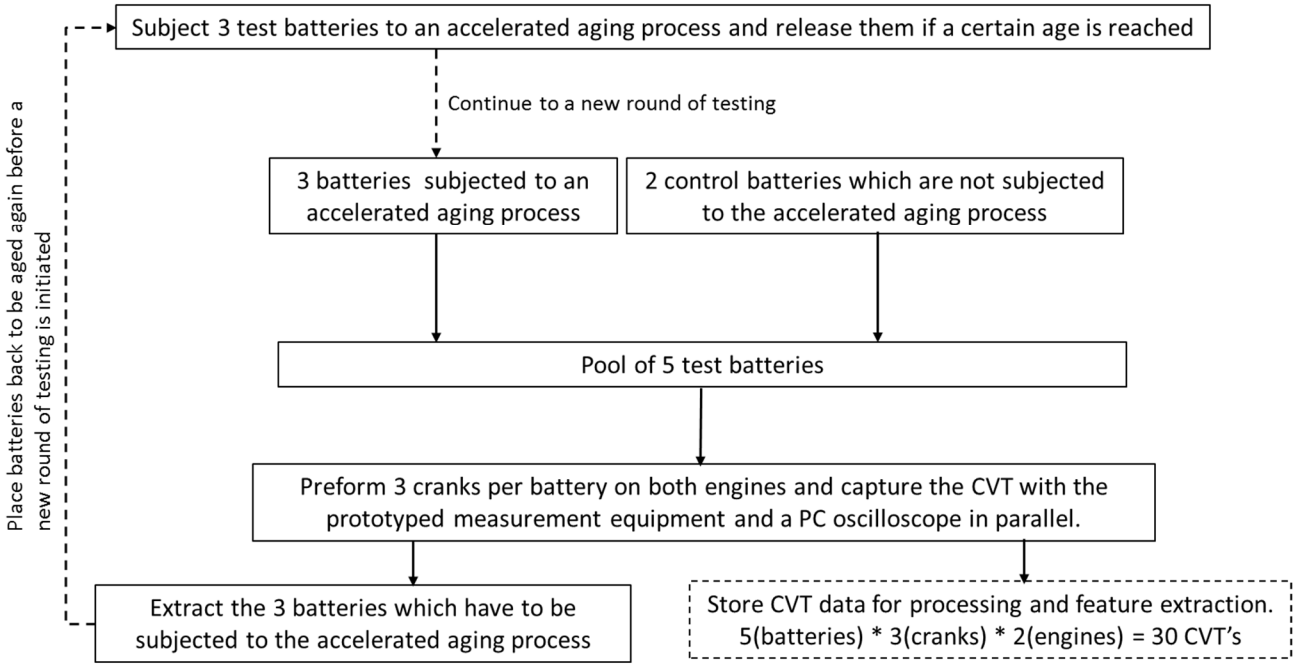

Figure 8-2: Testing procedure

As can be seen 3 of the 5 test batteries are subjected to an accelerated aging process. This is done to generate a dataset which is gradually stepping from new to old and failing batteries. Two batteries will be kept as a control and will not participate in the accelerated aging process. The complete pool of 5 test batteries will be put through three cranks per battery performed on both engines while the CVT's are captured. In this way 30 CVT's are generated which will be stored for processing and feature extraction. If the complete test pool has been subjected to the cranking events, the same 3 batteries as before will be subjected to the accelerated process again. If a certain age is reached the batteries are released form the accelerated aging process and a new round of testing is initiated.

8.2.1 Accelerated aging process

Batteries with a different state of health are required to generate CVT data which maps the service life of a battery. A dataset is required which is gradually stepping from new to old and failing batteries. An accelerated battery aging process is designed which enables the batteries to age in weeks instead of years. It involves keeping the batteries at an elevated temperature and put them through charge-discharge cycles. The method is based on a combination of failure tests as described in battery standards appendix xxx and advices from battery labs.

8.2.1.1 Accelerated aging method

The batteries are placed in a hot water bath which is kept at a constant temperature of 60 °C. The temperature is automatically regulated by a thermostat connected to a heating element. While at this elevated temperature the batteries are put heavy charge-discharge cycles. The cycling is controlled by a microcontroller similar to the one used for the prototyped measurement equipment.

The micro controller monitors the voltage of the batteries and drives high power relays to switch between charge and discharge. Three batteries will fit in the water tank as depicted in Figure 8-3.

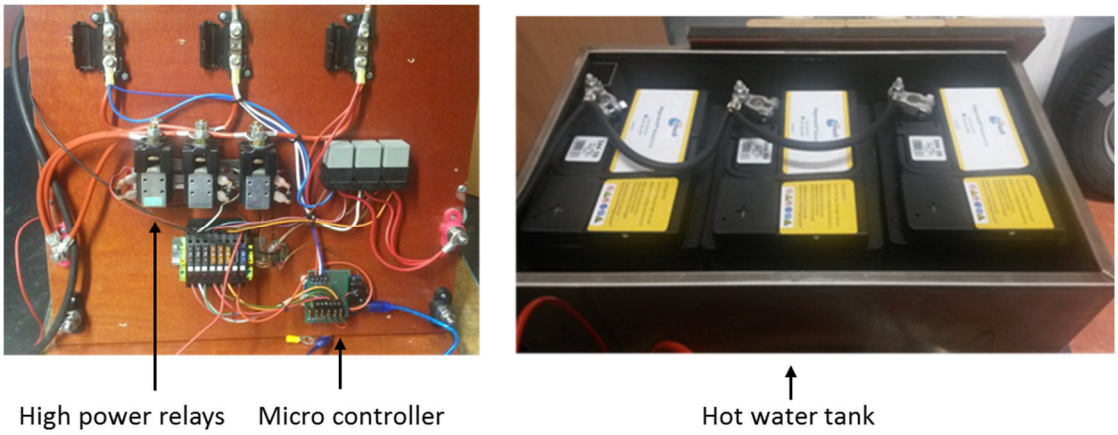

Figure 8-3: Battery aging device

To discharge the batteries a large resistor (with a small resistive value) is connected to the battery discharging it with a current of approximately 200 A. A configurable power source capable of delivering 1000 Watt is used to charge the batteries. The resistance and power source are depicted in Figure 8-4.

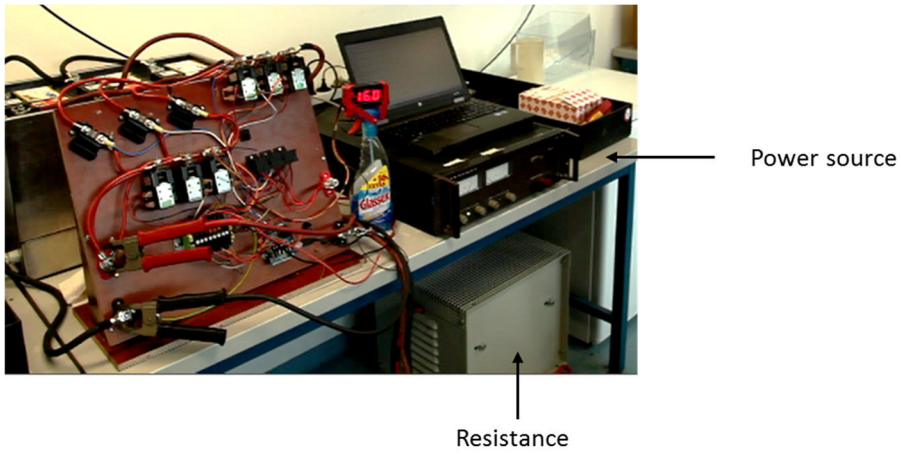

Figure 8-4: Battery aging power source and resistance

The power source is configured to charge the batteries according to a constant-current constant-voltage (CCCV) principle as depicted in Figure 8-5. In the beginning of the charging process a constant current of 40 A is supplied by the power source. If the battery nearing a higher state of charge it will no longer accept the 40 A of current unless the voltage is raised. To keep charging with a current of 40 A the voltage will automatically be raised until a threshold value of 16 volt is reached. If this threshold has been reached the voltage is kept constant at 16 volts while the current will vary. After a period of 5 minutes at 16 volt the microcontroller interrupts the charging process.

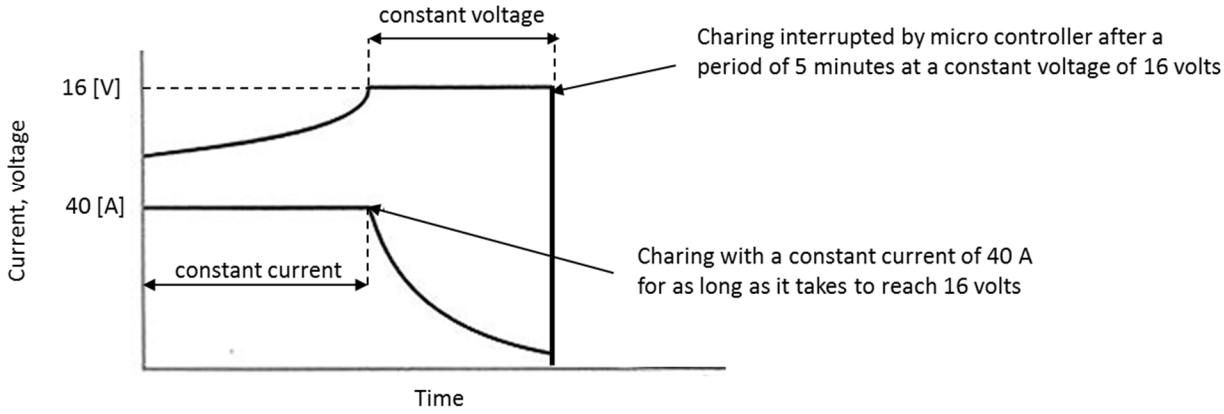

Figure 8-5: CCCV charging

The constant current and voltage values are chosen relatively high to accelerate the SOH degradation of the batteries, especially the constant voltage value which is set to be 16 volts. Charging a 12V flooded lead acid battery with 16 volts causes overcharging and excessive gassing which will accelerate the aging process.

The accelerated aging process triggers a combination of failure mechanisms as described in section 4.2.

8.2.2 Test battery pool

The test battery pool consists of five batteries. The batteries are of the same type, make and batch. For identification purposes the batteries are labelled from A to E. As explained 3 of the 5 test batteries will be subjected to a controlled, but accelerated aging process. The battery test pool is depicted in Figure 8-6.

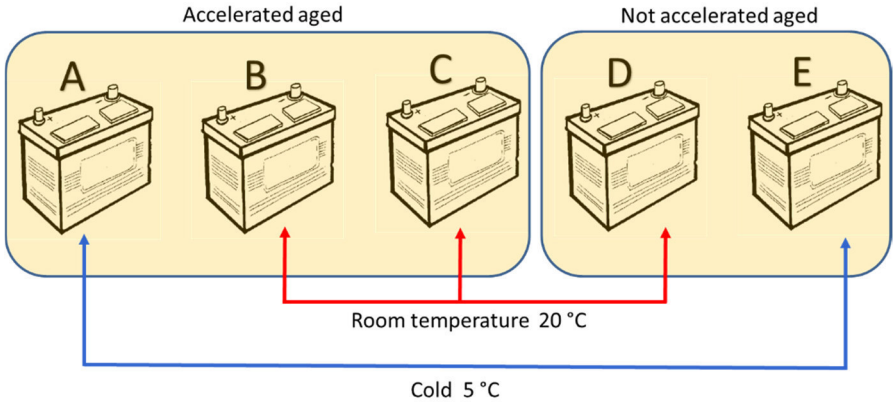

Figure 8-6: Test setup battery pool

As can be seen a temperature difference is introduced. This is done to discover if the features extracted from the CVT reveal a temperature dependence.

8.2.3 Testing preparations

As explained five batteries will be tested in combination with both engines of the test setup. Before using the batteries and engines of the test set up preparations have to be made including setting the correct temperatures for battery and engines and bringing the batteries to the a correct state of charge.

8.2.3.1 Temperatures

The engines and battery temperatures are kept constant where possible. To prepare the engines for testing they are warmed up by letting them idle for 5 minutes. As explained in section 8.2.2 three batteries have to be kept at a temperature of ± 20°C and two at ± 5°C. The latter are placed inside a refrigerator set to 5°C 24 hours prior to testing.

8.2.3.2 State of charge

Before testing all batteries are fully charged and have had an after-charge resting period of minimum 4 hours prior to testing.

9 CVT data processing

Before data can be analysed it has to be processed first. A first step in data processing is making the make the data identifiable. This is achieved by labelling the data. A personal table of labels is constructed for each test battery, so generated CVT data can be linked to that particular battery. Each CVT generated by the test setup receives an unique identification so they are distinguishable and can be linked to a particular cranking event. The CVT data is stored in a custom made folder and filename structure. A Matlab script imports the CVT data and uses the folder and filename structure to generate the CVT identification number. One the data is imported the data possessing can start. The data processing involves the selection of peaks and valleys contained by the shape of the CVT. All features extracted from the CVT data are based on the peaks and valleys, therefor the feature extraction process will start after the peak and valley selection has finished.

9.1 Table of labels

A table of labels is created for each test battery which registers al labels the battery contained through its service life. The labels exist next to the battery identification letter and will vary over the service life of a battery. The labels are based on three SOH estimators and one upcoming failure indicator.

9.1.1 SOH estimators

After each cycle aging session and before using the batteries in the test set up three different tests are conducted on each battery generating three SOH estimators. In this way the aging process can be tracked and CVT data can be linked to a particular SOH which is required for the data analysis process. Each battery receives a label containing the 3 SOH estimators before entering the test setup. Table 9-1 shows an example of the labels contained by a battery during the different rounds of testing. As explained each testing round belongs to a certain battery age i.e. a certain number of aging-cycles.

Number of aging cycles	CCA Midtronics	Heavy loading capacity	Reserve capacity
0	487	270	2820
15	475	228	2104
40	460	250	1845
60	426	302	1522
75	402	300	1220
90	375	68	424
125	349	60	166

Table 9-1: Battery SOH estimators

The CCA values depicted in the second column are determined by a Midtronics battery testing device. These values are purely based on internal resistance values of the battery. Although Midtronics is a leading battery tester manufacturer, by considering resistance alone they are missing out on an important SOH estimator: the effective capacity. Mapping the effective capacity of the batteries requires a different type of test.

The reserve capacity test is based on the reserve capacity check as explained in section 4.4.2.2. It involves discharging a fully charged battery with an average current of 25 A until the voltage reaches 10.5 volt. The discharge time is expressed in seconds and represents the reserve capacity.

The heavy loading capacity is based on the cranking performance check as described in section 5.3 of the battery standards which can be referenced in appendix xxx. For this test the battery is discharged with an average current of 200 A until the voltage reaches 7.5 volt. The discharge time is expressed in seconds and represents the heavy loading capacity.

9.1.2 Upcoming failure indicator

When batteries have gone through a complete round of testing a label is generated which indicates an upcoming cranking failure. This label is not based on a SOH estimator, but directly related to the batteries cranking performance. To generate the label and decide if a battery is about to fail the battery is hooked up to a non-starting diesel engine which is cranked for 15 seconds. If the battery makes it to the end of this cranking period without showing any effects of a degrading performance it is considered to be still in resalable shape. If a batteries fails or shows any sign of a degrading performance it is label as: “about to fail’

Aging cycles	CCA Midtronics	Heavy loading capacity	Reserve capacity	Upcoming failure indicator
0	487	270	2820	False
15	475	228	2104	False
40	460	250	1845	False
60	426	302	1522	False
75	402	300	1220	False
90	375	68	424	False
125	349	75	166	True

Table 9-2: Table of labels

9.1.3 CVT ID

Each CVT generated by the test setup receives an unique identification so they are distinguishable and can be linked to a particular cranking event. The identification number contains:

Battery ID	Aging-cycle number	Fuel type	Crank number
A	060	Petrol	02

Table 9-3: CVT identification number

The complete identification number resulting from the example given in Table 9-3 results in: A060B02. This label links this CVT to the third crank with test battery A in combination with the petrol engine at a cycle age of 60 cycles. The crank number starts at 00 and when three cranks are reached the crank number will be 02.

9.2 CVT data storage

The CVT data coming from the prototype device and lab scope is stored on a computer using predefined folder structures and file names. This is done to make the CVT’s distinguishable from each other and to be able to relate them to a specific cranking event. Figure 9-1 depicts the folder and filename structure used to store the CVT data.

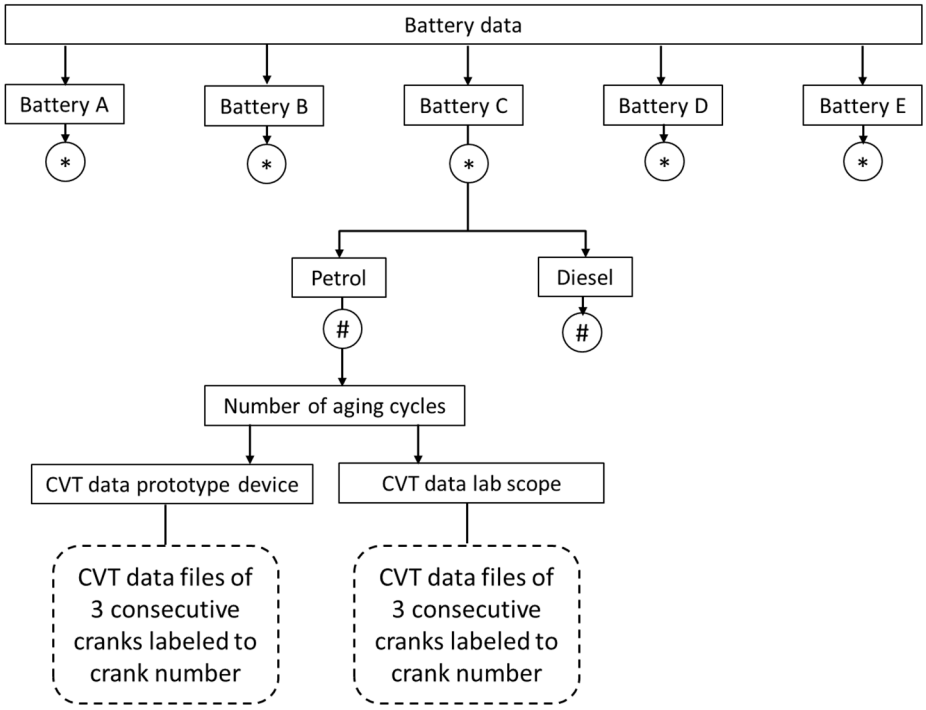

Figure 9-1: Folder and filename structure

A Matlab script is designed which imports and labels the CVT data based on the filename and folder structure. The script is designed to prepare a single CVT for processing and generate a data array containing the labels belonging to that particular CVT. The complete script can be referenced in appendix xxx. Figure 9-2 depicts a schematic overview of the script.

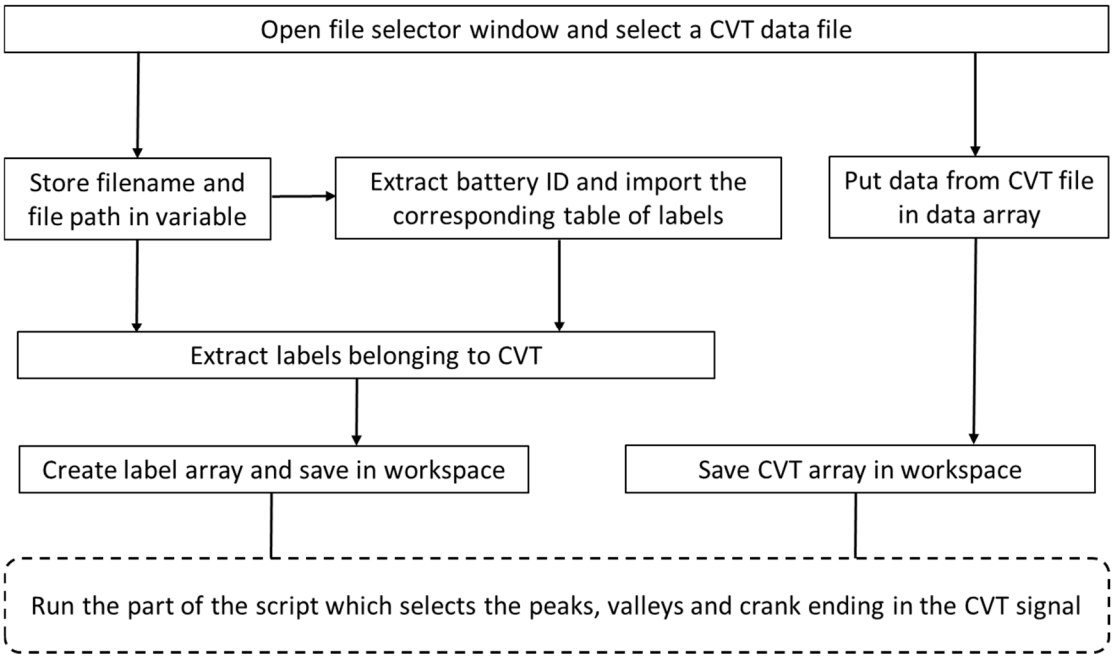

Figure 9-2: Data extracting part of script

9.3 Peak, valley and crank ending extraction

All features extracted from the CVT are based on peaks and valleys in the CVT signal shape. To find these peaks and valleys a clean signal is required. When graphing a CVT from raw data it shows a rough shape making it impossible for Matlab to distinguish major peaks and valleys from the minor peaks and valleys created by the rough shape. The raw data is cleaned first in order to perform proper peak and valley selection. Figure 9-3 depicts a CVT signal shape containing raw data together with the cleaned signal.

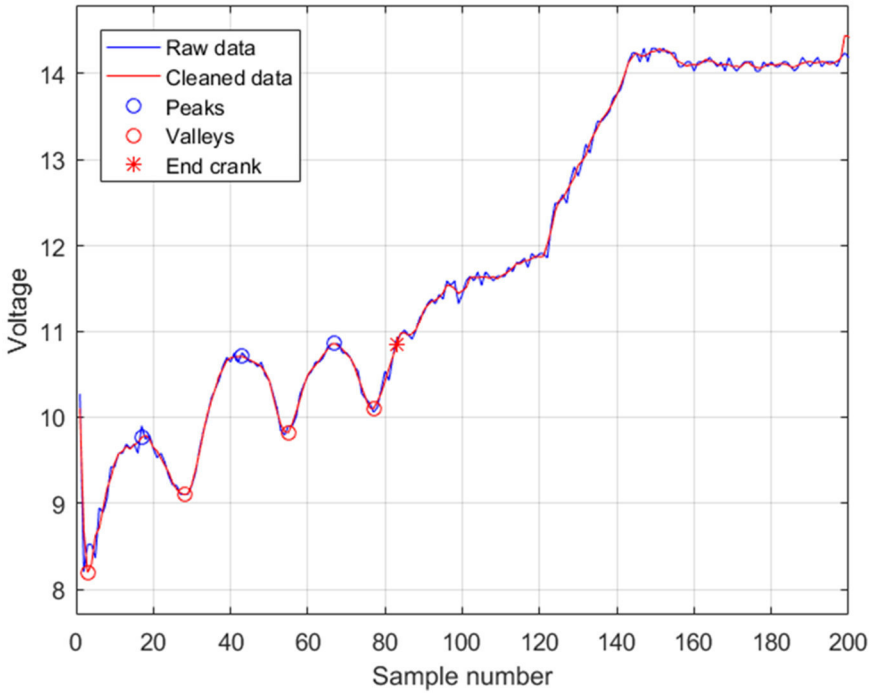

Figure 9-3: CVT signal

As can be seen, next to peaks and valleys the crank ending has to be determined. A proper definition of crank ending is important when using average values over the cranking period. The peaks and valleys of the CVT are determined using a Matlab script which iterates through all the samples. The complete script can be referenced in appendix xxx. A schematic overview of the script is depicted in Figure 9-4.

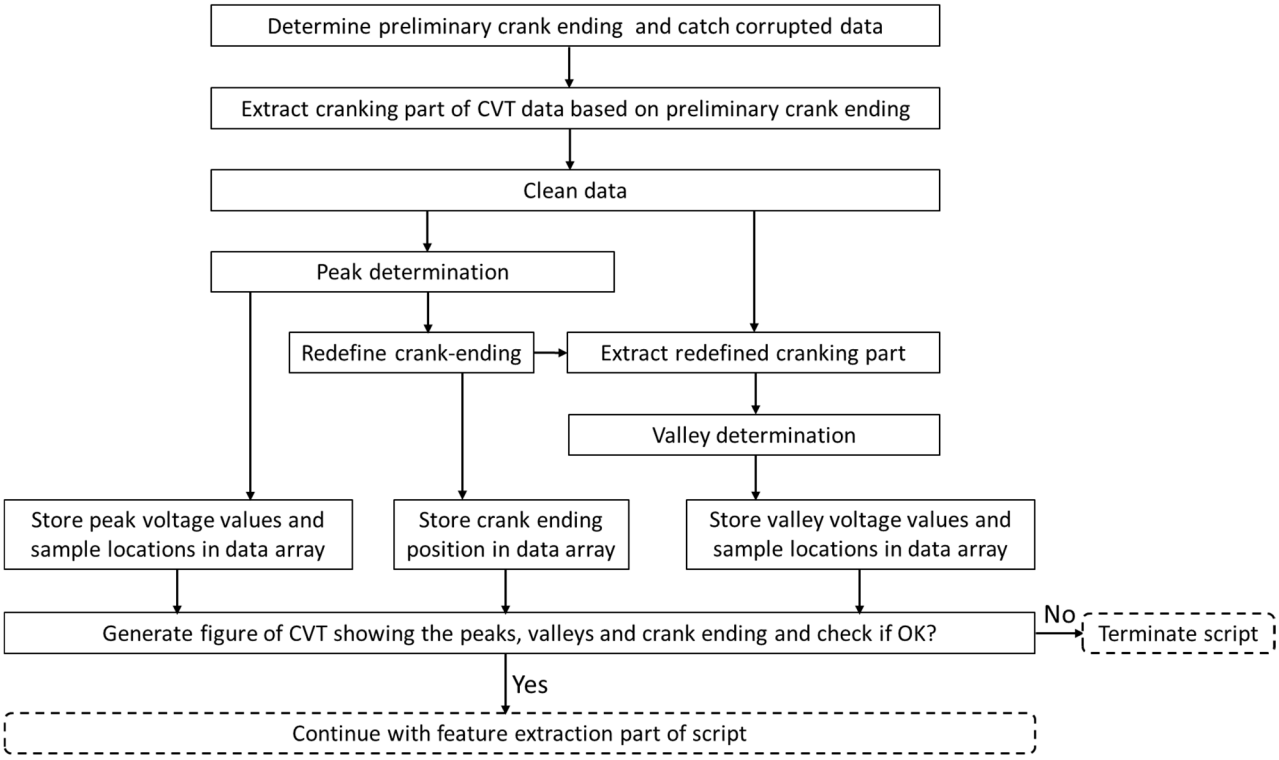

Figure 9-4: Peak, valley and crank ending selection part of script

The blocks of code will be discussed in more detail in in the next paragraphs.

9.3.1 Determine preliminary crank ending and catch corrupted data

In CVT data there is no clear indication of where the end of crank is situated. This part of the script determines a preliminary end of crank from raw uncleaned data. The preliminary crank ending is used to discard unusable parts of the CVT data. Determination of the preliminary crank ending is achieved by a process as depicted in Figure 9-5.

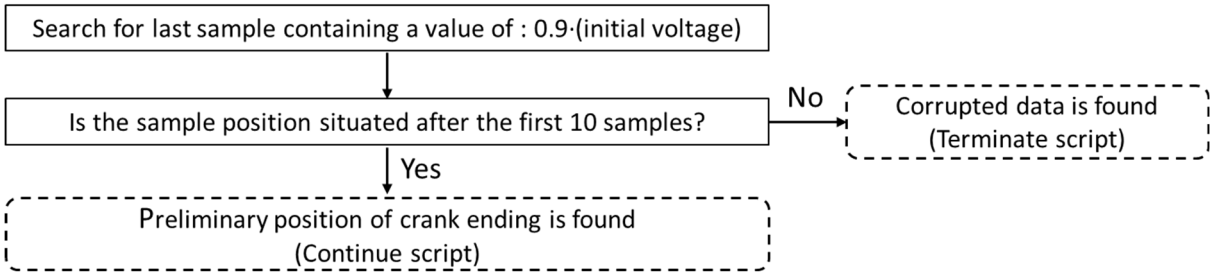

Figure 9-5: Preliminary end of crank determination

9.3.2 Cleaning data

Raw data is cleaned by use of a filter. The filter applies a polinomial fit to smoothen the raw CVT data. The order of polynomial and frame length are adapted to thesignal roughness. The filter settings are determined by a process as depicted in Figure 9-6.

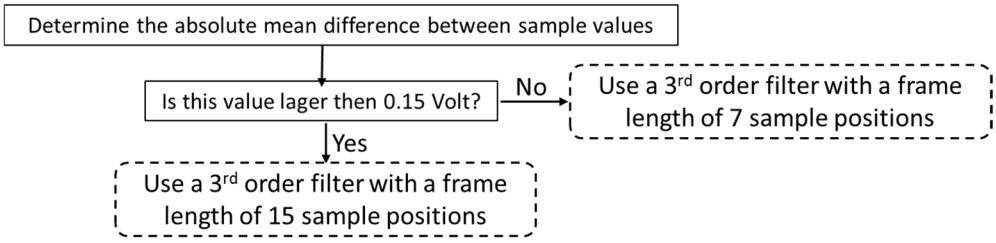

Figure 9-6: Data filter settings

Using this kind of filter smooths the CVT signal, making the peak and valley extraction possible. As depicted the zoomed part of Figure 9-7 the filtered voltage values correspond quite accurately to the voltage values of the original signal.

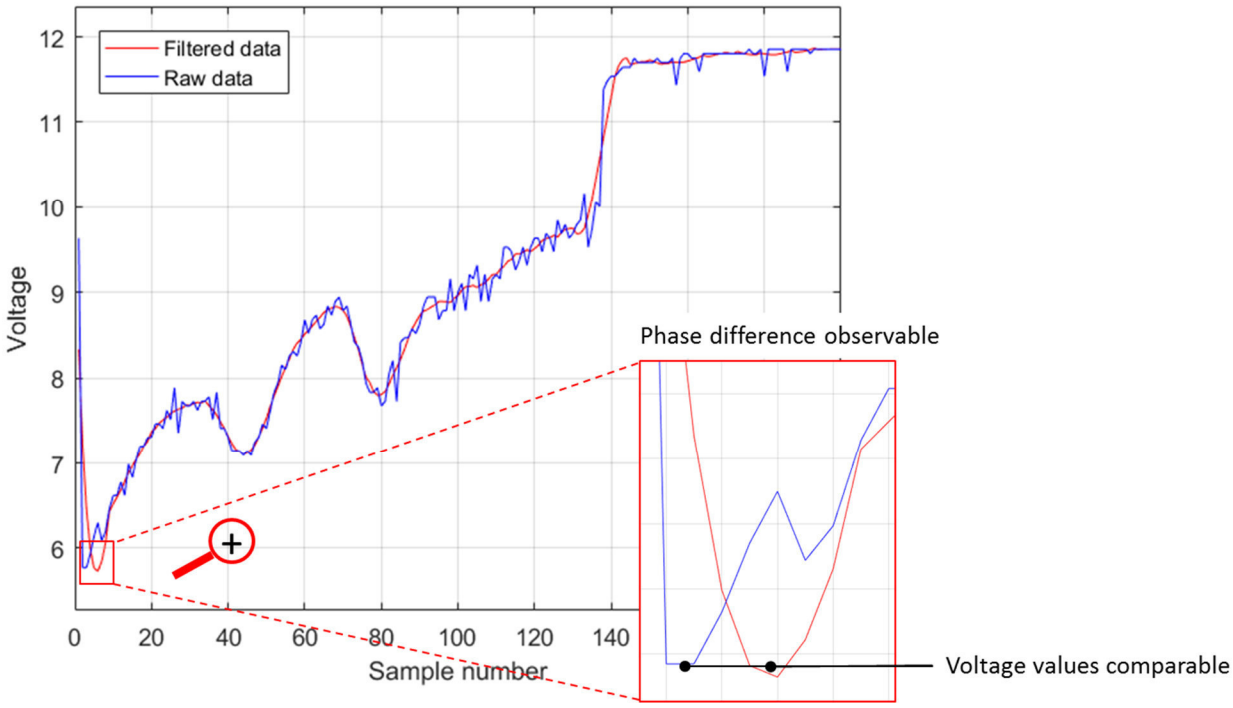

Figure 9-7: Filtered data and phase difference

As can be seen a phase difference is observable around the first and largest valley of the signal. This phase difference is mitigated by applying a higher order fit to the first part of the signal as depicted in Figure 9-8.

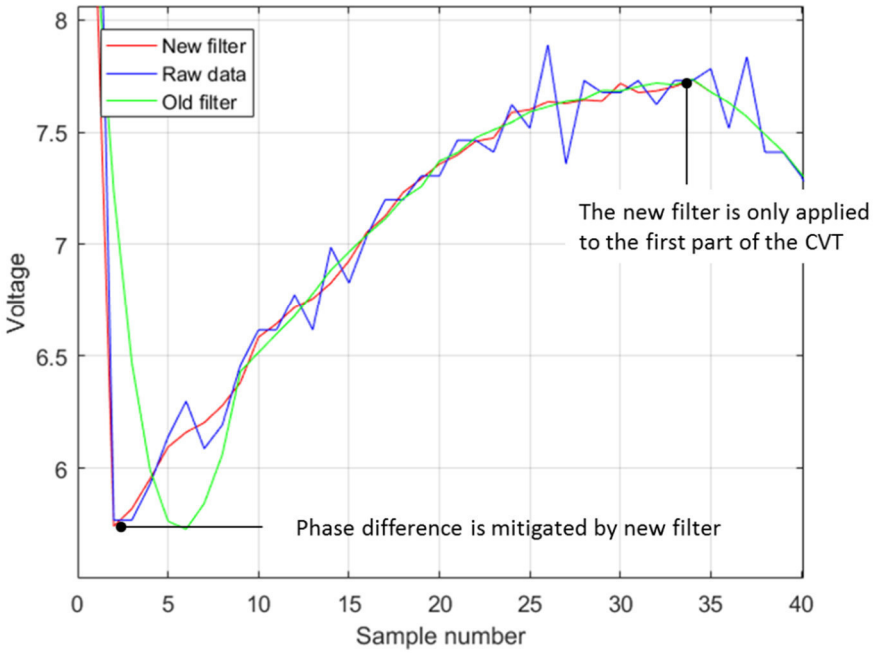

Figure 9-8: mitigation of phase difference

9.3.3 Peak selection

To determine the peaks in the CVT signal a loop iterates through the sample values and selects peaks based on a pre-defined set of rules. The iteration process is depicted in Figure 9-9.

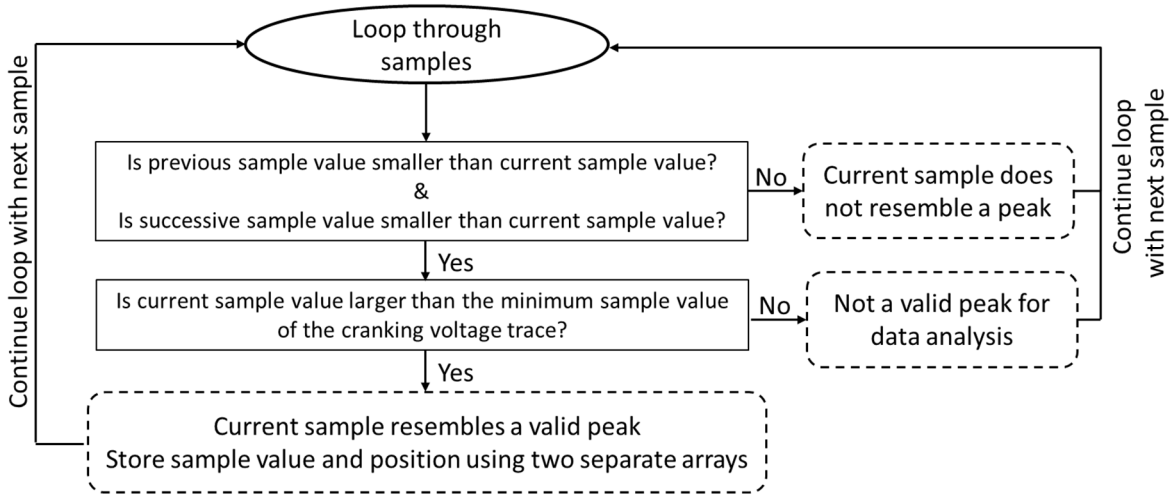

Figure 9-9: Peak selection loop

This iteration will select all peaks existing in the filtered signal as depicted by in Figure 9-10.

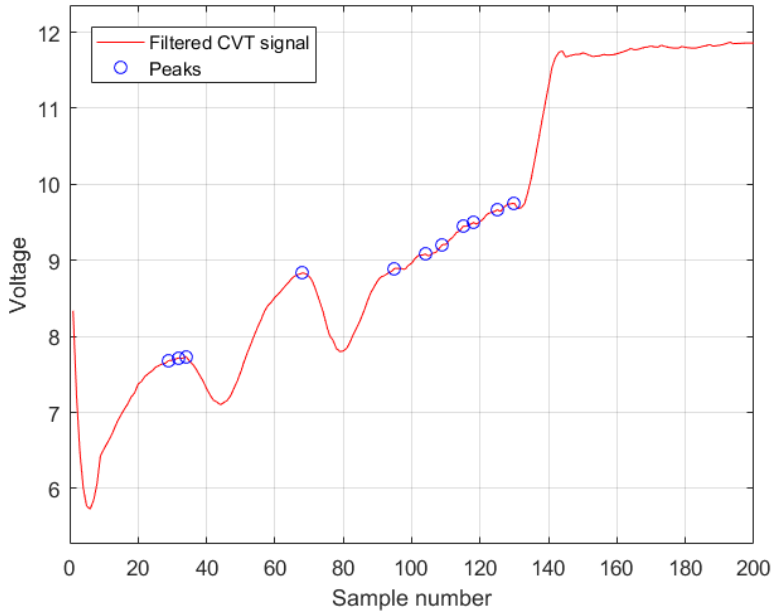

Figure 9-10: Peaks in filtered CVT signal

To obtain single peak values a second loop is executed, which iterates between the peak values instead of all sample values. This process is depicted in Figure 9-11.

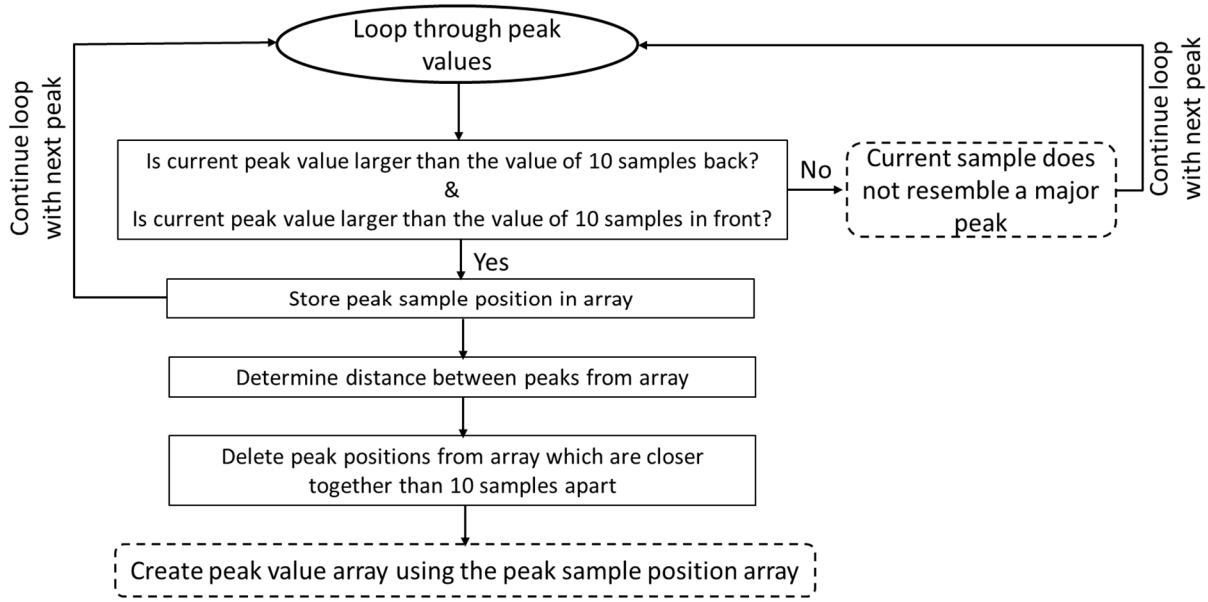

Figure 9-11: Second peak selection loop

Using this second loop single peak values are determined as depicted in Figure 9-12.

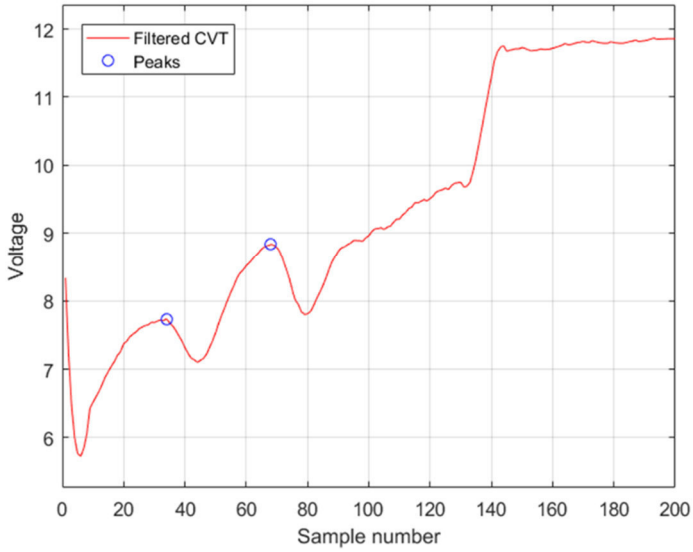

Figure 9-12: Single peaks in filters CVT signal

9.3.4 Redefine crank ending

The peak values are used to redefine the crank ending. The end of crank is a specific point which has to be the same for every crank. Keeping the ignition switch in the cranking position for a prolonged period changes the shape of the CVT as depicted in Figure 9-13.

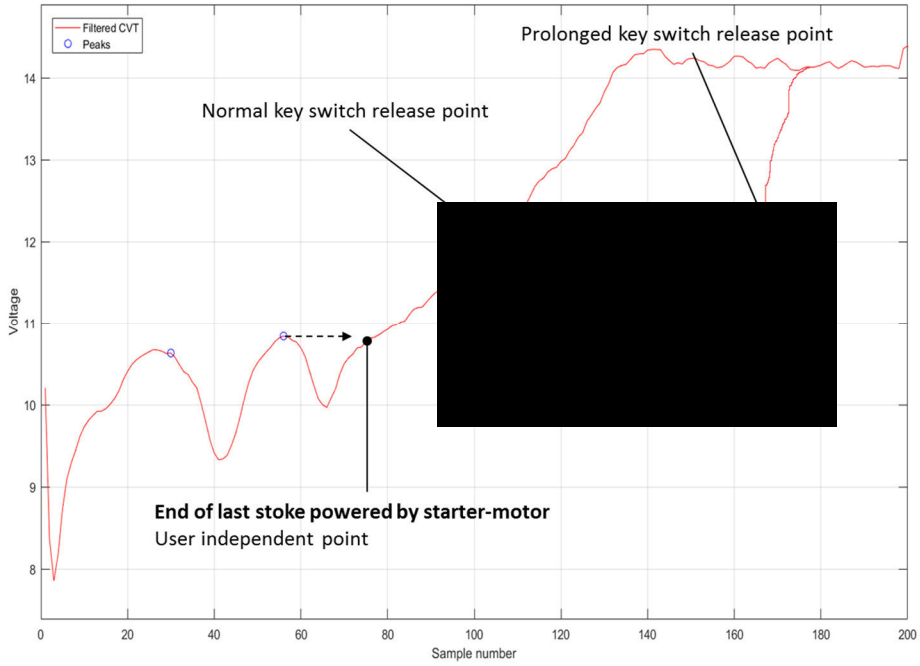

Figure 9-13: User independent end of crank

[redacted]

9.3.5 Valley selection

The valleys of the CVT signal are extracted using the same method as for the peak selection and will not be discussed.

9.3.6 Visual check

Having obtained all peaks, valleys and crank ending s a figure is generated to visually check if all points line up as expected. After the visual check as depicted in Figure 9-14, the script will be continued extracting features using the peaks, valleys and the end of crank.

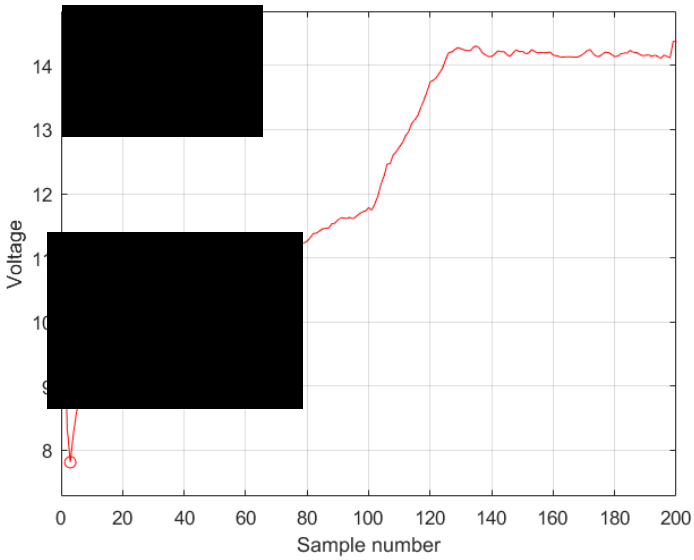

Figure 9-14: Visual check of peaks, valleys and end crank

9.4 Feature extraction

Having obtained all peaks, valleys and having obtained a user independent crank ending features can be extracted based on those points. As briefly explained in section the introduction of chapter 6 features represent common points occurring in ever CVT. The features will be stored in a table of features. Each row of the table of features will contain a set of extracted features belonging to a single CVT. In a later stage the table of features will be used in the data analysis.

9.4.1 Features imported from unprocessed CVT data

Some of the features do not have to be extracted from the CVT but can directly be imported from the CVT data array. Those features are stored in the first positions of the data array as explained in section 7.3.1.2. these features are depicted in Table 9-4.

[redacted]		
The sample rate used to sample the CVT	Temperature of environment.	Voltage while ignition is turned on just before cranking.

Table 9-4: Features imported from unprocessed CVT data

The initial voltage is equal to the battery voltage with ignition on just before cranking as depicted in Figure 9-15.

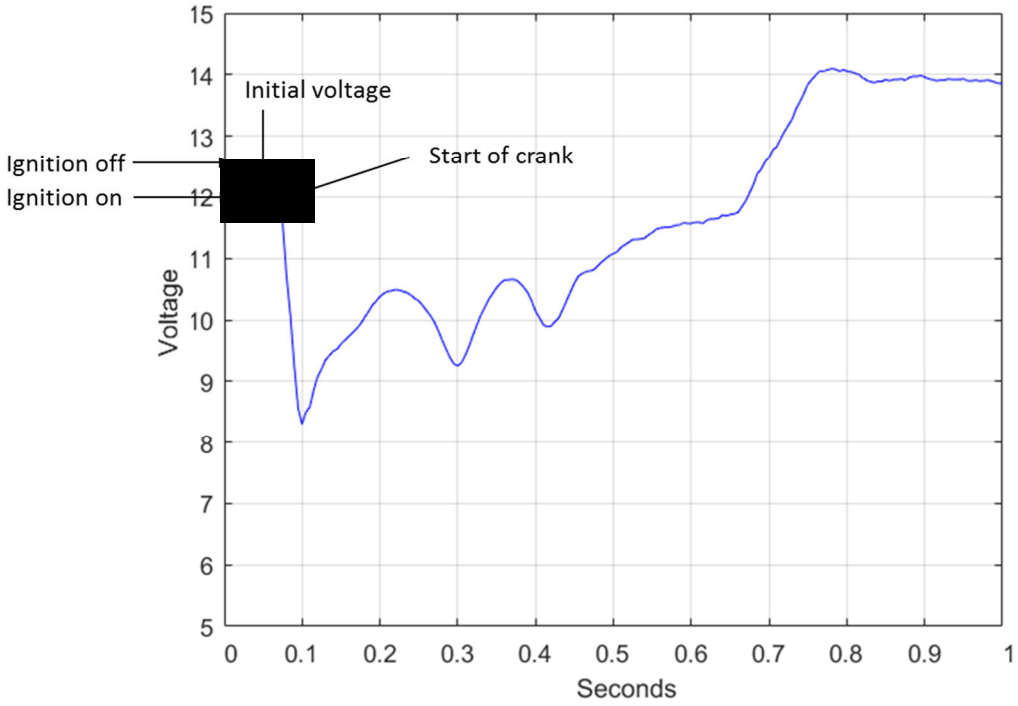

Figure 9-15: [redacted]

[redacted]

8.97 V	10.14 V	NaN	7.53	8.12	8.97

Table 9-5: [redacted]

[redacted]

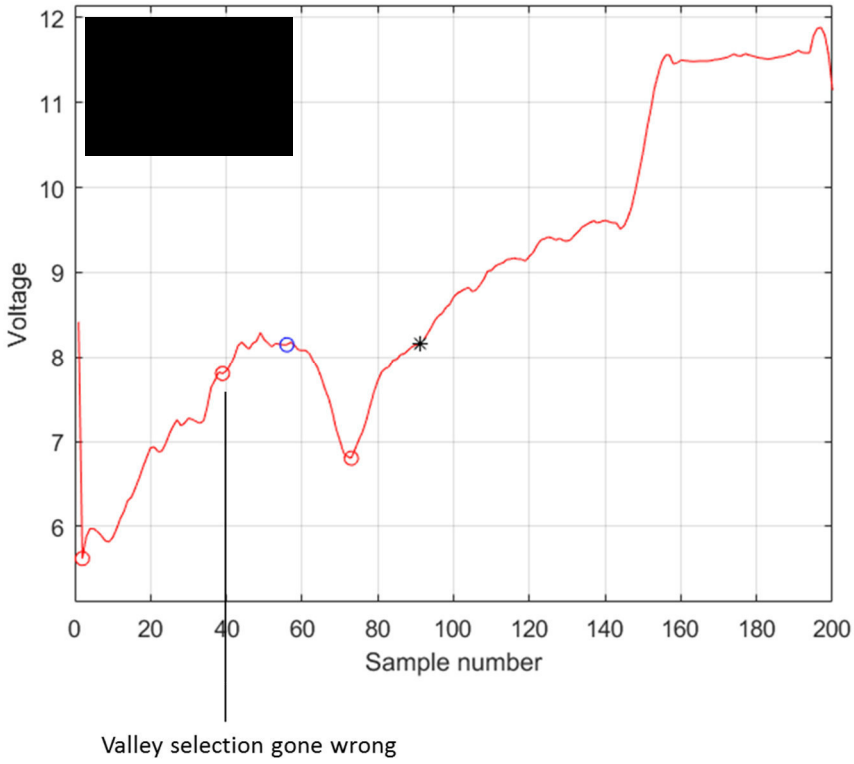

Figure 9-16: Fault in valley selection

[redacted]

[redacted]			
3.62	0,80	8.1	NaN

Table 9-6: [redacted]

[redacted]

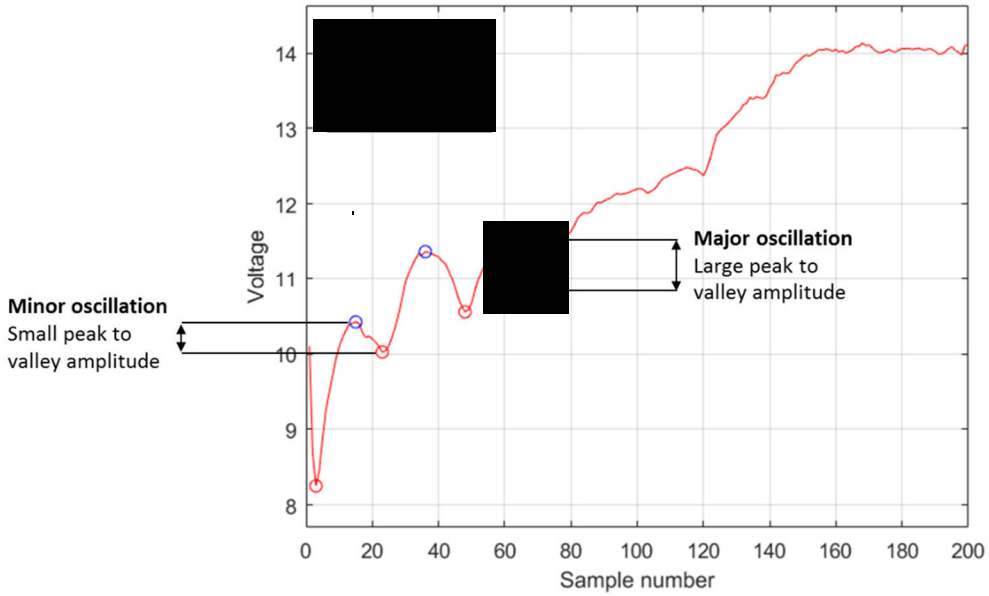

Figure 9-17: Oscillations in CVT

As depicted some CVT's show a minor oscillation at the beginning of the cranking event which is depending on the position of the moving parts inside the engine before crank.

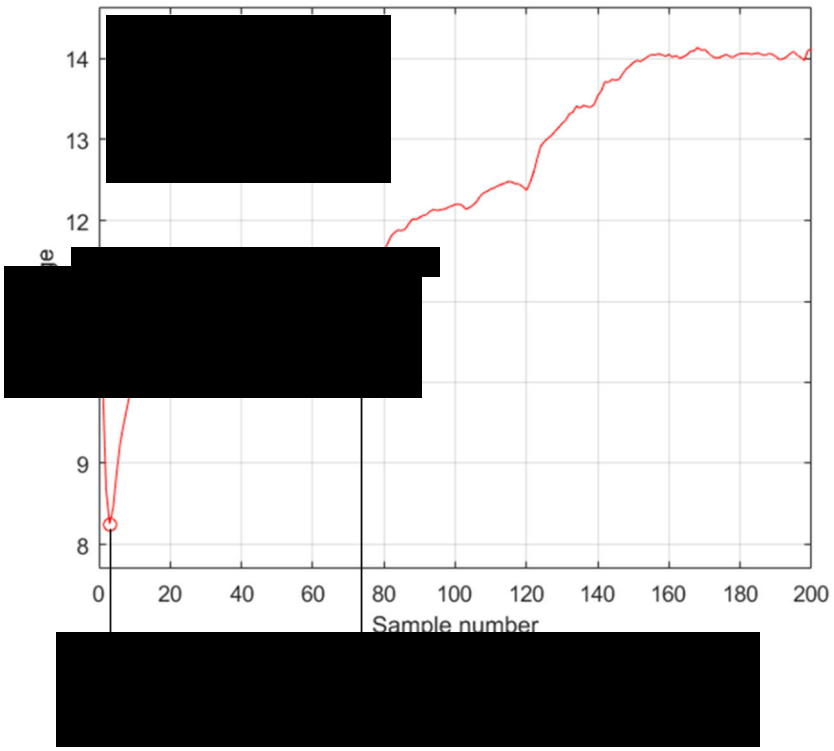

Figure 9-18:

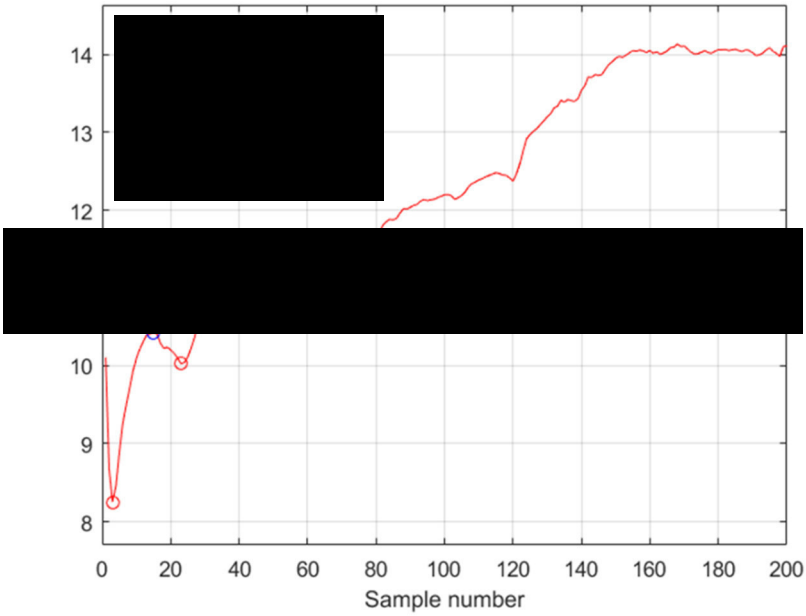

Figure 9-19:



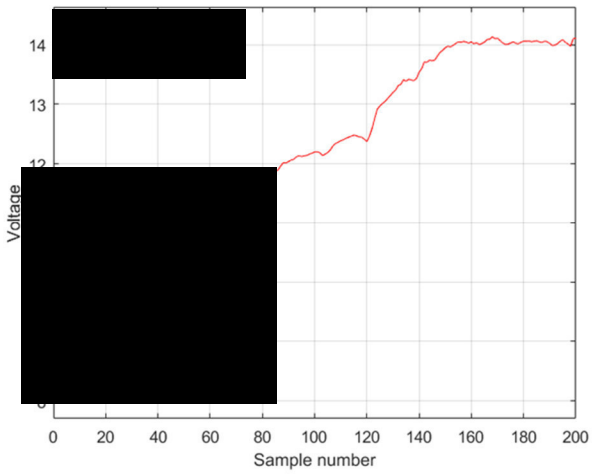

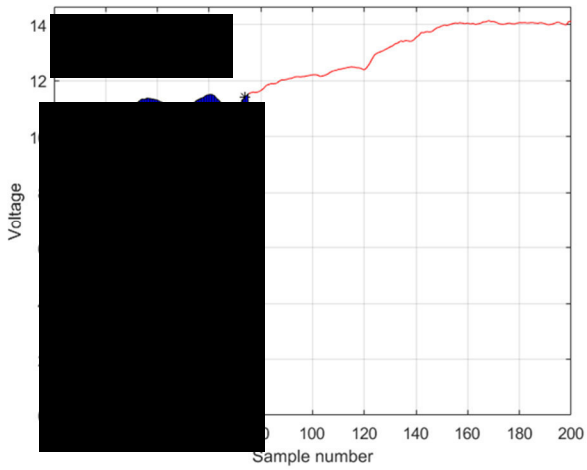

Figure 9-20:

9.4.9 Two areas above CVT

Two areas above the CVT are obtained by a numerical integrating process also using the trapezoidal rule. The two areas are selected for a feature as depicted in Figure 9-21. The integration process

starts at the sample position of the lowest valley and ends at crank end. The areas are relative to the voltage of the highest peak and the initial voltage.

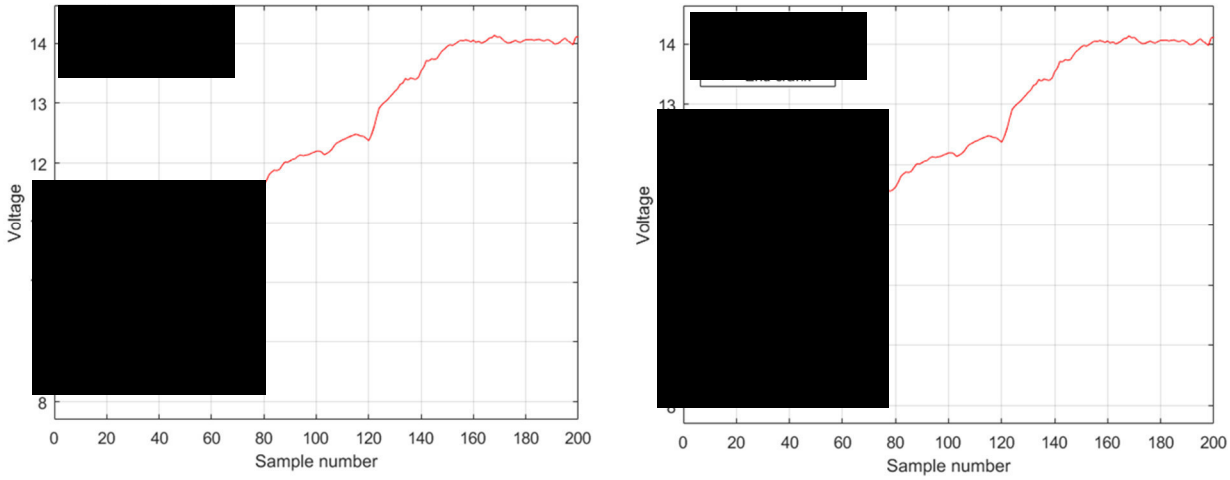

Figure 9-21: [redacted]

[redacted]

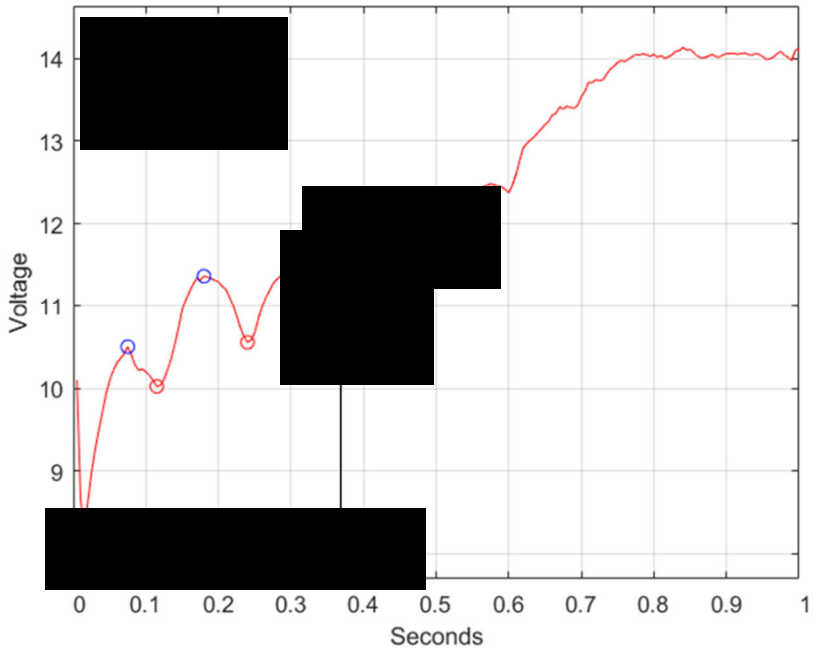

Figure 9-22: [redacted]

[redacted]

[redacted]						
0.02 s	0.12 s	0.24 s	0.08 s	0.18 s	0.31 s	0.37 s

Table 9-7: [redacted]

9.5 Table of features

After the feature extraction process a figure is generated giving a visual representation of most features. This enables a visual check of the feature extraction process. The script will be continued if no flaws are revealed by this visual check. All extracted features will be stored in the table of features. The first column of table of features contains the CVT identification number belonging to the feature set. Each table row contains a unique feature set which is labled using the table of labels as explained in section 9.1. The structure of the table of features is shown in Table 9-8.

CVT ID	[redacted]	abel ..1	Label ..2	Label …n
A060B02	Feature 1	Feature 2	Feature n	Label 1	Label 2	Label n

Table 9-8: Structure table of features

A total of 27 features has been extracted from the CVT signal. The features contained by the table of labels are shown in Table 9-9.

Feature number	Feature	Unit
[redacted]		



Table 9-9: All extracted features

The labels extracted from the table of labels and contained by the last columns of the table of features are shown in table Table 9-10.



Table 9-10: Labels

The complete table can be referenced in appendix xxx

10 Data analysis

This chapter describes the data analysis required to research the existence of a relation between features extracted from the CVT and the battery SOH. As explained in the previous chapter, 27 features are extracted from the CVT. These features will be classified and put through different analyses. In the process of analysis, the unusable features will be removed from the feature set resulting in a select set of features which is most capable of revealing a relation to battery SOH.

10.1 Classifying

One of the first steps in data analysis is classifying the data. Labelled data is obtained and stored in the table of features. Using these labels the data can be divided into separate classes. Since we want to monitor SPH, the aging cycles are used to classify the data. Increasing aging cycles correspond to a decreasing battery's SOH starting at 0 for new batteries. Table 10-1 shows an example of feature classification based on the aging cycles.

CVT				
B000D00	12,55	8,28	6,20	
B000D01	12,49	8,40	6,41	
B000D02	12,44	8,35	6,39	
B015D00	12,81	7,95	5,95	
B015D01	12,58	7,97	6,09	
B015D02	12,59	7,96	6,13	
B040D00	12,43	8,01	5,91	
B040D01	12,43	7,75	6,08	
B040D02	12,44	7,80	5,92	
B060D00	12,44	7,50	5,77	
B060D01	12,37	7,61	5,84	
B060D02	12,58	7,95	6,05	
B075D00	12,02	7,76	5,88	
B075D01	12,15	7,45	5,85	
B075D02	12,17	7,40	5,85	
B090D00	12,14	7,49	5,51	
B090D01	12,23	7,80	5,84	
B090D02	12,18	7,38	5,93	
B125D00	12,47	7,63	5,83	
B125D01	12,32	7,44	5,28	
B125D02	12,32	7,32	5,33	

Table 10-1: Feature classification based on aging cycles

As can be seen each aging cycle class contains three feature sets (rows). This can be explained by the testing procedure. As described in section 8.2. three cranks are performed using the same battery which has endured a particular number of aging cycles.

The aging cycles can be linked to the batteries SOH using the three SOH estimators and upcoming failure indicator as described in section 9.1.1. and section 9.1.2. Gathering this information in one

table created the a personal table of labels belonging to a single battery as described in section 9.1. The table of labels enables the aging cycles to be linked to battery SOH and upcoming failure indication shown in Table 10-2.

[redacted]

Table 10-2: Table of labels belonging to battery B

Using this table the aging class in which a battery was about to fail can be determined. For battery B which is depicted in the table, the aging class corresponding to a failing battery is 125. To generate a first indication on a relation between features and battery SOH or cranking performance labelled pairs of features can be plotted in a scatterplot as depicted in Figure 10-1.

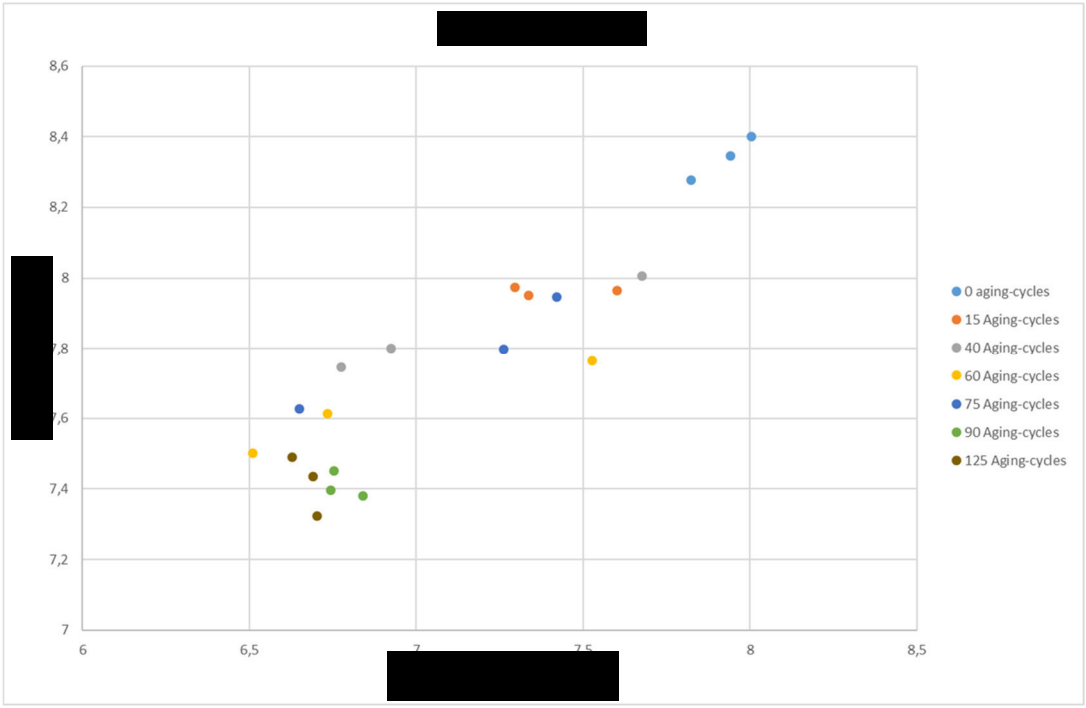

Figure 10-1: Labelled scatterplot of pair of features

Generating these kinds of plots for all pairs of features has been done which creates a first indication of a possible relation, but more importantly it helps to establish a feeling with the data. However, this approach is not very scientific and highly susceptible to misinterpretation of the data. For example scatterplots make it difficult so see relations originating from more than two features. Before generating scattered plots like this it is very useful to conduct an analysis on the feature set

itself. After analysis all unusable features can be discarded leaving fewer and better motivated options to generate scatterplots and continue the data analysis.

10.2 Feature analysis from a data perspective

[redacted]

10.2.1 Frequency of occurrence

As one can imagine not all features will occur in every CVT and are therefore missing in the feature set belonging to that CVT. Some features will occur in every CVT and have a 100 % frequency of occurrence, while other features will have a much lower frequency of occurrence. The frequency of occurrence belonging to a feature, is a first indicator for its usability. Figure 10-2 depicts the frequency occurrence of a selection of features. An overview of the complete feature occurrence can be referenced in appendix xxx.

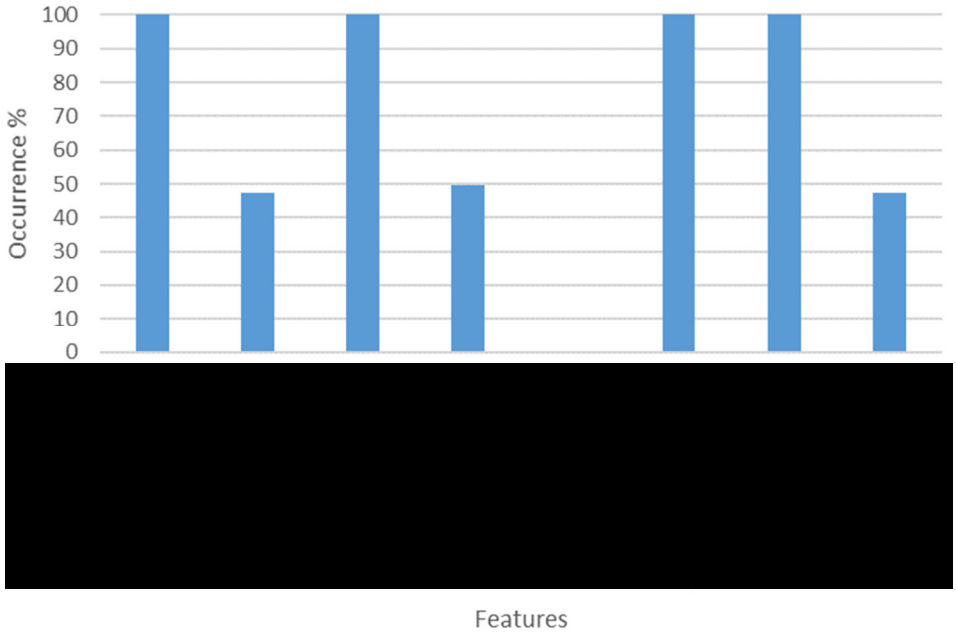

Figure 10-2: Percentage of feature occurrence

We like to have a robust feature set filled with features occurring in every CVT. All features having a less than 100% occurrence are removed from the table of features:

[redacted]

Table 10-3: Removed features

This leaves a smaller feature set which is subjected to further analysis

10.2.2 Correlation coefficient between features

Figure 10-1 depicts pairs of features revealing a trend line with an almost linear behaviour. On first sight this looks quite usable, but the linearity in the trendline is indicating that the features are likely to be highly correlated to each other. High correlation between features means the change in one feature highly effects the change in the other feature. To investigate the correlation between the features a correlation table is constructed showing the correlation between all features. Table 10-4 shows an example of this correlation table. The complete tables can be referenced in appendix xxx.

[redacted]	[redacted]			
[redacted]				
	0.			
	0.	0.		
	0.	0.	0.	
	0.	0.	0.71	0.74
	0.	0.	0.65	0.
	0.	0.	0.06	0.
	0.	0.	0.23	0.
	0.	0 48	-0.22	-0.60
	0.	0.		0,70
	0.	0.	0.70	
	0.	0.	0.53	0.

Table 10-4: Correlation Coefficient matrix

The correlation is expressed using normalized values in a range of $-1 \leq 0 \geq 1$. The upper and lower limit indicating a positive or negative one to one correlation (they are identical) and zero meaning indicating no correlation. Crossing the correlation of all features in a table will create a diagonal of ones on the crossing point of two identical features. If other ones are present outside of the diagonal it means one of the two crossed features is redundant and can be eliminated from the feature set. The redundant features removed from the feature set are depicted in Table 10-5.

[redacted]

Table 10-5: redundant features

After the removal of these redundant features a smaller feature set remains for further examination.

10.2.3 Standard deviation

The next step is to discover if the features reveal a certain change. If features remain almost constant while other features are changing with battery SOH they cannot be linked to the failure

process. To indicate the change of a particular feature, the standard deviation is computed for all features left in the feature set as depicted in Figure 10-3.

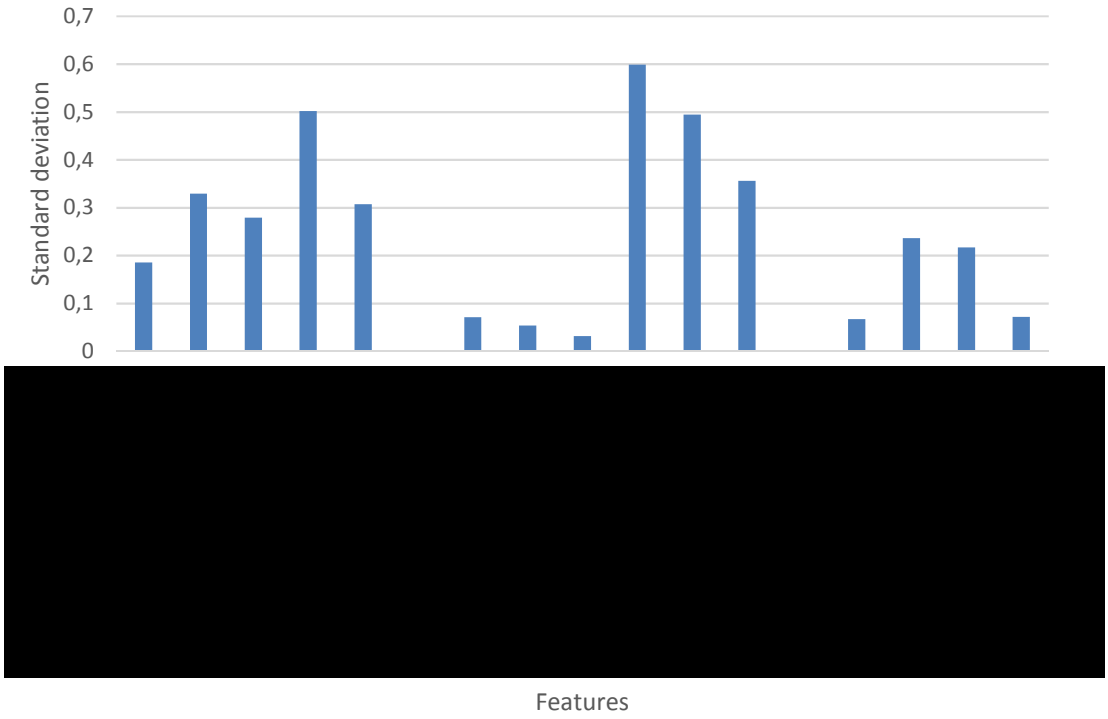

Figure 10-3: Standard deviation

[redacted]

Table 10-6: 10 remaining features

When looking from a data perspective, these remaining features show potential. But If these remaining features show any relation to the battery's SOH still has to be investigated.

10.3 Feature analysis from a relation perspective

A new level in the data analysis process is reached. In the previous paragraph features have been discriminated on their usability looking from a data perspective and are removed from the data set. From now on features will be discriminated on their relation to failure indicators, battery SOH and cranking performance.

10.3.1 Feature correlation with failure indicators

The correlation between the features and the failure indicators is investigated. All 10 remaining features are correlated to the three SOH estimators as explained in [redacted] contradiction to section 10.2.2, we are now looking for a high correlation. In this case high correlation coefficients are indicating a high correlation between features and failure indicators, meaning they can be used for failure indication. Figure 10-4 depicts the correlation coefficients of the remaining features.

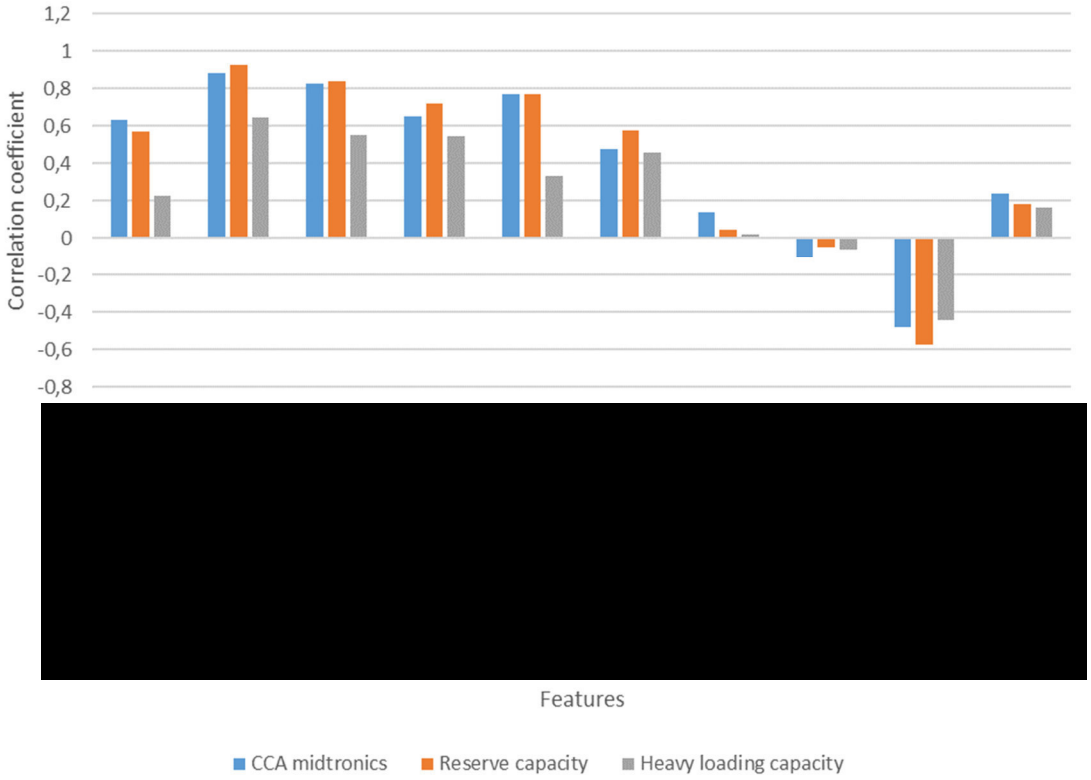

Figure 10-4: Correlation to failure indicators

[redacted]

10.3.2 Feature value change over the cycle aging classes

The 7 remaining features show a certain behaviour when they are changing. Ideally feature values show a steady change in one direction. As explained features are divided into different classes. Per class three data points will be present originating from three cranks. Within these classes the change has to be minimal. If there exists a large change within a class, the feature shows inconsistent behaviour and is probably unusable. In other words: we want to see minimal change within a class,

but a steady change between the classes. Figure 10-5 depicts the feature values within their aging cycle classes.

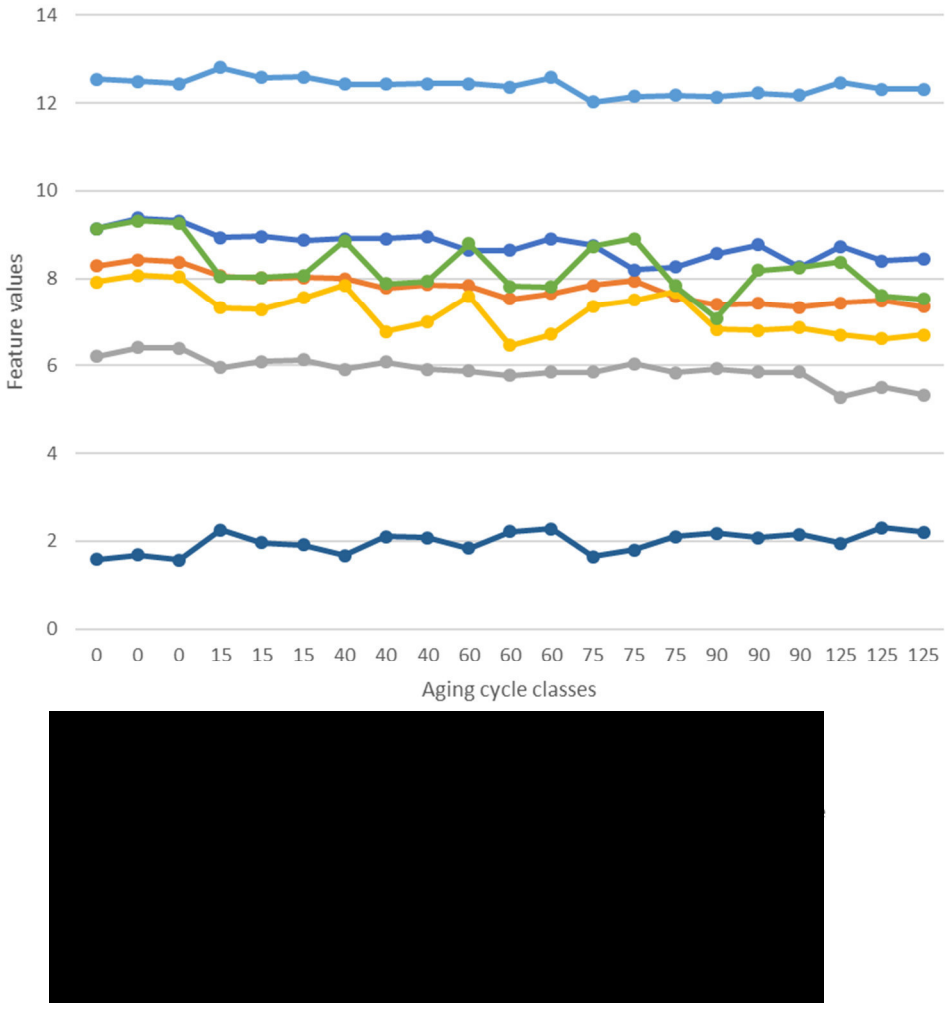

Figure 10-5: Feature change behaviour

As can be seen some features are inconsistent within the classes and do not reveal a steady state change over the aging cycles. Before removing these features from the data set further examination is needed.

10.3.3 Linear regression solving for aging cycle classes

To indicate the contribution of the features to the aging cycle classes, a linear regression is executed using the aging cycle classes as the dependent variables and the features as independent variables (regressors). The resulting regression coefficients indicate the degree of contribution of a particular feature, they can be thought of as weighing factors . Figure 10-6 depicts the linear regression coefficients of the 7 left over features:

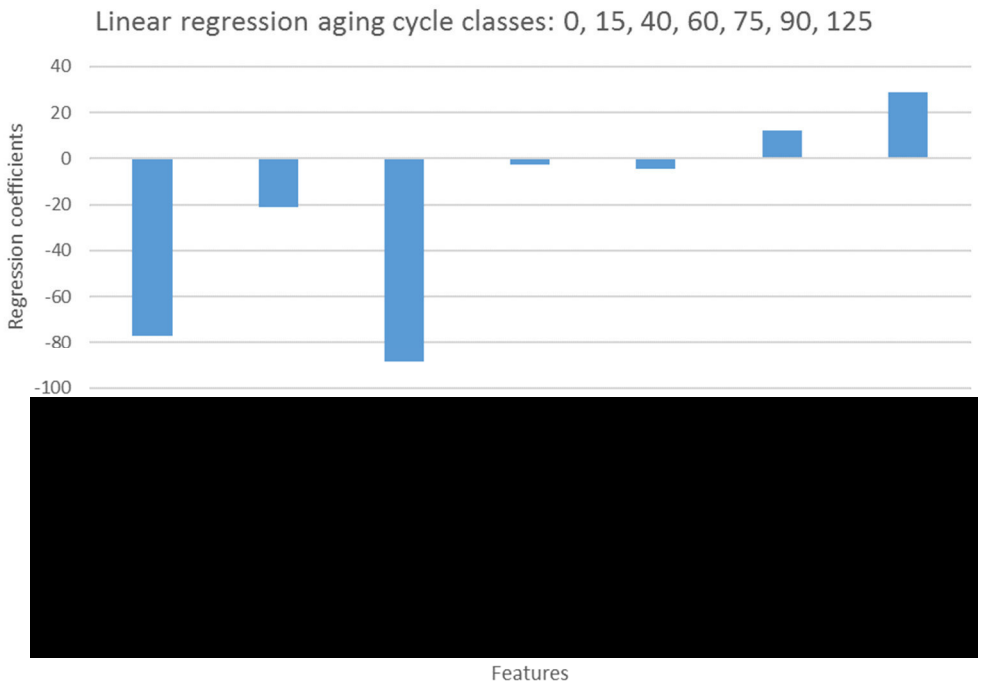

Figure 10-6: Linear regression coefficients

[redacted]

10.3.4 Linear regression solving for 3 classes

Three classes can be defined using a combination of aging cycles, failure indicators and the extra cranking performance test. The three classes: new, middle-aged and failing, will be used in the linear regression as dependent variables while the features will be the regressors. Table 10-7 shows how these classes are constructed.

[redacted]

Table 10-7: Three classes: new , middle-aged and failing

Performing a linear regression and solving for those three classes should reveal the features most capable of discriminating between new, middle -aged and failing batteries. Figure 10-7 depicts the regression coefficients based on the three classes.



Figure 10-7: Regression coefficients solved for 3 for: new, middle aged and failing



10.3.5 Linear regression SOH estimators

Three SOH estimators can be mapped to the aging cycles as described in section 10.1. These SOH estimators provide a better indication of the battery's SOH over the cycle-aging process. Applying a linear regression and solving for this SOH estimators will provide a better understanding of features capable of SOH prediction.

Internal resistance

As described in section 4.4.1.1 is an importand SOH estimator which increases over battery life. The table of labels contains CCA values measured by the Midtronics device. As depicted in Figure 10-8, the internal resistance is directly and negative related to the CCA values measured by the Midtronics device.

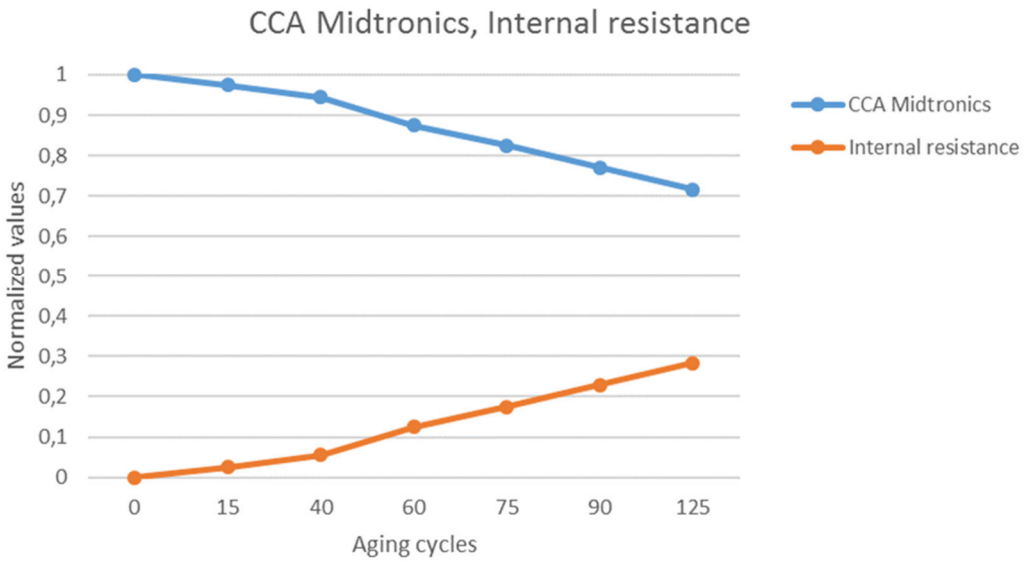

Figure 10-8: CCA , Internal resistance versus service life

The internal resistance reveals a steady increase over battery service life with a marginal steeper incline at the end of service life. Due to this steady increase it is hard to predict an upcoming battery failure, but it can be argued that a 30% increase indicates the end of service life. Applying a linear regression and solving for the internal resistance reveals the features most related to the increase of the internal resistance.

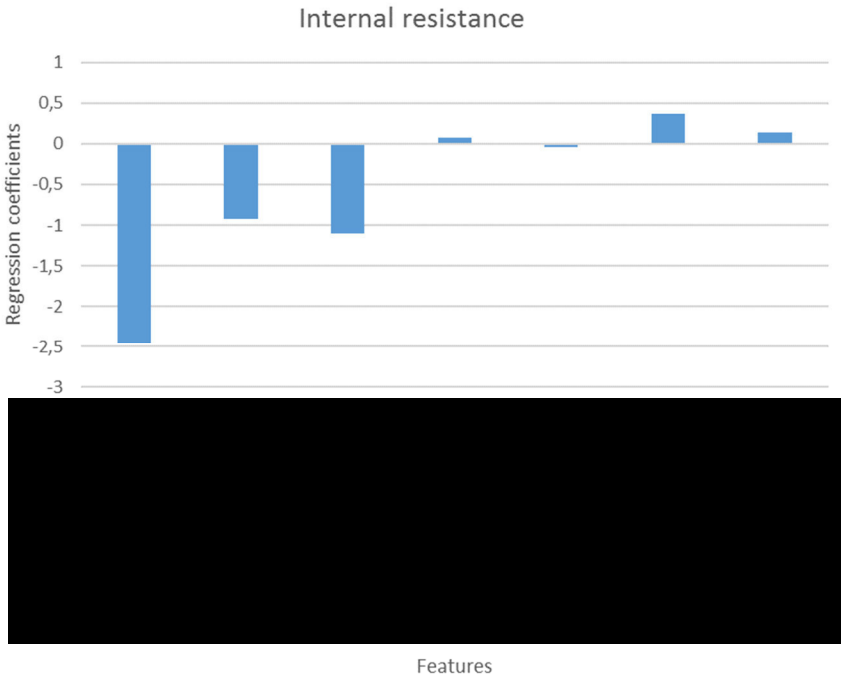

Figure 10-9: Linear regression coefficients internal resistance

[redacted]

negative relation meaning the internal resistance and voltage values change in opposite directions (both are decreasing while the internal resistance is increasing). The decrease in voltage can be explained by ohm's law, which explains an increasing resistance will decrease voltage values caused by a voltage drop over this resistance.

Reserve capacity

This failure indicator is most related to the effective capacity of the battery.

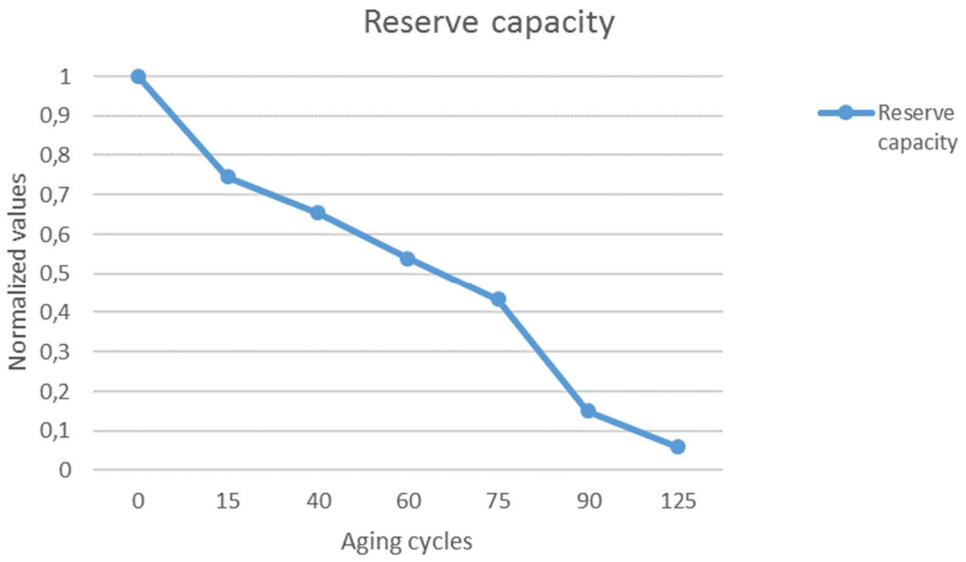

Figure 10-10: reserve capacity

The effective capacity is gradually and steady decreasing over battery life. Therefore this SOH indicator is very useful to see a decrease in battery SOH instead of only a prediction on failure. Applying a linear regression and solving for the reserve capacity will reveal the features most related to the reserve capacity and therefore to a steady decrease in SOH.

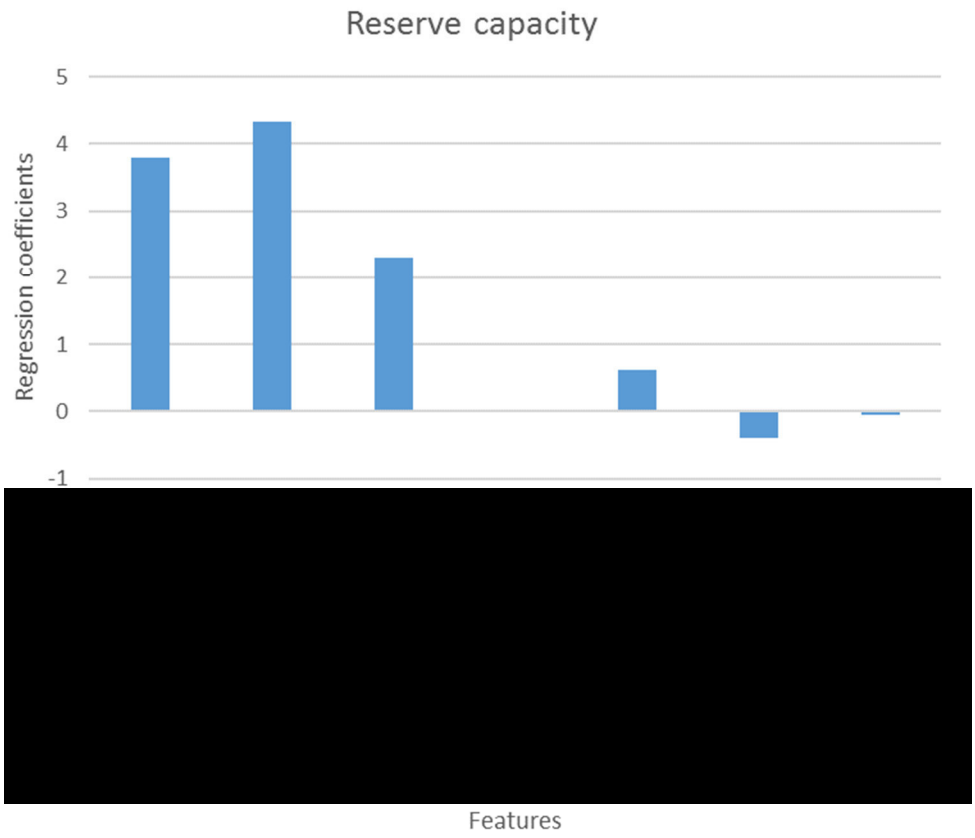

Figure 10-11: Linear regression coefficients reserve capacity

[redacted]

Heavy loading capacity

This is also a capacity based SOH indicator, but this one is most related to the battery's cranking performance since a cranking event is loading the battery very heavily. The heavy loading capacity first shows a small decrease, before getting larger and is dropping very steeply at the battery's end of service life as depicted in Figure 10-12.

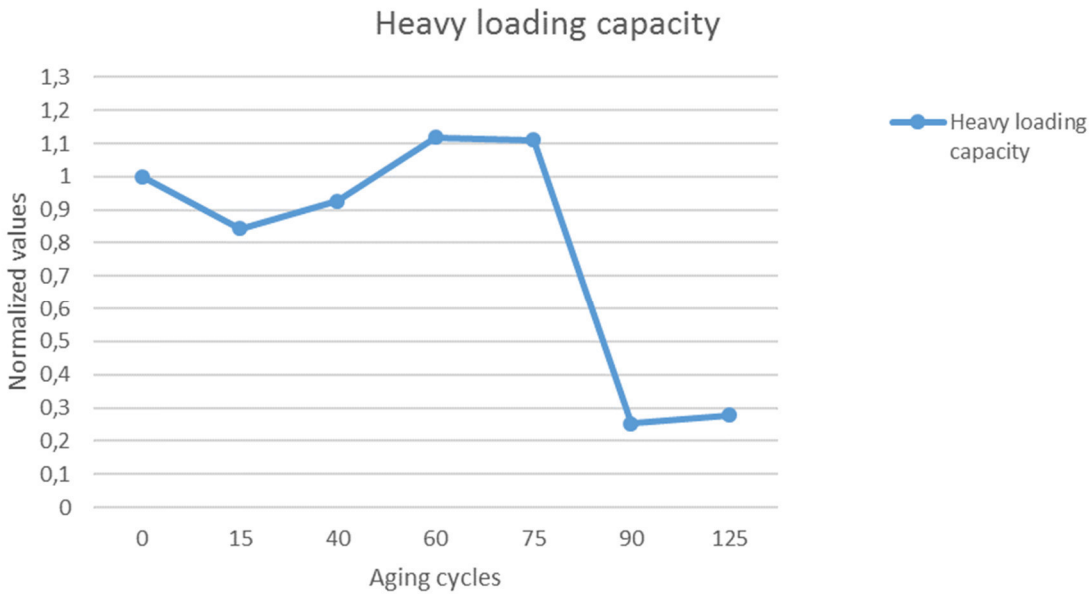

Figure 10-12: Heavy loading capacity

As can be seen there exists a steep decrease of the heavy loading towards the end of battery service life. According to the heavy loading capacity the batteries first start to perform better and have a harsh decrease in performance towards the end of service life. The behaviour is typical for this type of batteries. The increase in performance is caused by the activation of the electrochemical processes after first use. When electrochemical processes are no longer supported by the active materials (battery is worn out) a quick failure is observed. This is one of the reasons why it is hard to predict an upcoming battery failure. As explained the heavy loading capacity mimics this behaviour and is therefore one of the best SOH predictors for batteries used for SLI applications. Applying a linear regression and solving for the heavy loading capacity reveals the features most related to the heavy loading capacity and therefore most capable of predicting an upcoming battery failure.

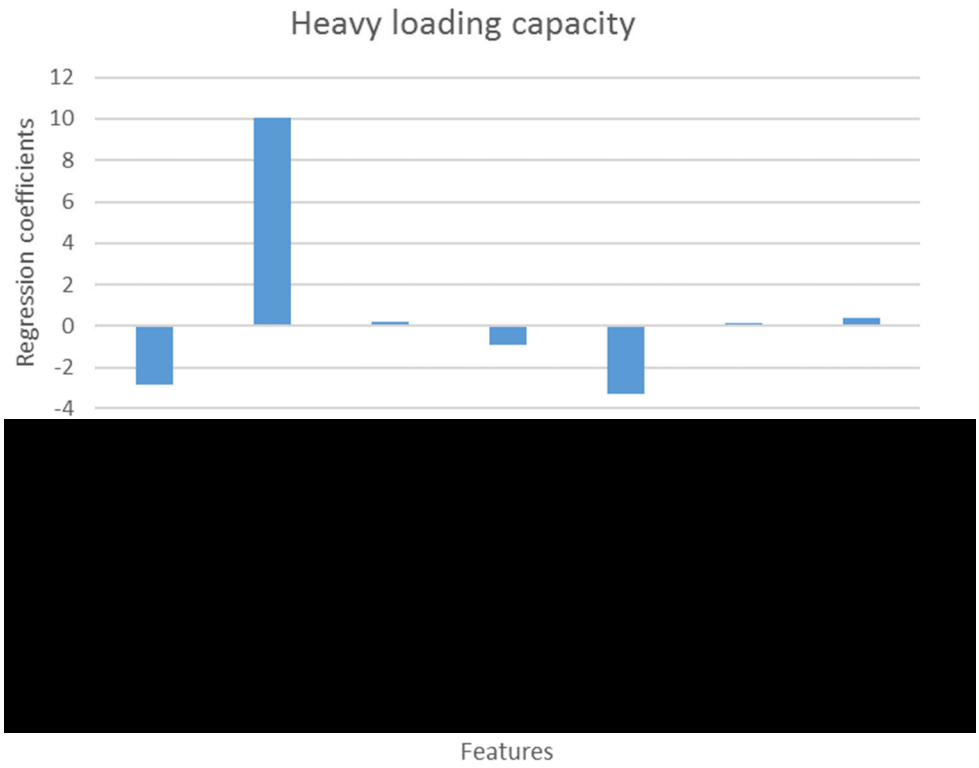

Figure 10-13: linear regression coefficients heavy loading capacity

[redacted]

10.3.6 Selected features

[redacted]

10.4 Relation analysis

In the preceding paragraphs the we obtained three features most related to the SOH indicators. The existence of a relation between these features and batty SOH related to cranking performance will be investigated in this paragraph. As described in the previous paragraph the three features left compromise: [redacted]

10.4.1 3d plots

To generate a first indication and to visualize the behaviour of this set of features, they are mapped inside a three-dimensional graph. The mapping creates data points where the feature values intercept each other. The data points are colour marked according to their cycle aging class as depicted in Figure 10-14.

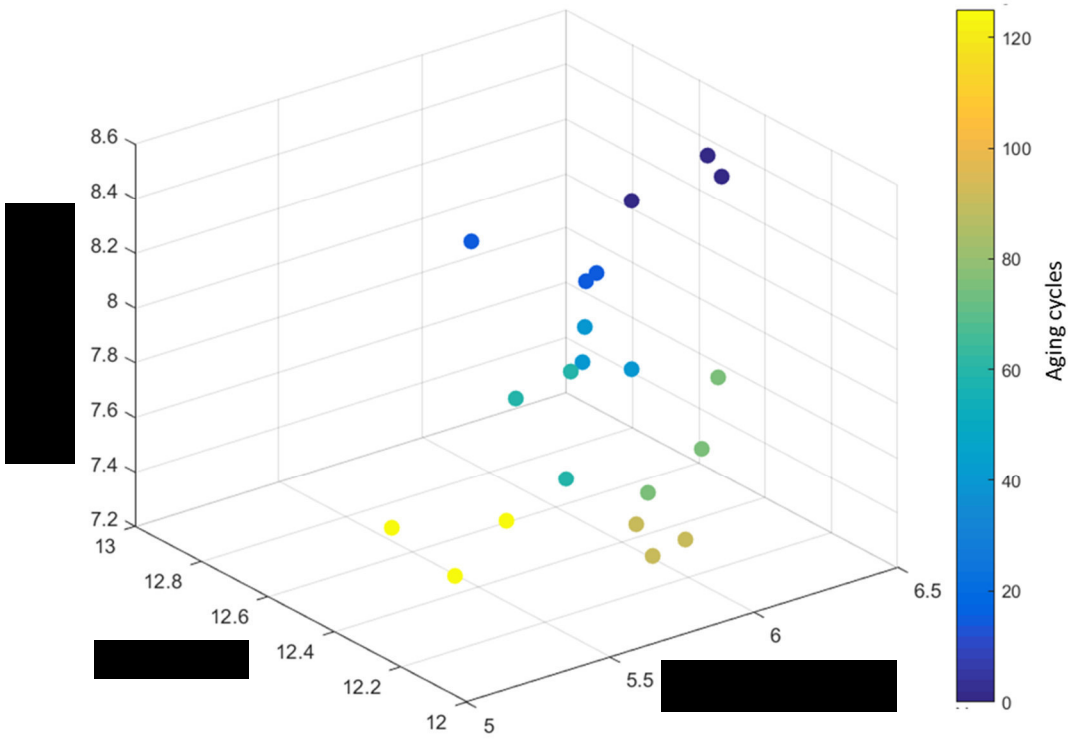

Figure 10-14: 3D scatterplot

[redacted]

10.4.2 Plotting pairs of features

Using features contained by the feature set to make pairs, yields to three possible combinations. The combinations are greyed out in Table 10-8. The correlation between a pair of features is also shown.

[redacted]	[redacted]	
[redacted]	0,49	
	0,23	0,81

Table 10-8: Pairs of features with their correlation coefficients

As can be seen all combinations have a positive correlation coefficient smaller than 1. This means there is no one to one relation between these features, indicating they will behave differently from each other. The greyed out combinations will be used to create three two dimensional graphs.

[redacted]

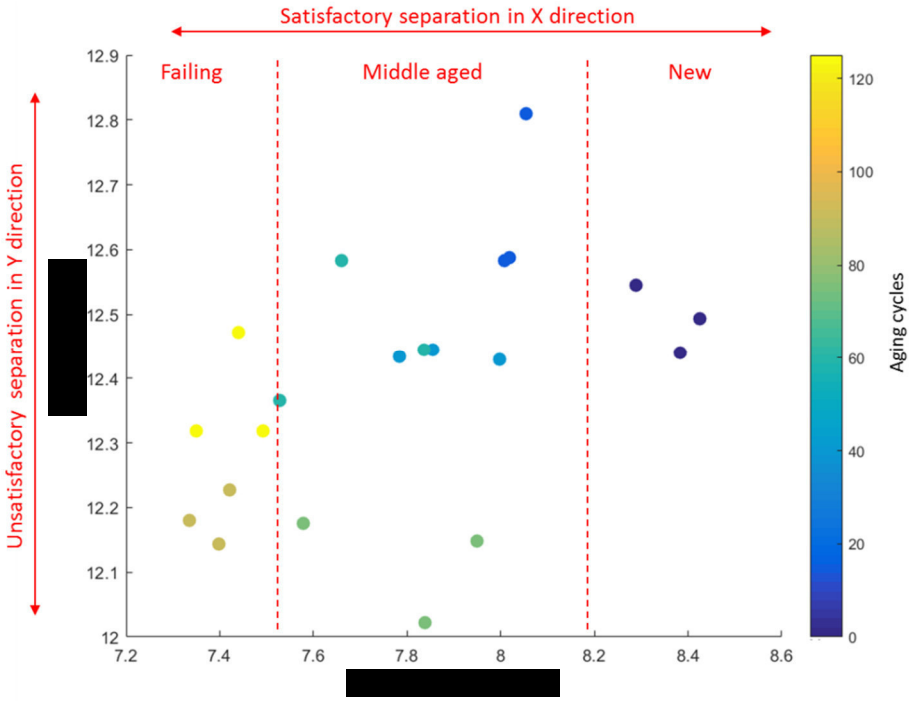

Figure 10-15: [redacted]

[redacted]

[redacted]

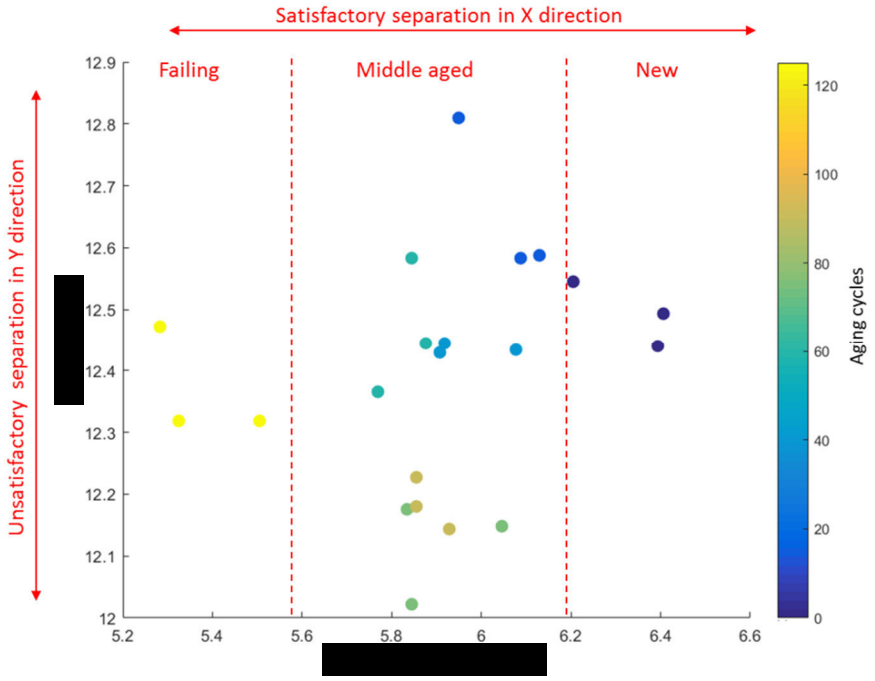

Figure 10-16: [redacted]

[redacted]

[redacted]

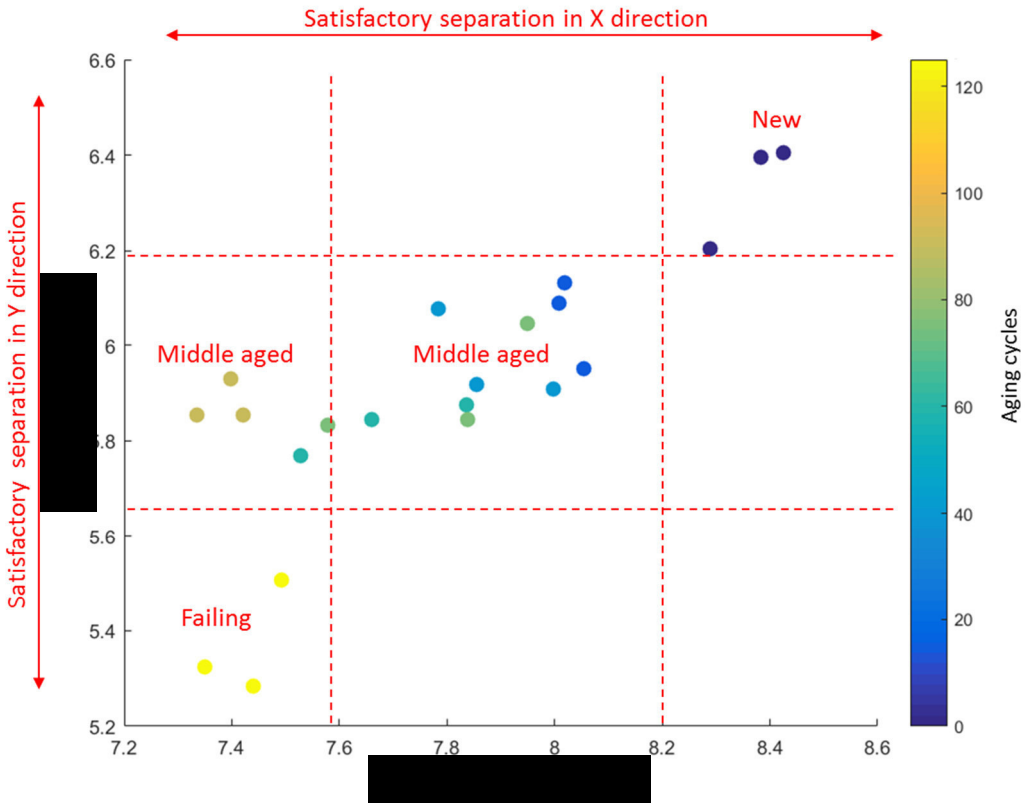

Figure 10-17: [redacted]

[redacted]

10.5 Chosen pair of features

[redacted]

10.5.1 Motivation considering polarisation effects

Section 2.2.2 describes the polarisation effects occurring in working cells. These effects will also occur in energy producing batteries since they are built-up from these cells. A battery used in a cranking event is producing energy and therefore susceptible to polarisation effects. A decreased SOH will increase the polarisation effects. The polarisation effects describe a deviation of the voltage and since both selected features are based on voltage they have a close relation to the polarisation effects.

[redacted]

[redacted]

[redacted]

[redacted]

[redacted]

10.5.2 Motivation considering battery SOH estimators

Battery failure is caused by a combination of failure mechanisms as described in section 4.2. Progression of the failure mechanisms is unobservable on the outside of the battery and therefore it is difficult to determine its SOH. As described in section 9.1.1 resistance and capacity based SOH estimators can be used to for estimations on battery SOH. The features selected show strong relations with these estimators.

[redacted]

[redacted]

10.5.3 Motivation considering the cranking system

As explained in section 5.1, the cranking system comprises an electric starter-motor. This motor influences the voltage values measured during a cranking event. Both selected features can be related to the functioning of the starter motor.

[redacted]

10.5.4 Temperature dependence

As described in section 8.2.2, a battery temperature difference was introduced to discover the existence of a temperature dependence. As depicted in Figure 8-5, the test battery pool contains two control batteries of different temperature. [redacted] values of those two batteries reveals a temperature dependence as depicted in Figure 10-18.

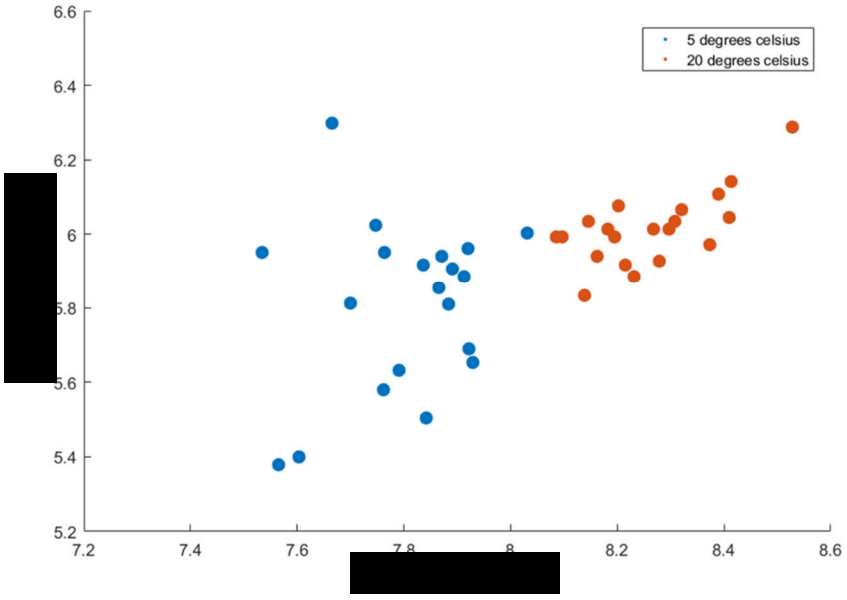

Figure 10-18: Temperature dependence



11 Continuous state of health monitoring and failure warning

This chapter describes the implementation of the selected features in a continuous battery SOH monitoring method. There will be investigated if the method is capable of generating an upcoming battery failure warning. A battery's fail rate is very dependent on usage and temperature as explained in section 4.3. Therefore every battery engine combination behaves differently and will generate different feature values. To make results comparable all feature values are normalized. This is done by scaling them to a baseline value. The normalized values will be used for a SOH monitoring method, capable of generating an upcoming failure warning.

11.1 Baseline

Batteries can be compared to living organisms having a certain life span which is strongly dependent on the healthiness of the living circumstances. Because of this, every battery engine combination will



this baseline will create normalized values which are still capable of revealing a change. The baseline is created using averaged values belonging to new batteries which endure their first cranking events. The personal baseline of test battery B in combination with the diesel engine is shown in Table 11-1.

CVT ID	[redacted]		
B000D00	8,29	6,20	
B000D01	8,42	6,41	
B000D02	8,38	6,39	
Baseline	8,37	6,33	

Table 11-1: Baseline battery B + diesel engine

All feature values belonging to cranks after the baseline value was captured are scaled to this baseline creating normalized values as shown in Table 11-2.

CVT ID	[redacted]		
B015D00	0,96	0,94	
B015D01	0,96	0,96	
B015D02	0,96	0,97	
B040D00	0,96	0,93	
B040D01	0,93	0,96	
B040D02	0,94	0,93	
B060D00	0,94	0,93	
B060D01	0,90	0,91	
B060D02	0,92	0,92	

B075D00	0,94	0,92	
B075D01	0,95	0,95	
B075D02	0,91	0,92	
B090D00	0,88	0,94	
B090D01	0,89	0,92	
B090D02	0,88	0,92	
B125D00	0,89	0,83	125
B125D01	0,90	0,87	125
B125D02	0,88	0,84	125

Table 11-2: Normalized values battery B + diesel engine

Figure 11-1 depicts the intersection points of the normalised values of the lowest valley and initial voltage. The intersection points are coloured corresponding to their aging cycle class.

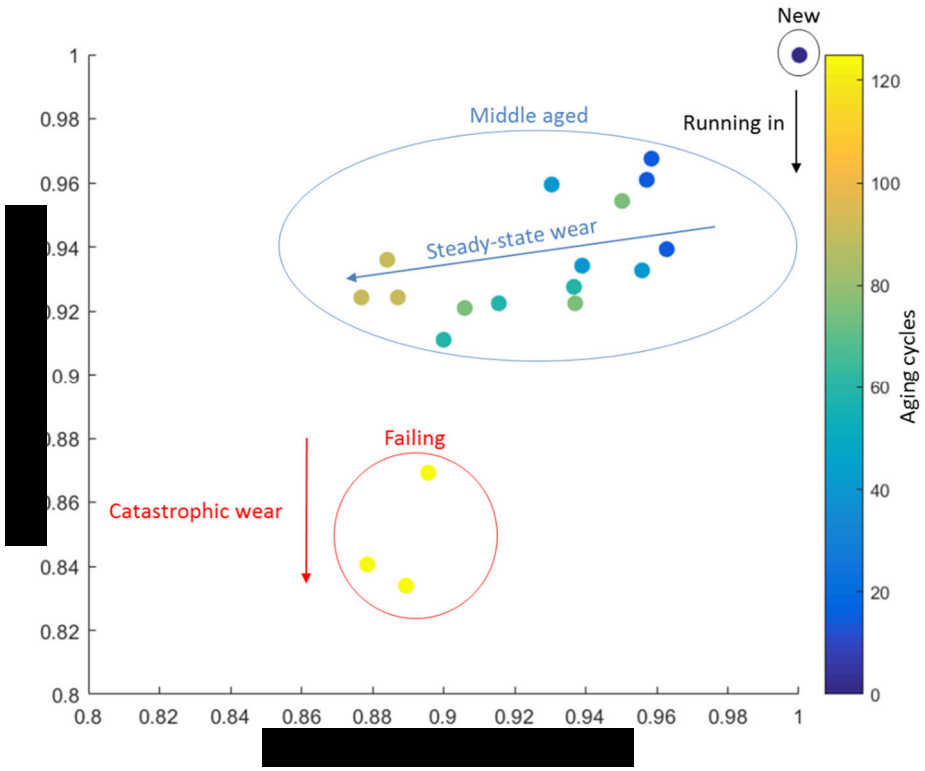

Figure 11-1: two-dimensional graph using normalized values

As can be seen this figure has a strong resemblance to Figure 10-17 and a clear distinction between failing and the middle aged and new batteries can still be made. The new batteries are now grouped together, but they can also be distinguished from the middle aged and failing batteries. The grouping is caused by the scaling to a baseline based on new batteries.

Because the failing batteries are so clearly separated from the rest, a failure warning can be generated using this separation. A line of separation is designed which separates the failing batteries from the rest as depicted in Figure 11-2.

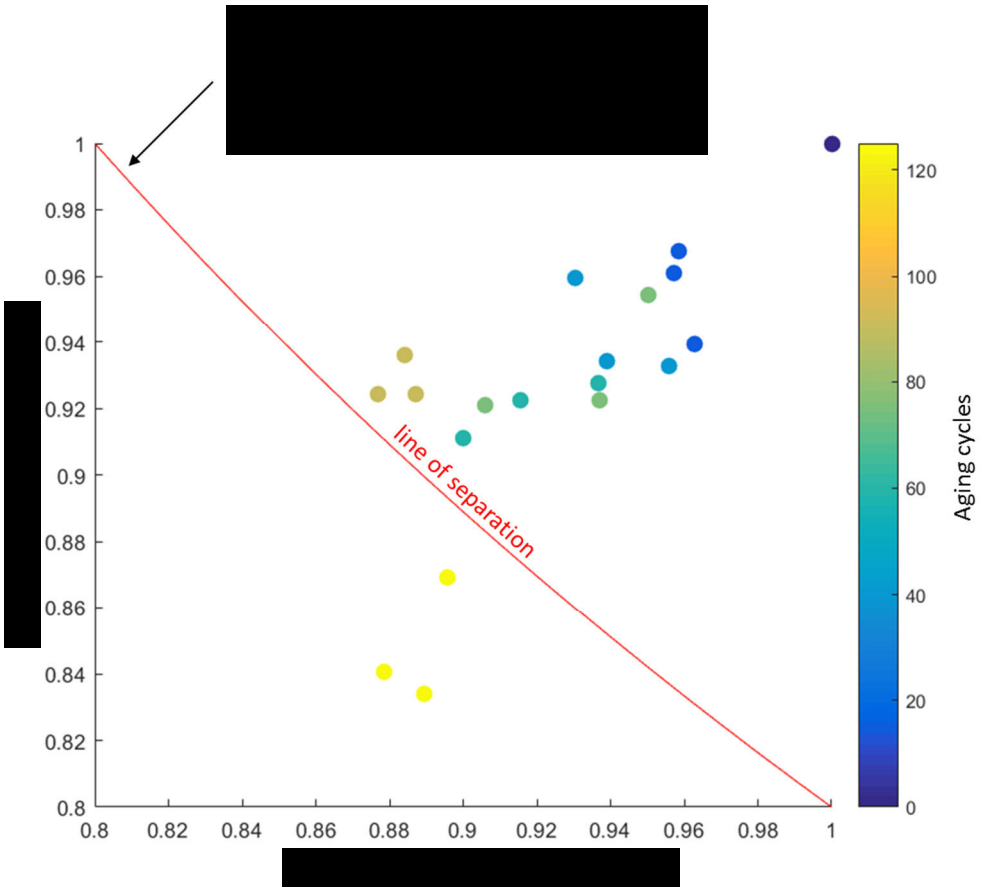

Figure 11-2: Line of separation

The data depicted in Figure 11-2 belongs to battery B which started to produce signs of failure at 125 aging cycles but was still able to crank the engine. This battery generated an upcoming failure label as described in section 9.1.2 at 125 cycles, indicating an upcoming battery failure was prominent. Using the equation belonging to the line of separation a rule has been constructed which predicts an upcoming battery failure:

The equation belonging to the line of separation is:

Equation 11-1: Line of separation

Using this equation a failure prediction rule has been constructed:

Equation 11-2 Rule predicting an upcoming battery failure

This rule is tested on the complete test set and resulted in a list of upcoming battery failure predictions as shown in Table 11-3. The corresponding figures visualizing the line of separation can be referenced in appendix xxx.

CVT ID	

A090D00		0,85	0,84		
A090D01		0,84	0,92		
A125D00		0,82	0,87	125	
A125D01		0,82	0,81	125	
A125D02		0,81	0,81	125	
B125D00		0,89	0,83	125	
B125D01		0,90	0,87	125	
B125D02		0,88	0,84	125	
C125D00		0,83	0,81	125	
C125D01		0,85	0,82	125	
C125D02		0,85	0,82	125	

Table 11-3: Upcoming battery failure predictions

As can be seen no failures are predicted in combination with the petrol engine, which is in line with reality. All batteries failing on the diesel engine failing batteries kept working fine in combination with the petrol engine. Another observation which can be made is that for battery A failure predictions started at 90 aging cycles instead of 125. This is also in line with which occurred in reality. As described in section 8.2.3.1 battery A was chilled to 5 °C and therefore started to fail earlier than the batteries kept on room temperature. The prediction check as shown in the last column is based on the upcoming failure indicator as described in section 9.1.2. All batteries predicted to fail also generated an upcoming failure label.

11.2 Normalized change



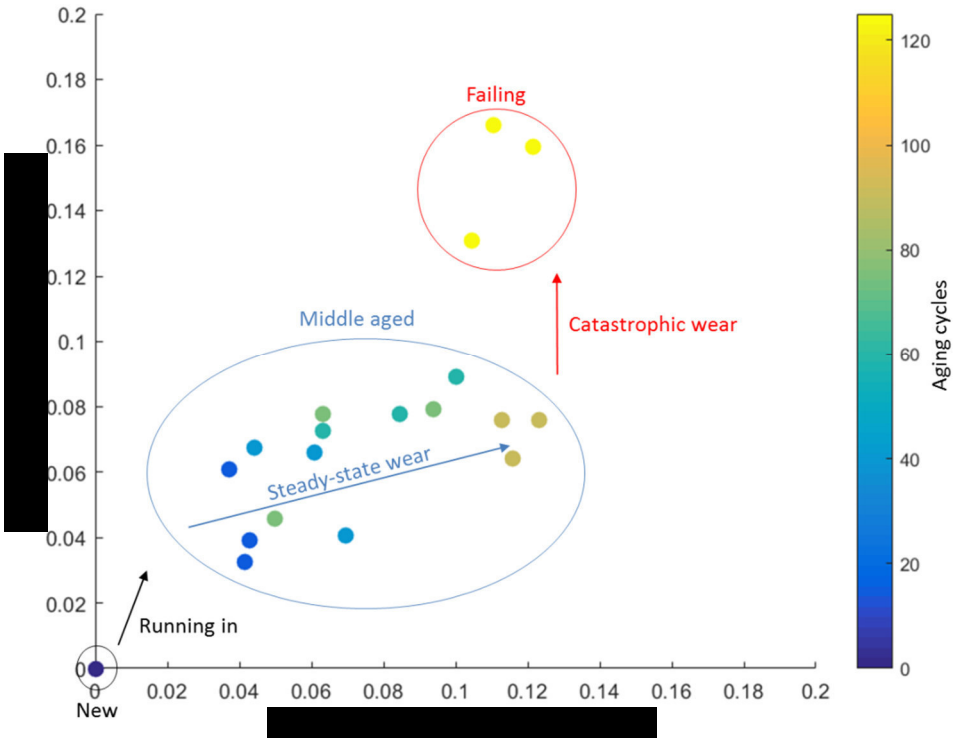

Figure 11-3: Normalized change values

As can be seen an inversed picture is painted compared to Figure 11-1 and the data points belonging to the new batteries now start in the origin of the axes. This makes it easier to apply trendline equations. An example of a trendline equation depicted in Figure 11-4 using an exponential function with a fractured exponent.

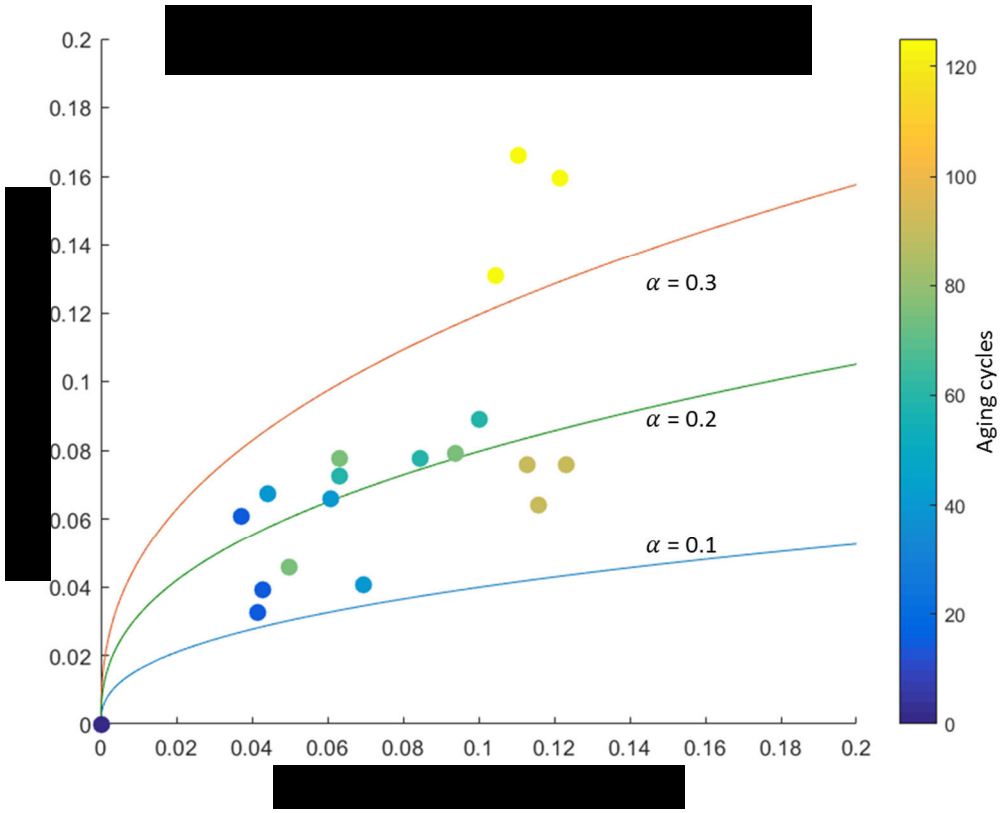

Figure 11-4: Example trendline equations

12 Conclusion & recommendation

12.1 Conclusion

A method has been examined to estimate battery SOH using non-invasive electric measuring methods. The method is based on the discharge voltage during a cranking event. This discharge voltage signal has a distinctive shape and is named: ”the cranking voltage trace” (CVT). To make the measurements non-invasive the CVT has to be captured via the on-board diagnostics port (OBD). A CVT capturing device has been prototyped using simple hardware, proving the CVT can be captured via the OBD port by use of simple hardware.

A test setup has been created to generate CVT data. The test set up contains a diesel and petrol engine. A pool of 5 test batteries has been created which is used to crank both engines of the test setup while the CVT data is captured and stored.

A battery accelerated ageing device has been created which has successfully aged 3 of the 5 test batteries within weeks instead of years. At different instances during the aging process CVT data is generated which maps the battery life from new to old and failing.

When the 3 aged batteries started to produce failures in combination with the diesel engine, they continued to work fine in combination with the petrol engine. From this it is concluded that a failure is system dependent i.e. dependent on a particular battery engine combination.

The CVT data revealed constant differences between the petrol and diesel engine. From this it is concluded that ever battery engine combination is unique.

CVT data is processed resulting in 27 features extracted from a single CVT.

A data quality driven feature analysis is executed which discarded unusable features based on: frequency of occurrence, correlation coefficients and standard deviation. This has resulted in 10 remaining features which are subjected to a second analysis discriminating on the ability to show a relation. The relation analysis was based on: correlation to SOH estimators, value change over service life, linear regressions solving for aging classes and linear regressions solving for SOH estimators.

Three features remained and were selected to be subjected to an analysis which investigated the [redacted] combination. The personal baseline is constructed using values belonging to the first cranks performed by the battery engine combination with a new battery. Normalization is achieved by [redacted]

Using a combination of the normalized [redacted] revealed a relation to battery SOH with the capability of an upcoming failure warning.

Three upcoming failure warning methods were proposed from which two proved to be most robust: the line of separation and a variance based method.

The proposed relation between the combination of the [redacted] be used in a SOH monitoring system which is capable of generating an upcoming failure warning. The prototyping process proved the practical achievability of a remotes SOH monitoring system using dongles (OBD connectible devices) as intended by the ANWB. To make such a system [redacted] have to be corrected for temperature, and scaled to personal and temperature corrected baseline values.

12.2 Recommendation

In this study the type of battery is kept constant. Successive study is required to test the applicability on other types of batteries starting with VRLA batteries.

A temperature dependence is revealed. Successive study is required to establish the temperature [redacted]

Three batteries are aged and used to generate data coming from aged batteries. The relation of the [redacted] to battery SOH has to be tested on a larger scale.

List of figures

Figure 2-1 : Lead Acid Cell 7
Figure 2-2: Active materials lead in charged lead acid cell 8
Figure 2-3: Lead acid cell on discharge 9
Figure 2-4: Automotive battery design 11
Figure 3-1: 20 hr capacity vs discharge rate at 25°C [1] 15
Figure 3-2: Temperature dependence [1] 16
Figure 3-3: State of charge versus OCV [1] 17
Figure 3-4: Battery hydrometer 19
Figure 4-1: Most common failure modes [1] 20
Figure 4-2: Amorphous & crystalline structures 24
Figure 4-3: Operating temperature vs service life [1] 25
Figure 4-4: Capacitor and Resistor 26
Figure 4-5: Equivalent circuit single cell 27
Figure 4-6: Voltage & current waveforms 28
Figure 4-7: Impedance spectrum of a lead acid battery [5] 28
Figure 5-1: Cranking system 31
Figure 5-2: Combustion engine 32
Figure 5-3: Cranking voltage trace 33
Figure 6-1:Cranking voltage trace of new and old battery 34
Figure 6-2: proposed SOH monitoring method 35
Figure 7-1: CVT sampled at 1000Hz 38
Figure 7-2: Most prominent voltage value in first voltage drop 39
Figure 7-3: On-board diagnostics port 40
Figure 7-4: Dongle 40
Figure 7-5: Prototyping measuring equipment 41
Figure 7-6: Controller chip 42
Figure 7-7: Voltage divider 42
Figure 7-8: Initialization part prototype software 45
Figure 7-9: Looping part prototype software 45
Figure 7-10: cranking voltage captured with an oscilloscope 46
Figure 8-1: Test categories 48
Figure 8-2: Testing procedure 49
Figure 8-3: Battery aging device 50
Figure 8-4: CCCV charging 51
Figure 8-5: Test setup battery pool 51
Figure 9-1: Folder and filename structure 54
Figure 9-2: Data extracting part of script 55
Figure 9-3: CVT signal 56
Figure 9-4: Peak, valley and crank ending selection part of script 56
Figure 9-5: Preliminary end of crank determination 57
Figure 9-6: Data filter settings 57
Figure 9-7: Filtered data and phase difference 57
Figure 9-8: mitigation of phase difference 58
Figure 9-9: Peak selection loop 58

Figure 9-10: Peaks in filtered CVT signal 59
Figure 9-11: Second peak selection loop. 59
Figure 9-12: Single peaks in filters CVT signal 60
Figure 9-13: [redacted] 60
Figure 9-14: Visual check of peaks, valleys and end crank. 61
Figure 9-15: [redacted] 62
Figure 9-16: Fault in valley selection 63
Figure 9-17: [redacted] 64
Figure 9-18: [redacted] 65
Figure 9-19: [redacted] 65
Figure 9-20: [redacted] 66
Figure 9-21: [redacted] 66
Figure 9-22: [redacted] 66
Figure 10-1: Labelled scatterplot of pair of features. 72
Figure 10-2: Percentage of feature occurrence 73
Figure 10-3: Standard deviation 75
Figure 10-4: Correlation to failure indicators. 76
Figure 10-5: Feature change behaviour 77
Figure 10-6: Linear regression coefficients 78
Figure 10-7: Regression coefficients solved for 3 for: new, middle aged and failing 79
Figure 10-8: CCA , Internal resistance versus service life. 80
Figure 10-9: Linear regression coefficients internal resistance 80
Figure 10-10: reserve capacity 81
Figure 10-11: Linear regression coefficients reserve capacity 82
Figure 10-12: Heavy loading capacity. 83
Figure 10-13: linear regression coefficients heavy loading capacity. 84
Figure 10-14: 3D scatterplot. 85
Figure 10-15: [redacted] 86
Figure 10-16: [redacted] 87
Figure 10-17: [redacted] 88
Figure 10-18: Temperature dependence 90
Figure 11-1: two-dimensional graph using normalized values 93
Figure 11-2: Line of separation. 94
Figure 11-3: Normalized change values 96
Figure 11-4: Example trendline equations 97

List of tables

Table 3-1: CCA test standards 16
Table 4-1: Failure mechanisms 21
Table 5-1: Cranking process 32
Table 7-1: OBD Socket pinout 40
Table 8-1: Test setup 47
Table 8-2: Engine specifications 48
Table 9-1: Battery SOH estimators 53
Table 9-2: CVT identification number 53
Table 9-3: Features imported from unprocessed CVT data 61
Table 9-4: [redacted] 62
Table 9-5: 63
Table 9-6: 67
Table 9-7: Structure table of features 67
Table 9-8: Features 68
Table 9-9: Labels 68
Table 10-1: Feature classification based on aging cycles 71
Table 10-2: Table of labels belonging to battery B. 72
Table 10-3: Removed features 73
Table 10-4: Correlation Coefficient matrix. 74
Table 10-5: redundant features 74
Table 10-6: 10 remaining features 75
Table 10-7: Three classes: new , middle-aged and failing. 78
Table 10-8: Pairs of features with their correlation coefficients 86
Table 11-1: Baseline battery B + diesel engine 92
Table 11-2: Normalized values battery B + diesel engine 93
Table 11-3: Upcoming battery failure predictions 95

References

[1] P. Reasbeck, 1997. *Batteries for Automotive Use (Electronic and Electrical Engineering Research Studies: Power Sources Technology, Vol. 2)*. Edition. Research Studies Pre.

[2] H.A. Kiehne, 2003. *Battery technology handbook (Tailor & Francis group)*. Second Edition.

[3] Cleve B. Moler, 2008. *Numerical Computing with MATLAB, Revised Reprint*. 2 Edition. Society for Industrial and Applied Mathematics.

[4] H.J. Bergveld, 2005. *Battery Management Systems: Design by Modelling (Philips Research Book Series)*. 2002 Edition. Springer.

[5] J. Ross Macdonald, 2005. *Impedance Spectroscopy: Theory, Experiment, and Applications*. 2 Edition. Wiley-Interscience.

[6] F. Schaffer, 2010. *Autodiagnose met OBD: Theory, OBD I, OBD II and KW1281*. 2 Edition. Elektor International Media.

[7] Basic to Advanced Battery Information from Battery University. 2016. *Basic to Advanced Battery Information from Battery University*. [ONLINE] Available at: http://batteryuniversity.com

[8] AGM, EFB, ECM: welke accu moet er in?. 2016. *AGM, EFB, ECM: welke accu moet er in?*. [ONLINE] Available at: http://www.amt.nl/techniek/nieuws/2010/12/agm-efb-ecm-welke-accu-moet-er-in-10114075

[9] DigiKey Electronics - Electronic Components Distributor . 2016. DigiKey Electronics - Electronic Components Distributor . [ONLINE] Available at: http://www.digikey.com

[10] Catherino, H.A., 2004. Sulfation in lead-acid batteries. Journal of Power Sources, 129, 113-120.

[11] Alber, G. Predicting Battery Performance Using Internal Cell Resistance. Albercorp, 1, 7.

[12] Instruments, Gamry. Basics of Electrochemical Impedance Spectroscopy. Application Note, 1, 17.

[13] Miraglio, R, 1994. Passivation and corrosion phenomena on lead-calcium-tin alloys of lead/acid battery positive electrodes. Journal of power sources, 53, 8.

[14] Bose , SCS. Battery state of health estimation trough coup de fouet: field experience. Valence technology Inc., 1, 4.

[15] Xiao, B, 2010. A universal state-of-charge algorithm for batteries. Electrical engeneering dept. University of calafornia, Los Angeles, 1, 6.

[16] Champlin, K.S., 1992. Electronic tester for assessing battery/cell capacity. United States Patent, 5,140,269, 22.

[17] Champlin, K.S., 1975. Electronic battery testing device. United States Patent, 3,909,708, 14.

[18] Hsiang Chao, K, 2011. State-of-health estimator based on extension theory with a learning mechanism for lead acid batteries. Expert systems with applications, 38, 24.

[19] Gou , J, 2014. Modelling of cranking and charging processes of conventional valve regulated lead acid batteries in micro-hybrid applications. Journal of power sources, 263, 16.

[20] Li, Y, 2014. Real-time estimation of lead acid battery parameters: A dynamic driven approach. journal of power sources, 268, 12.

[21] Galeotti, M, 2015. Performance analysis and SOH evaluation of lithium polymer batteries trough electrochemical impedance spectroscopy. Energy, 678, 16.

[22] Delaille, A, 2006. Study of the "coup de fouet" of lead acid cells as a function of their state-of-charge and state-of-health. Journal of power sources, 158, 18.

[23] Mejia-Aguilar, A, 2009. Electrical Impedance Measurement Using Voltage/Current Pulse Excitation. IMEKO world congress fundamental and applied metrology, 1, 10.